

Analysis of Drug Impurities by Means of Chromatographic Methods: Targeted and Untargeted Approaches



Dissertation zur Erlangung des naturwissenschaftlichen
Doktorgrades an der Fakultät für Chemie und Pharmazie
der Julius-Maximilians-Universität Würzburg

vorgelegt

von

Jonas Wohlfart

aus Würzburg

Würzburg 2022

Eingereicht bei der Fakultät für Chemie und Pharmazie am

Gutachter der Dissertation

1. Gutachter: _____

2. Gutachter: _____

Prüfer des öffentlichen Promotionskolloquiums

1. Prüfer: _____

2. Prüfer: _____

3. Prüfer: _____

Tag des öffentlichen Promotionskolloquiums

Doktorurkunde ausgehändigt am

Die vorliegende Arbeit wurde unter Anleitung von
Prof. Dr. Ulrike Holzgrabe
am Lehrstuhl für Pharmazeutische und Medizinische Chemie
des Instituts für Pharmazie und Lebensmittelchemie
der Julius-Maximilians-Universität Würzburg angefertigt.

Vielen Dank für das mir entgegengebrachte Vertrauen und die
Möglichkeit, mich in verschiedenen Projekten und Fragestellungen
einzubringen und sowohl fachlich als auch menschlich weiterentwickeln
zu können.

Außerdem danke ich Prof. Dr. Fritz Sörgel und Dr. Martina Kinzig vom
IBMP in Nürnberg-Heroldsberg sowie Dr. Elisabeth Jäckel und Dr. Dirk
Jung von Arevipharma für die gute und aufschlussreiche
Zusammenarbeit.

Vielen Dank an alle Mitglieder des AK Holzgrabe!

Adrian, Alex, Christiane, Christine, Cristian, Daniela, Emilie, Florian,
Klaus, Laura, Liling, Lukas, Markus, Mohamed, Nelson, Niclas, Nicolas,
Nina, Jonas U., Joshua, Rasmus, Ruben, Sebastian, Sylvia, Theresa

Curd, Jens, Lina, Ludwig, Martina, Fr. Möhler

Eva-Maria, Renate, Silke

Besonderer Dank gebührt Jonas U. und Rasmus für den
aufschlussreichen und vielfältigen Austausch.

Danke an Nina für die Unterstützung in der Anfangszeit sowie
Alexander, Antonio und Joshua für die Unterstützung in der Synthese
und Charakterisierung von Verunreinigungen.

Danke an Adrian, Jonas U., Sebastian S. und Sebastian Z. für die
gemeinsame Betreuung des 8. Semesters.

Table of Contents

1	Introduction.....	1
1.1	Control of impurities in active pharmaceutical ingredients and medicinal products by regulatory authorities	1
1.1.1	Related substances: side- and degradation products	1
1.1.2	Mutagenic impurities	2
1.1.3	Other impurities.....	3
1.2	Analytical approaches in the control of impurities	5
1.2.1	Principles of high-performance liquid chromatography	5
1.2.2	Important detection principles	6
1.3	References	12
2	Aims of the work.....	19
3	Results	21
3.1	Analysis of Histamine and Sisomicin in Gentamicin: Search for the Causative Agents of Adverse Effects	21
3.2	The nitrosamine contamination of drugs, part 3: Quantification of 4-Methyl-1-nitrosopiperazine in rifampicin capsules by LC-MS/HRMS	35
3.3	Analysis of Naproxen-PEG-Esters in Soft Gel Capsule Formulations	49
3.4	Impurity Profiling of Bisoprolol Fumarate by Liquid Chromatography-High-Resolution Mass Spectrometry: A Combination of Targeted and Untargeted Approaches using a Synthesis Reaction Matrix and General Unknown Comparative Screening.....	61
4	Final Discussion	129
4.1	Sources of impurities in active pharmaceutical ingredients and medicinal products	129
4.2	Methods in the analysis of drug impurities.....	130
4.2.1	Targeted approaches	130
4.2.2	Untargeted approaches.....	132
4.3	References	133
5	Summary.....	137
6	Zusammenfassung.....	139
7	Appendix	141
7.1	List of publications	141
7.2	Documentation of authorship.....	141

List of abbreviations

ACN	acetonitrile
AMP	1-amino-4-methylpiperazine
APCI	atmospheric-pressure chemical ionization
API	active pharmaceutical ingredient
CAD	charged aerosol detector
CEP	Certification of suitability to the monographs of the European Pharmacopoeia
CF	correction factor
CPNP	4-cyclopentyl-1-nitrosopiperazine
CRS	chemical reference substance
DC	direct current
DMF	N,N-dimethylformamide
EDQM	European Directorate for the Quality of Medicines and HealthCare
EFPIA	European Federation of Pharmaceutical Industries and Associations
EI	electron impact ionization
ESI	electrospray ionization
EtOH	ethanol
FA	formic acid
FDA	US Food and Drug Administration
FT-ICR	Fourier-transform ion cyclotron resonance
GC	gas chromatography
GUCS	general unknown comparative screening
HILIC	hydrophilic interaction liquid chromatography
HPLC	high-performance liquid chromatography

HRMS	high-resolution mass spectrometry
ICH	International Council for Harmonisation of Technical Requirements for Pharmaceuticals for Human Use
ICP-MS	inductively coupled plasma-mass spectrometry
IDA	information-dependent acquisition
IS	internal standard
LC	liquid chromatography
MALDI	matrix-assisted laser desorption ionization
MEKC	micellar electrokinetic chromatography
MeNP	1-methyl-4-nitrosopiperazine
MeOH	methanol
MRM	multiple reaction monitoring
MS	mass spectrometry / mass spectrometer
MS/MS	tandem mass spectrometry
m/z	mass-to-charge ratio
NDEA	N-nitrosodiethylamine
NDIPA	N-nitrosodiisopropylamine
NDMA	N-nitrosodimethylamine
NMR	nuclear magnetic resonance
NPEG	naproxen-PEG-ester
NSAID	nonsteroidal anti-inflammatory drug
PEG	polyethylene glycol
PEP	post-exposure prophylaxis
PhEur	European Pharmacopoeia
PI	potential impurity

PTSA	p-toluenesulfonic acid
RF	response factor
RP	reversed phase
SEC	size exclusion chromatography
SIM	single-ion monitoring
SSP	stock standard preparation
SWATH	sequential window acquisition of all theoretical fragments
TIC	total ion current
TLC	thin-layer chromatography
TOF	time-of-flight
USP	United States Pharmacopoeia
QIT	quadrupole ion trap
qOrbitrap	quadrupole-orbitrap
qTOF	quadrupole-time-of-flight
QqQ	triple quadrupole
RCF	relative centrifugal force
WSP	working standard preparation
XIC	extracted ion chromatogram

1 Introduction

1.1 Control of impurities in active pharmaceutical ingredients and medicinal products by regulatory authorities

The control of impurities in active pharmaceutical ingredients (API) and medicinal products is a highly regulated field of activity. A variety of guidelines regarding the quality control of drug substances/products and respective analytical procedures has been elaborated and published by the *International Council for Harmonisation of Technical Requirements for Pharmaceuticals for Human Use* (ICH), whose members are the regulatory authorities of e.g. several European countries, the European Union, USA and Japan as well as industry associations like EFPIA (European Federation of Pharmaceutical Industries and Associations) [1]. In pharmacopoeias like the *European Pharmacopoeia* (PhEur) and the *United States Pharmacopoeia* (USP) methods for the analysis of APIs and excipients are provided in general and specific monographs to ensure a suitable quality of APIs and drug products [2, 3].

1.1.1 Related substances: side- and degradation products

Impurities due to starting products, impurities of starting products, side-reactions during the synthesis and degradation of APIs are, amongst others, controlled by the ICH guidelines Q3A (R2) and Q1A (R2), respectively [4, 5]. The guidelines propose limits and requirements for non-mutagenic impurities considering the maximum daily doses of APIs (Table 1). Impurities exceeding the respective *reporting threshold* must be indicated, but the identity of the impurity must only be elucidated above the *identification threshold*. If the *qualification threshold* is exceeded, further investigations are required to assess the biological safety of the respective impurity. In forced degradation studies, APIs and medicinal products are subjected to elevated temperatures, humidity, oxidizing agents, acidic/basic conditions, and photolysis to derive relevant degradation products. Furthermore, long-term studies are conducted as a basis for the definition of suitable storage conditions and expiry dates.

Table 1 Thresholds for impurities in new APIs according to ICH guideline Q3A (R2) [4]

Maximum daily dose	Reporting threshold	Identification threshold	Qualification threshold
≤ 2 g	0.05%	0.1% or 1.0 mg*	0.15% or 1.0 mg*
> 2 g	0.03%	0.05%	0.05%

*whichever is lower

PhEur monographs of individual APIs state a test for *related substances* and provide the chemical structures of impurities covered by this test [6]. Only *specified impurities* have acceptance criteria which are authorized by the authorities, while *other detectable impurities*, which are not expected to exceed the *identification threshold*, are given for information purposes only.

1.1.2 Mutagenic impurities

ICH guideline M7 (R1) describes strategies in the control of mutagenic impurities with the aim of limiting any potential carcinogenic risk [7]. It requires an assessment of the entire production process to estimate the potential of the formation of mutagenic impurities for new APIs, but also for marketed products after relevant production changes, like changes of the synthesis route or the dosage form. Furthermore, a *Threshold of Toxicological Concern* of 1.5 µg/day is defined as an acceptable intake for most mutagens. The mutagenic potential is usually estimated based on bacterial mutagenicity assays like the *Ames test* and the *Salmonella-reverse-mutation assay* [8]. Furthermore, the guideline states a *cohort of concern* including impurities with the potential for high mutagenicity like nitrosamines, for which even lower limits might be appropriate [7].

Amongst the known classes of DNA-reactive compounds, like aldehydes, carbamates, hydrazines, aniline derivatives, Michael acceptors, etc., nitrosamine impurities have attracted particular attention in 2018 and prompted a worldwide scandal after their occurrence in valsartan and other tetrazole containing sartans upon a change of the synthesis by the manufacturer [9-12]. Decomposition of the subsequently used solvent N,N-dimethylformamide (DMF) set free dimethylamine [13, 14], which reacted with the simultaneously present quenching agent sodium nitrite, to form the corresponding nitrosamine N-nitrosodimethylamine (NDMA) [15]. Besides NDMA, other nitrosamines like N-nitrosodiethylamine (NDEA) and N-nitrosodiisopropylamine (NDIPA) were detected, whose emergence could be explained by the presence of the respective amines as impurities of the solvent [16]. In consequence, the PhEur established the new general chapter *N-Nitrosamines in active substances* describing the analysis of seven nitrosamines in sartans by means of GC-MS, GC-MS/MS and LC-MS/MS, focusing on APIs of the sartan class containing a tetrazole moiety [17]. Furthermore, production statements were added to the monographs of the affected sartans (candesartan cilexetil, irbesartan, losartan potassium, olmesartan medoxomil, and valsartan), addressing the potential of nitrosamine formation upon manufacturing in

PhEur 10.4 [18-22]. The sartan scandal prompted the search for nitrosamines in other drug substance classes, which revealed the contamination of various, chemically diverse drugs like ranitidine, metformin, and rifampicin [23-25].

1.1.3 Other impurities

Besides related substances and mutagenic impurities, APIs may be contaminated with a variety of other impurities of diverse sources. Another group of synthesis related contaminants is the class of *elemental impurities*, which is addressed by ICH guideline Q3D (R1) [26, 27]. *Permitted daily exposures* for such impurities are defined considering the toxicity of the respective element and the route of administration (oral, parenteral, inhalation). *Elemental impurities*, previously called *heavy metals*, might be present in APIs as residuals of catalysts, due to contamination of water and as leachables from manufacturing equipment and containers. Besides reagent-based limit tests, e.g. precipitation of heavy metals with thioacetamide [28], PhEur suggests the use of instrumental analytics for elemental impurities, like atomic emission/absorption spectroscopy, x-ray fluorescence spectrometry and inductively coupled plasma-mass spectrometry (ICP-MS) [29].

Furthermore, impurities and degradation products of raw materials can lead to contamination of drug substances, as became obvious with the histamine contamination of gentamicin sulfate in 2016 [30]. The biogenic amine occurred in low-quality fish peptone used for the fermentative production of gentamicin and was carried through the whole process into the final product. Intravenous application of affected drug products to horses led to anaphylactic reactions including tachycardia, tachypnoea, and sweating [31]. Later, also humans were affected with one fatality [32]. In consequence of these events, the PhEur general monograph *Products of fermentation* was adapted. Since PhEur 10.4 it requires testing of raw materials for free histidine to prevent the emergence of histamine through bacterial decarboxylation, and the purification processes must be able to “remove histamine and other biogenic amines from fishery products used in raw materials” [33].

Moreover, interaction products of APIs with excipients and primary packaging materials can occur in medicinal products, which are addressed by ICH guideline Q3B (R2) [34]. Reactive impurities of excipients like aldehydes, organic acids, reducing sugars, elemental impurities and peroxides can cause incompatibilities, resulting in degradation of the API and/or formation of (reactive) impurities [35, 36]. For example,

peroxides present in polymeric excipients like polysorbates, and polyethylene glycol can react with Michael systems, forming reactive epoxide derivatives [37].

Residual solvents pose a potential risk and are controlled by ICH guideline Q3C (R6) and its respective general monograph in PhEur [38, 39]. Solvents are grouped into three classes: *solvents to be avoided* like benzene and carbon tetrachloride, *solvents to be limited* like chloroform and methanol (MeOH), and *solvents with low toxic potential* like acetone and ethanol (EtOH). Furthermore, appropriate limits and methods for the establishment of thresholds are provided. Headspace gas chromatography is the most used technique for the quantification of residual solvents. However, if only nontoxic solvents are used, a less specific method like *loss on drying* can be used.

In addition to all these well-known and highly controlled sources of impurities, still not all potential impurities are covered by the discussed guidelines. For example, unexpected impurities might emerge upon reactions of solvents with APIs or intermediates: halogenated hydrocarbon solvents such as chloroform are known to participate in reactions during drug synthesis, leading e.g. to chloromethyl derivatives [40, 41]. Another possible source of toxicologically relevant impurities is the crystallization of drug salts by reactions of the used acid/base and the solvent without participation of the API: chloroalkanes and sulfonate esters can emerge during the preparation of hydrochlorides or sulfonates (e.g. tosylates), respectively, when solvents with free alcohol groups (MeOH, EtOH, etc.) are used for the salification [42]. ICH guideline Q3A (R2) requires an appraisal of the synthesis procedure in order to predict possible impurities [4]. However, the presented variety of sources for impurities illustrates the challenge of predicting all relevant impurities which might emerge during the synthesis and storage of the API as well as its interactions with excipients and primary packaging.

Pharmacopeial monographs provide methods for the identification, quantification, and purity assessment of APIs, but cover only the impurities related to the production method(s) considered upon the development of the respective monograph [6]. Manufacturers can be granted a CEP (*Certification of suitability to the monographs of the European Pharmacopoeia*) if their product complies with the requirements of the monograph and the impurities concomitant with their production method are suitably controlled [43]. Otherwise, the existing methods have to be adapted or new methods need to be developed and validated [44].

1.2 Analytical approaches in the control of impurities

For quality control of drugs, a separation of APIs and their impurities is necessary and mostly achieved by chromatography. Chromatographic separation is based on different affinities of the analytes towards two immiscible phases: A mobile phase, which can be a liquid, gas, or supercritical fluid, is moved over a solid or liquid stationary phase, which is immobilized on a solid or gel [45]. The solute analytes are carried forwards by the mobile phase and are retained on the stationary phase by different mechanisms like partition, adsorption, size exclusion and ionic interactions. Common types of chromatography applied in drug analysis are thin-layer chromatography (TLC), gas chromatography (GC) and high-performance liquid chromatography (HPLC), being the gold standard in the analysis of APIs, drug products and their impurities.

1.2.1 Principles of high-performance liquid chromatography

The main components of HPLC instruments are a pumping system to move the mobile phase through the system, an injector, a column incorporating the stationary phase, a detector and a system for instrument control and data evaluation [46].

The stationary phase can be selected from diverse available materials depending on the physicochemical properties of the analytes [47]. Often, chemically derivatized silica gels or polymers are used in the analysis of drugs, e.g. octyl (C8), octadecyl (C18) and phenyl phases in reversed phase (RP) chromatography [48]. Further variants like chiral chromatography, HILIC (hydrophilic interaction liquid chromatography), SEC (size exclusion chromatography) and mixed-mode chromatography incorporate suitable stationary phases for many analyte classes and challenging separations [49].

Mobile phases used in RP chromatography normally consist of mixtures of water with organic modifiers, e.g. methanol, acetonitrile and tetrahydrofuran. Buffering agents for different pH areas like phosphate, borate and acetate buffers are often added to modify the separation [46, 50]. Moreover, ion-pairing agents like alkylammonium salts and perfluorinated carboxylic acids are used to achieve separation of anions and cations, respectively, using RP stationary phases [51]. Yet, the type of detector also influences the choice of additives. For example, volatile additives and buffering agents (like formic or acetic acid and their ammonium salts) must be used with aerosol-based detectors, like the charged aerosol detector (CAD) and mass spectrometers (MS) [52, 53].

1.2.2 Important detection principles

1.2.2.1 UV-Vis detector

The UV-Vis detector is one of the most used detectors in HPLC due to its great range of detectable analytes, robustness, and cost-effectiveness [54, 55]. It consists of a light source, a monochromator, a flow cell, a device capable of the detection of electromagnetic radiation, and a data processing system [56]. The UV-Vis detector is capable of detecting analytes containing a chromophore, which is a system of excitable electrons like conjugated double-bonds and free electron pairs of heteroatoms [48]. The detection is based on the absorption of electromagnetic radiation in the UV and the Vis range of 180-400 nm and 400-800 nm, respectively [56]. The Beer-Lambert law describes the linear relationship of analyte concentration and absorbance [57].

Most APIs and related substances are detectable by the UV-Vis detector. The concentrations of related substances are relevant in the range of the thresholds given in ICH guideline Q3A (R2), i.e. 0.03% or higher, which can typically be analyzed by UV-Vis detectors [4]. However, considerably lower concentrations need to be quantified when it comes to mutagenic impurities. Furthermore, not all APIs and impurities contain chromophores [58, 59]. Hence, more sensitive and versatile detectors like MS or the CAD are needed for such applications.

1.2.2.2 Mass spectrometric detectors

The components of mass spectrometers are an ion source responsible for the generation of desolvated and charged analyte molecules, a mass analyzer and an ion detection system [60]. Ions of different mass-to-charge ratios (m/z) are separated by the mass analyzer and then hit the detector, most commonly electron multipliers [61].

1.2.2.2.1 Ionization techniques

Several ionization techniques with different properties have been developed, like electron impact (EI), matrix-assisted laser desorption ionization (MALDI), electrospray ionization (ESI, Figure 1) and atmospheric-pressure chemical ionization (APCI). They cover a wide range of analyte classes [60].

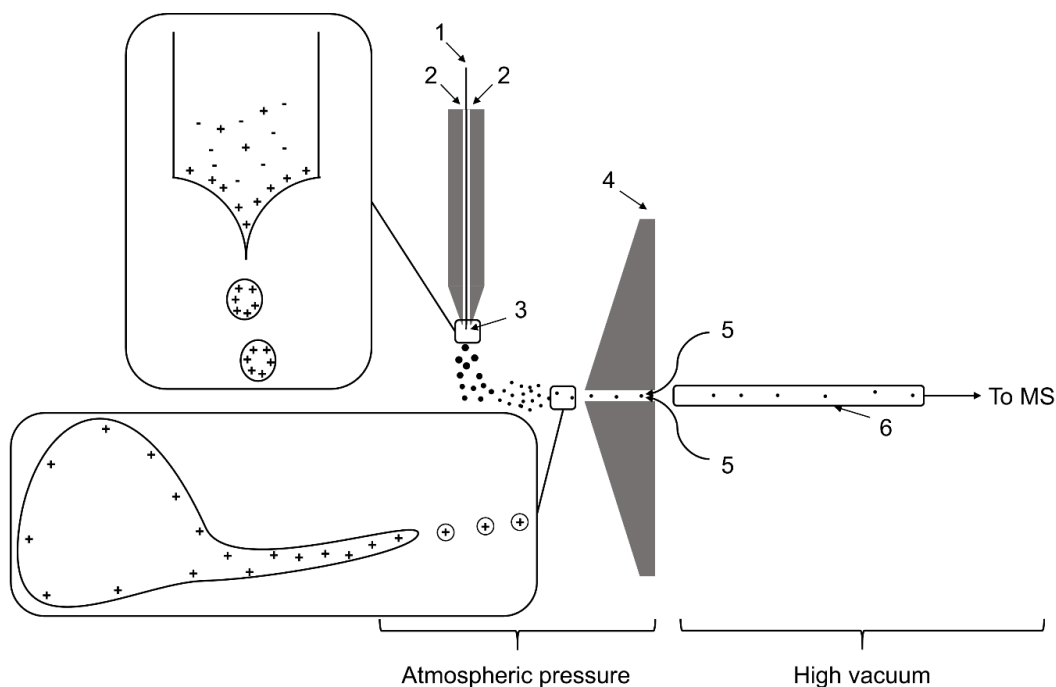


Figure 1 Schematic setup of an ESI source in positive mode (1: Eluent from HPLC, 2: Nebulizer Gas, 3: Spray capillary tip with Taylor cone, 4: Orifice plate, 5: Desolvation/sheath gas, 6: Glass capillary) [62, 63]

ESI is a soft ionization technique well suitable for the coupling with HPLC [63]. The eluent (1) is nebulized with the aid of a nebulizer gas (2), usually nitrogen. The spray capillary tip (3) and the orifice plate (4) serve as electrodes, to which a potential of several kilovolts is applied. Depending on the nature of the analytes, the polarity can be switched between positive and negative mode for the analysis of cations and anions, respectively. The desolvation/sheath gas (5) aids with the desolvation of the droplets and protects the MS from contamination. Due to the strong electric field at the thin spray capillary, an aerosol of multiple charged droplets is formed from a *Taylor Cone* [64]. Classical theories assume that the droplets decrease in size until, at the *Rayleigh Limit*, the excess charge exceeds the surface tension and smaller droplets are formed in a *Coulomb Explosion*. Other works suggest the release of smaller droplets from protuberances of parent droplets (see Figure 1). The mechanisms leading to free analyte ions in the gas phase are not fully understood yet and hence, further investigated [62, 65]. A cascade of such reactions eventually sets free protonated or deprotonated species. These are transferred through a glass capillary (6) and ion optics towards the mass analyzer. The formation of multiple charged species enables the analysis of macromolecules like proteins despite the limited m/z ranges of mass analyzers [66, 67]. Furthermore, adducts with e.g. sodium cations and water, as well as clusters are often detected [63, 68]. To avoid contamination of the ion

optics, the source geometry has been optimized to the orthogonal design shown in Figure 1 and *Z-Spray* [69]. For ESI, the presence of charged analyte molecules in the sample solution is crucial, which limits this ionization technique to relatively polar molecules. As this requirement is met by a great majority of drug substances, ESI is the most used ion source in drug analysis. The ionization efficiency depends on the mobile phase composition, source parameters and analyte properties like pK_a , $\log P$, and nonpolar surface area [70].

Less polar substances can be ionized by APCI. Here, ionization occurs within the aerosol by a corona discharge needle [64]. Therefore, the nebulization is not performed under the influence of a high voltage, but pneumatically [63]. Besides the dominating protonated or deprotonated species [60], APCI also yields radical ions, which can be explained by the ionization process (example given for positive mode) [71]: Nitrogen molecules, as the most abundant species in the ion source, form radical cations $N_2^{+\bullet}$ in the high electric field surrounding the corona discharge needle. These radical cations can react with solvent molecules, which then ionize analyte molecules forming $[M+H]^+$ as well as $[M]^{+\bullet}$ ions.

1.2.2.2.2 Mass analyzers

The “heart” of a mass spectrometer is its mass analyzer, which is responsible for the separation of analyte ions. Several techniques based on different physical principles have been developed, e.g. magnetic sectorfield, quadrupole, three-dimensional quadrupole ion trap (QIT), orbitrap, Fourier-transform ion cyclotron resonance (FT-ICR), and time-of-flight (TOF) analyzers [60, 63]. Hybrid instruments like quadrupole-TOF (qTOF) and quadrupole-orbitrap (qOrbitrap) have been developed to combine the strengths of single techniques to powerful devices, especially for tandem mass spectrometry (MS/MS).

A quadrupole is the quadratic arrangement of four parallel, cylindrical or hyperbolic rod electrodes (Figure 2) [63]. Ions of specific mass-to-charge ratios (m/z) can be selected by application of a direct current (DC) and a radio frequency, which determine the trajectories of ions through the quadrupole. Only selected ions show stable trajectories and can be detected, while other ions show instable trajectories and collide with the rods. Development of this technique led to triple quadrupole (QqQ) mass spectrometers [72], and the triple quadrupole linear ion trap, which enable the investigation of single and multiple fragmentation reactions (MS^n), respectively [73].



Figure 2 Photographs of a quadrupole used in Sciex mass spectrometers (photo by Jonas Wohlfart)

Another option for the acquisition of MS^n spectra is the three-dimensional QIT [60, 63]. It consists of two hyperbolic electrodes and a ring electrode. Similar as with linear quadrupoles, ions of selected m/z (ranges) are isolated by applying suitable DC potentials and radio frequencies to produce stable trajectories for the respective ions. The ions enter and leave the QIT through holes in the electrodes. Contrary to QqQ instruments, the QIT selects and fragments ions at the same place and not in a separate collision cell [74].

MS^n experiments provide information on the chemical structure of analytes and are an important tool in the structure elucidation of small molecules [75]. Yet, a determination of molecular formulae is not possible with quadrupole and QIT instruments, as they show insufficient resolution powers. TOF, orbitrap and FT-ICR instruments can be used for high-resolution mass spectrometry (HRMS) to deduce molecular formulae based on the exact mass and isotope pattern of analytes [76].

In TOF analyzers, ions are accelerated by a defined voltage of about 10-20 kV into a field free flight path [60, 77]. The velocity of ions depends on their m/z and thus, the time required for the passage of a flight tube (25 to 150 cm) can be used to determine their m/z . An optimization of the resolution power of TOF instruments lead to reflector TOF mass analyzers [63]. Reflectors are electrostatic mirrors consisting of ring-shaped electrodes with rising potential. In hybrid instruments like the qTOF, ions of the same m/z might show different velocities due to diffusion within the ion beam emitted by the ion source, which broadens the signal in the mass spectrum. Faster ions penetrate deeper into the reflector and spend more time in the reflector than slower ions: the difference in the measured flight times decreases and significantly sharper signals are obtained. The effect can be extended by the combination of two or more reflectors (Figure 3).

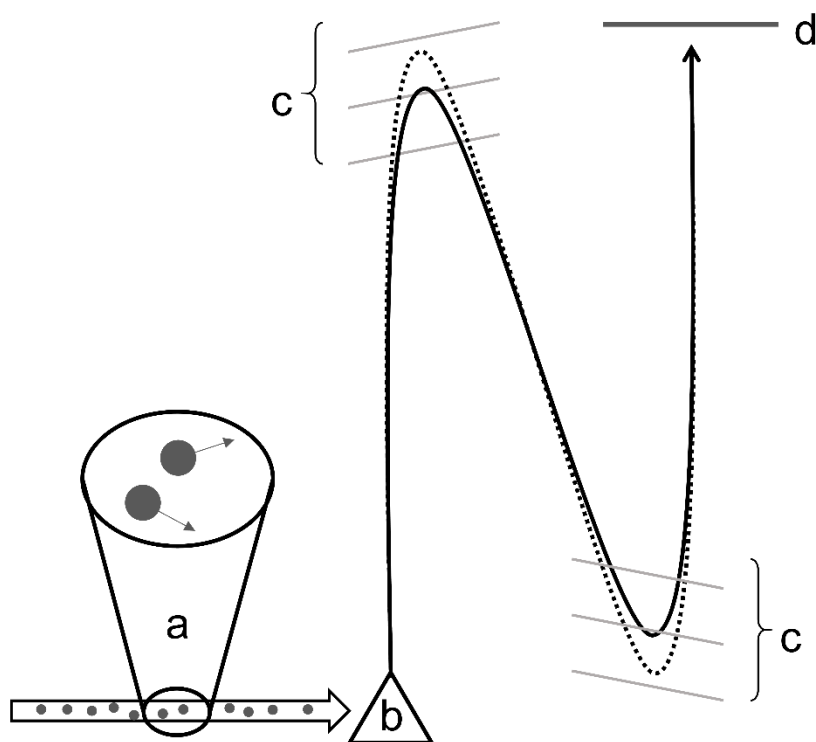


Figure 3 Setup of a TOF instrument with two reflectors. Ions with diffusion-based differences in their starting velocities (a) are accelerated orthogonal (b) into the analyzer. The flight paths of two ions with the same m/z are shown: the faster ion (dotted line) penetrates deeper into the reflectors (c) than the slower ion (continuous line), followed by detection (d) [63]

High-resolution fragment spectra can be acquired using qTOF hybrid instruments, which consist of two quadrupoles and a TOF analyzer. The two quadrupoles are used in the same way as in QqQ instruments. After selection and fragmentation of ions, the ions are accelerated in orthogonal direction into the TOF analyzer [78].

1.2.2.2.3 Acquisition modes

Mass spectral information can be acquired in different modes, depending on the type of mass spectrometer used and the analytical task. In *complete spectrum mode*, all present ions in a selected mass range are recorded. The results are a *total ion current* (TIC) chromatogram and mass spectra over the entire mass range. Ions of interest can be examined by creating *extracted ion chromatograms* (XIC) [79]. In contrast, only ions with a selected m/z are selected and detected in *single-ion monitoring* (SIM). In quantitative analyses, measurements are commonly performed in *multiple reaction monitoring* (MRM): one or several m/z are selected for fragmentation and specific fragments are detected [60]. QqQ instruments are often operated in this mode and can reach excellent selectivity and sensitivity [80, 81].

In untargeted approaches, *information dependent acquisition* (IDA), *sequential window acquisition of all theoretical fragments* (SWATH) and *MS/MS^{All}* are used to generate fragment spectra of hypothetically all present analytes in a sample [82]. These techniques are used especially with qTOF instruments, which are predestined for the identification of unknown substances due to their high mass accuracy, sensitivity, and short cycle times [83]. Molecular formulae can be determined based on the exact m/z of a molecule and the abundance of its isotope signals [76]. Fragment spectra can be used to draw conclusions concerning the structural formulae. This can be supported by *in-silico* fragmentation, where fragment spectra are simulated following predefined rules by a computer to estimate the plausibility of respective structures [84]. However, any tentative identification or elucidation should be verified by comparison with fragment spectra of authentic reference material or mass spectral libraries [85-87].

In targeted approaches, potential impurities are derived based on the synthesis procedure of drug substances, which can be supported by reaction matrices [88], and searched in specific assays. However, the variety of sources of impurities of an API presented above illustrate the unlikeliness to predict all impurities emerging during the production of a medicinal product. Untargeted approaches (IDA, SWATH) are potentially capable of detecting all present impurities without prior information. Hence, a combination of both targeted and untargeted approaches is desirable to establish comprehensive impurity profiles. Especially when it comes to mutagenic impurities and long-term therapeutics, highly sensitive and thorough analytics are required to ensure a maximum of patient safety.

1.3 References

- [1] International Council for Harmonisation of Technical Requirements for Pharmaceuticals for Human Use, Overview of ICH. https://admin.ich.org/sites/default/files/2021-06/OverviewOfICH_2021_0614.pdf, 2021 (accessed 24 August 2021)
- [2] Substances for Pharmaceutical Use in: European Pharmacopoeia 10.0, Council of Europe, Strasbourg, France, 2020
- [3] The United States Pharmacopeial Convention, An Overview of USP Monographs. <https://www.usp.org/about/public-policy/overview-of-monographs>, 2021 (accessed 19 March 2021)
- [4] International Council for Harmonisation of Technical Requirements for Pharmaceuticals for Human Use, ICH Topic Q3A (R2) Impurities in new Drug Substances, 2006
- [5] International Council for Harmonisation of Technical Requirements for Pharmaceuticals for Human Use, ICH Topic Q1A (R2) Stability Testing of new Drug Substances and Products, 2003
- [6] 5.10 Control of Impurities in Substances for Pharmaceutical Use in: European Pharmacopoeia 10.0, Council of Europe, Strasbourg, France, 2020
- [7] International Council for Harmonisation of Technical Requirements for Pharmaceuticals for Human Use, ICH guideline M7 (R1) on assessment and control of DNA reactive (mutagenic) impurities in pharmaceuticals to limit potential carcinogenic risk, 2015
- [8] P. Escobar, R. Kemper, J. Tarca, J. Nicolette, M. Kenyon, S. Glowienke, S. Sawant, J. Christensen, T. Johnson, C. McKnight, Bacterial mutagenicity screening in the pharmaceutical industry, *Mutat Res/Rev Mutat Res* 752 (2013) 99-118
- [9] S. S. Bharate, Critical Analysis of Drug Product Recalls due to Nitrosamine Impurities, *J Med Chem* 64 (2021) 2923-2936
- [10] F. Sörgel, M. Kinzig, M. Abdel-Tawab, C. Bidmon, A. Schreiber, S. Ermel, J. Wohlfart, A. Besa, O. Scherf-Clavel, U. Holzgrabe, The contamination of valsartan and other sartans, part 1: New findings, *J Pharm Biomed Anal* 172 (2019) 395-405
- [11] Bundesinstitut für Arzneimittel und Medizinprodukte, Valsartan: chargenbezogener Rückruf valsartanhaltiger Arzneimittel, deren Wirkstoff von dem chinesischen Hersteller Zhejiang Huahai Pharmaceutical produziert wurde. <https://www.bfarm.de/SharedDocs/Pressemitteilungen/DE/2018/pm5-2018.html>, 2018 (accessed 4 January 2021)
- [12] U.S. Food & Drug Administration, FDA Updates and Press Announcements on Angiotensin II Receptor Blocker (ARB) Recalls, <https://www.fda.gov/drugs/drug-safety-and-availability/fda-updates-and-press-announcements-angiotensin-ii-receptor-blocker-arb-recalls-valsartan-losartan>, 2018 (accessed 4 January 2021)
- [13] W. Liu, C. Chen, H. Liu, Dimethylamine as the key intermediate generated in situ from dimethylformamide (DMF) for the synthesis of thioamides, *Beilstein J Organ Chem* 11 (2015) 1721-1726

- [14] J. Muzart, N, N-Dimethylformamide: much more than a solvent, *Tetrahedron* 65 (2009) 8313-8323
- [15] Aliphatische Stickstoffverbindungen in: T. Schirmeister, C. Schmuck, P. R. Wich, Beyer/Walter | *Organische Chemie*, 25th edition, S. Hirzel Verlag, Stuttgart, Germany, 2015
- [16] H. Buschmann, U. Holzgrabe, Noch mehr Nitrosamine. NDMA, NDEA, NDIPA – wie kommen die Verunreinigungen in die Sartane, *Deutsche Apotheker Zeitung* 159-1/2 (2019) 50-54
- [17] European Directorate for the Quality of Medicines & HealthCare, Ph. Eur. Commission adopts a new general chapter for the analysis of N-nitrosamine impurities. <https://www.edqm.eu/en/news/ph-eur-commission-adopts-new-general-chapter-analysis-n-nitrosamine-impurities>, 2020 (accessed 22 January 2021)
- [18] Monograph Candesartan cilexetil in: *European Pharmacopoeia 10.4*, Council of Europe, Strasbourg, France, 2021
- [19] Monograph Irbesartan in: *European Pharmacopoeia 10.4*, Council of Europe, Strasbourg, France, 2021
- [20] Monograph Losartan potassium in: *European Pharmacopoeia 10.4*, Council of Europe, Strasbourg, France, 2021
- [21] Monograph Olmesartan medoxomil in: *European Pharmacopoeia 10.4*, Council of Europe, Strasbourg, France, 2021
- [22] Monograph Valsartan in: *European Pharmacopoeia 10.4*, Council of Europe, Strasbourg, France, 2021
- [23] U.S. Food & Drug Administration, FDA Updates and Press Announcements on NDMA in Zantac (ranitidine). <https://www.fda.gov/drugs/drug-safety-and-availability/fda-updates-and-press-announcements-ndma-zantac-ranitidine#:~:text=Glenmark%20Pharmaceutical%20Inc.-,FDA%20has%20advised%20companies%20to%20recall%20their%20ranitidine%20if%20testing,conduct%20their%20own%20laboratory%20testing.>, 2020 (accessed 4 January 2021)
- [24] U.S. Food & Drug Administration, FDA Updates and Press Announcements on NDMA in Metformin. <https://www.fda.gov/drugs/drug-safety-and-availability/fda-updates-and-press-announcements-ndma-metformin>, 2020 (accessed 4 January 2021)
- [25] U.S. Food & Drug Administration, FDA works to mitigate shortages of rifampin and rifapentine after manufacturers find nitrosamine impurities. <https://www.fda.gov/drugs/drug-safety-and-availability/fda-works-mitigate-shortages-rifampin-and-rifapentine-after-manufacturers-find-nitrosamine>, 2020 (accessed 11 December 2020)
- [26] Chapter 5.20 Elemental Impurities in: *European Pharmacopoeia 10.0*, Council of Europe, Strasbourg, France, 2020
- [27] International Council for Harmonisation of Technical Requirements for Pharmaceuticals for Human Use, ICH guideline Q3D (R1) on elemental impurities, 2019
- [28] Chapter 2.4.8 Heavy metals in: *European Pharmacopoeia 10.0*, Council of Europe, Strasbourg, France, 2020

- [29] Chapter 2.4.20 Determination of elemental impurities in: European Pharmacopoeia 10.0, Council of Europe, Strasbourg, France, 2020
- [30] European Medicines Agency, Histamine contamination of gentamicin medicinal products for human and veterinary use, Chronology of events, EMA/65677/2018, 2018
- [31] V. Stammwitz, Ä. Honnens, D. Hochhuth, H.-J. Schuberth, Increase of Adverse Events After Intravenous Injection of Gentamicin in Horses Between 2015 and 2017 – From Marketing Authorization Holder's Point of View, *Front Vet Sci* 8 (2021) 8:71057
- [32] European Medicines Agency, Assessment report, Procedure under Article 5(3) of Regulation EC (No) 726/2004, Procedure no EMEA/H/A-5(3)/1468, INN/active substance: gentamicin (solution for infusion/solution for injection), 2018
- [33] Products of Fermentation in: European Pharmacopoeia 10.4, Council of Europe, Strasbourg, France, 2021
- [34] International Council for Harmonisation of Technical Requirements for Pharmaceuticals for Human Use, Impurities in New Drug Products Q3B (R2), 2006
- [35] Y. Wu, J. Levons, A. S. Narang, K. Raghavan, V. M. Rao, Reactive Impurities in Excipients: Profiling, Identification and Mitigation of Drug–Excipient Incompatibility, *AAPS PharmSciTech* 12 (2011) 1248-1263
- [36] K. Zhang, J. D. Pellett, A. S. Narang, Y. J. Wang, Y. T. Zhang, Reactive impurities in large and small molecule pharmaceutical excipients – A review, *Trends Anal Chem* 101 (2018) 34-42
- [37] K. C. Waterman, R. C. Adami, K. M. Alsante, J. Hong, M. S. Landis, F. Lombardo, C. J. Roberts, Stabilization of pharmaceuticals to oxidative degradation, *Pharm Dev Technol* 7 (2002) 1-32
- [38] International Council for Harmonisation of Technical Requirements for Pharmaceuticals for Human Use, ICH guideline Q3C (R6) on impurities: guideline for residual solvents, 2019
- [39] Chapter 5.4 Residual Solvents in: European Pharmacopoeia 10.0, Council of Europe, Strasbourg, France, 2020
- [40] A. H. Gainza, Reaction of halogenated hydrocarbon solvents with tertiary amines: Spectrophotometric and conductimetric study, *Int J Chem Kinet* 36 (2004) 500-509
- [41] V. G. Dongre, P. D. Ghugare, P. Karmuse, D. Singh, A. Jadhav, A. Kumar, Identification and characterization of process related impurities in chloroquine and hydroxychloroquine by LC/IT/MS, LC/TOF/MS and NMR, *J Pharm Biomed Anal* 49 (2009) 873-879
- [42] H. Buschmann, D. Jung, U. Holzgrabe, Unerwartet verunreinigt, *Deutsche Apotheker Zeitung* 159-20 (2019) 50-59
- [43] European Directorate for the Quality of Medicines & HealthCare, Fact Sheet: The Certification procedure (CEP procedure). https://www.edqm.eu/sites/default/files/medias/fichiers/Factsheets/Certification_of_suitability/factsheet_certification_of_suitability_cep_july_2020.pdf, 2020 (accessed 24 March 2021)

- [44] International Council for Harmonisation of Technical Requirements for Pharmaceuticals for Human Use, Validation of analytical procedures: Text and Methodology Q2 (R1), 2005
- [45] Chapter 2.2.46 Chromatographic separation techniques in: European Pharmacopoeia 10.0, Council of Europe, Strasbourg, France, 2020
- [46] Chapter 2.2.29 Liquid chromatography in: European Pharmacopoeia 10.0, Council of Europe, Strasbourg, France, 2020
- [47] C. S. Young, R. J. Weigand, An efficient approach to column selection in HPLC method development, *LC GC N Am* 20 (2002) 464-473
- [48] M. H. Gey, *Instrumentelle Analytik und Bioanalytik: Biosubstanzen, Trennmethode, Strukturanalytik, Applikationen*, 3rd edition, Springer-Verlag GmbH, Heidelberg, Germany, 2015
- [49] K. Zhang, X. Liu, Mixed-mode chromatography in pharmaceutical and biopharmaceutical applications, *J Pharm Biomed Anal* 128 (2016) 73-88
- [50] L. R. Snyder, J. J. Kirkland, J. W. Dolan, *Introduction to modern liquid chromatography*, 3rd edition, John Wiley & Sons, Inc., Hoboken, New Jersey, USA 2011
- [51] T. Cecchi, *Ion-pair chromatography and related techniques*, 1st edition, Informa UK Limited, London, United Kingdom, 2009
- [52] D. Corradini, J. Cazes, *Handbook of HPLC*, 2nd edition, Informa UK Limited, London, United Kingdom, 2010
- [53] P. H. Gamache, *Charged aerosol detection for liquid chromatography and related separation techniques*, 1st edition, John Wiley & Sons, Inc., Hoboken, New Jersey, USA, 2017
- [54] K. G. Kraiczek, R. Bonjour, Y. Salvadé, R. Zengerle, Highly Flexible UV–Vis Radiation Sources and Novel Detection Schemes for Spectrophotometric HPLC Detection, *Anal Chem* 86 (2014) 1146-1152
- [55] R. Nageswara Rao, V. Nagaraju, An overview of the recent trends in development of HPLC methods for determination of impurities in drugs, *J Pharm Biomed Anal* 33 (2003) 335-377
- [56] Chapter 2.2.25 Absorption spectrophotometry, ultraviolet and visible in: European Pharmacopoeia 10.0, Council of Europe, Strasbourg, France, 2020
- [57] Beer-Lambert law (or Beer-Lambert-Bouguer law) in: A. D. McNaught, A. Wilkinson, *Compendium of Chemical Terminology*, Web 2.0 version, International Union of Pure and Applied Chemistry, Durham, North Carolina, USA, 2019
- [58] A. Soliven, I. A. H. Ahmad, J. Tam, N. Kadrichu, P. Challoner, R. Markovich, A. Blasko, A simplified guide for charged aerosol detection of non-chromophoric compounds – Analytical method development and validation for the HPLC assay of aerosol particle size distribution for amikacin, *J Pharm Biomed Anal* 143 (2017) 68-76
- [59] S. McCrossen, D. Bryant, B. Cook, J. Richards, Comparison of LC detection methods in the investigation of non-UV detectable organic impurities in a drug substance, *J Pharm Biomed Anal* 17 (1998) 455-471

- [60] Chapter 2.2.43 Mass spectrometry in: European Pharmacopoeia 10.0, Council of Europe, Strasbourg, France, 2020
- [61] D. W. Koppenaal, C. J. Barinaga, M. B. Denton, R. P. Sperline, G. M. Hieftje, G. D. Schilling, F. J. Andrade, J. H. Barnes, MS Detectors, *Anal Chem* 77 (2005) 418A-427A
- [62] P. Kebarle, L. Tang, From ions in solution to ions in the gas phase-the mechanism of electrospray mass spectrometry, *Anal Chem* 65 (1993) 972A-986A
- [63] J. H. Gross, *Massenspektrometrie: Ein Lehrbuch*, 1st edition, Springer-Verlag GmbH, Heidelberg, Germany, 2013
- [64] A. E. Ashcroft, *Ionization methods in organic mass spectrometry*, Royal Society of Chemistry, London, United Kingdom, 1997
- [65] L. Konermann, E. Ahadi, A. D. Rodriguez, S. Vahidi, Unraveling the Mechanism of Electrospray Ionization, *Anal Chem* 85 (2013) 2-9.
- [66] K. Strupat, Molecular weight determination of peptides and proteins by ESI and MALDI, *Methods Enzymol* 405 (2005) 1-36
- [67] E. J. Finehout, K. H. Lee, An introduction to mass spectrometry applications in biological research, *Biochem Mol Biol Educ* 32 (2004) 93-100
- [68] B. O. Keller, J. Sui, A. B. Young, R. M. Whittal, Interferences and contaminants encountered in modern mass spectrometry, *Anal Chim Acta* 627 (2008) 71-81
- [69] C. Ghosh, C. P. Shinde, B. S. Chakraborty, Influence of ionization source design on matrix effects during LC-ESI-MS/MS analysis, *J Chromatogr B* 893 (2012) 193-200
- [70] P. Liigand, J. Liigand, K. Kaupmees, A. Kruve, 30 Years of Research on ESI/MS response: trends, contradictions and applications, *Anal Chim Acta* (2020) 238117
- [71] L. C. Herrera, J. S. Grossert, L. Ramaley, Quantitative aspects of and ionization mechanisms in positive-ion atmospheric pressure chemical ionization mass spectrometry, *J Am Soc Mass Spectrom* 19 (2008) 1926-1941
- [72] G. Hopfgartner, E. Varesio, V. Tschäppät, C. Grivet, E. Bourgoigne, L. A. Leuthold, Triple quadrupole linear ion trap mass spectrometer for the analysis of small molecules and macromolecules, *J Mass Spectrom* 39 (2004) 845-855
- [73] J. W. Hager, A new linear ion trap mass spectrometer, *Rapid Commun Mass Spectrom* 16 (2002) 512-526
- [74] J. N. Louris, R. G. Cooks, J. E. Syka, P. E. Kelley, G. C. Stafford, J. F. Todd, Instrumentation, applications, and energy deposition in quadrupole ion-trap tandem mass spectrometry, *Anal Chem* 59 (1987) 1677-1685
- [75] T. Kind, O. Fiehn, Advances in structure elucidation of small molecules using mass spectrometry, *Bioanal Rev* 2 (2010) 23-60
- [76] A. A. Doucette, R. A. Chisholm, Molecular-Formula Determination through Accurate-Mass Analysis: A Forensic Investigation, *J Chem Educ* 96 (2019) 1458-1464
- [77] F. Xian, C. L. Hendrickson, A. G. Marshall, High resolution mass spectrometry, *Anal Chem* 84 (2012) 708-719

- [78] G. L. Glish, D. J. Burinsky, Hybrid mass spectrometers for tandem mass spectrometry, *J Am Soc Mass Spectrom* 19 (2008) 161-172
- [79] Basic Definitions, in: M. Smoluch, G. Grasso, P. Suder, J. Silberring, *Mass Spectrometry: An Applied Approach*, 2nd edition, John Wiley & Sons, Inc., Hoboken, New Jersey, USA, 2019
- [80] R. W. Kondrat, G. A. McClusky, R. G. Cooks, Multiple reaction monitoring in mass spectrometry/mass spectrometry for direct analysis of complex mixtures, *Anal Chem* 50 (1978) 2017-2021
- [81] A. K. Yocum, A. M. Chinnaiyan, Current affairs in quantitative targeted proteomics: multiple reaction monitoring–mass spectrometry, *Brief Funct Genom Proteom* 8 (2009) 145-157
- [82] X. Zhu, Y. Chen, R. Subramanian, Comparison of Information-Dependent Acquisition, SWATH, and MSAll Techniques in Metabolite Identification Study Employing Ultrahigh-Performance Liquid Chromatography–Quadrupole Time-of-Flight Mass Spectrometry, *Anal Chem* 86 (2014) 1202-1209
- [83] M. Zedda, C. Zwiener, Is nontarget screening of emerging contaminants by LC-HRMS successful? A plea for compound libraries and computer tools, *Anal Bioanal Chem* 403 (2012) 2493-2502
- [84] F. Allen, A. Pon, M. Wilson, R. Greiner, D. Wishart, CFM-ID: a web server for annotation, spectrum prediction and metabolite identification from tandem mass spectra, *Nucleic Acids Res* 42 (2014) W94-W99
- [85] S. Dresen, M. Gergov, L. Politi, C. Halter, W. Weinmann, ESI-MS/MS library of 1,253 compounds for application in forensic and clinical toxicology, *Anal Bioanal Chem* 395 (2009) 2521-2526
- [86] T. Huan, C. Tang, R. Li, Y. Shi, G. Lin, L. Li, MyCompoundID MS/MS Search: Metabolite Identification Using a Library of Predicted Fragment-Ion-Spectra of 383,830 Possible Human Metabolites, *Anal Chem* 87 (2015) 10619-10626
- [87] S. Broecker, S. Herre, B. Wüst, J. Zweigenbaum, F. Pragst, Development and practical application of a library of CID accurate mass spectra of more than 2,500 toxic compounds for systematic toxicological analysis by LC–QTOF-MS with data-dependent acquisition, *Anal Bioanal Chem* 400 (2011) 101-117
- [88] A. Leistner, S. Haerling, J.-D. Kreher, I. Becker, D. Jung, U. Holzgrabe, Risk assessment report of potential impurities in cetirizine dihydrochloride, *J Pharm Biomed Anal* 189 (2020) 113425

2 Aims of the work

Different marketed APIs should be analyzed concerning new impurities. The occurrence of histamine in gentamicin sulfate 2016 prompted the question whether histamine was responsible for deaths in the 1990s after intravenous administration of the antibiotic in the USA. The aim was to quantify histamine in batches of gentamicin sulfate already analyzed in the context of the 1990s cases of death to determine whether the biogenic amine was the causative agent for the fatalities.

In 2020 the potential carcinogen 1-methyl-4-nitrosopiperazine (MeNP) was found as new impurity in medicinal products containing the antibiotic rifampicin. The contents of MeNP in rifampicin capsules purchased in Comoros, India, Nepal, and Tanzania were to be determined applying an already published LC-MS/HRMS method. Furthermore, the potential for the formation of nitrosamines upon the synthesis of rifampicin should be investigated.

Chemical reactions of APIs and excipients are a potential source of impurities in drug products. One example for such reactions is the formation of esters of the nonsteroidal anti-inflammatory drug naproxen and polyethylene glycol in soft capsule formulations. The influence of different parameters on the formation of such esters should be investigated by incubation of different formulations and quantification of naproxen-PEG-ester using an LC-UV method developed for this purpose.

In cooperation with *Arevipharma*, a comprehensive impurity profile of the API bisoprolol fumarate should be elaborated. Therefore, an LC-MS/HRMS method suitable for the untargeted search for unknown impurities should be developed. Based on the synthesis pathway of bisoprolol fumarate, *Arevipharma* created a reaction matrix to derive potential impurities of the API. The targeted search for these impurities should be combined with an untargeted analysis to detect all unknown impurities. The aim was to create an impurity profile as complete as possible by a combination of different chromatographic and mass spectrometric conditions. Moreover, a quantification of the impurities was intended.

3 Results

3.1 Analysis of Histamine and Sisomicin in Gentamicin: Search for the Causative Agents of Adverse Effects

Jonas Wohlfart, Ulrike Holzgrabe

Reprinted with Permission from

Archiv der Pharmazie 2021, e2100260

Abstract

In 1998, the aminoglycoside antibiotic gentamicin sulfate caused several cases of deaths in the United States, after the switch from twice- to once-daily application. Endotoxins were discussed as the cause for the adverse effects and sisomicin was identified as the lead impurity; batches containing sisomicin were contaminated with more impurities and were responsible for the fatalities. In 2016, anaphylactic reactions in horses, and later in humans with one fatality, were observed after application of gentamicin sulfate contaminated with histamine. To determine whether histamine was responsible for the 1990s death cases as well, histamine was quantified by means of liquid chromatography-tandem mass spectrometry (LC-MS/MS) in 30 samples of gentamicin sulfate analyzed in previous studies. Furthermore, a relative quantification of sisomicin was performed to check for a correlation between histamine and the lead impurity. A maximum amount of 11.52 ppm histamine was detected, which is below the limit for anaphylactic reactions of 16 ppm, and no correlation of the two impurities was observed. However, the European Medicines Agency recommends a stricter limit with regard to the maximum single dose of gentamicin sulfate to reach a greater gap between the maximum histamine exposition of 4.3 µg and the quantity known to cause hypotension of 7 µg. The low amounts of histamine and the fact that there is no connection with the contamination of sisomicin showed that histamine was not the cause for the death cases in the United States in 1998, and endotoxins remain the most probable explanation.

3.1.1 Introduction

The antibiotic gentamicin was first described in 1963 as a mixture of closely related aminoglycosides produced by *Micromonospora purpurea*. [1] The gentamicins C₁, C_{1a}, C₂, C_{2a}, and C_{2b} (Figure 1) are the main components and show similar antibacterial activities [2,3]. The sulfate salt of the broad-spectrum antibiotic is used in the treatment of severe infections with various Gram-negative and Gram-positive microorganisms like *Staphylococcus aureus*, *Klebsiella pneumoniae*, and *Acinetobacter pittii* [4]. The oral bioavailability of gentamicin is low because of its hydrophilic (logP = -3.1) and cationic character, with five basic nitrogen atoms in the pK_a range of 5.7-9.9 [5,6]. Hence, an intravenous or intramuscular application is necessary for systemic antibiotics [7]. Moreover, the topical application of gentamicin via (eye) ointments and eye drops is common in the therapy of local infections, often in combination with glucocorticoids [8,9]. Several resistance mechanisms like enzymatic drug modification (e.g., acetylation and phosphorylation), target modification (16S rRNA methylation), and efflux-mediated resistance have been described for aminoglycosides [10].

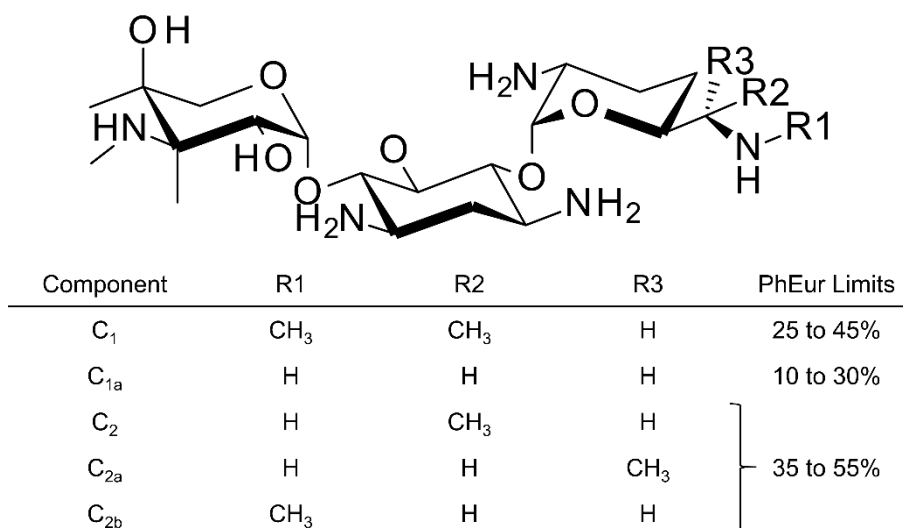


Figure 1 Main components of gentamicin and their limitations [2]

Like for other aminoglycosides, the most relevant adverse effects of gentamicin are ototoxicity and nephrotoxicity [11]. During the first years after its introduction, the market authorization holders stated twice- or thrice-daily dosing (every 8-12 h) [12]. In the 1990s, a lower nephrotoxicity was discussed for single daily dosing when compared to a multiple daily dosing regimen [13-15]. However, a distinct increase in deaths following severe endotoxin-like reactions was reported after a once-daily application of gentamicin sulfate in the United States [16], even though the endotoxin

concentrations of the affected batches were within the limits proposed by the US Food and Drug Administration. Perhaps, these limits were inappropriate as they considered multiple daily dosing. It was argued that higher peak concentrations of endotoxins were reached after application of a single, but higher dose of gentamicin sulfate when compared to multiple lower doses. As a result, the immunogenicity of the endotoxins exceeded tolerable limits and led to severe reactions [17]. Interestingly, an endotoxin contamination was never proven unequivocally as the root cause for the reported fatalities.

Following up these events, the Holzgrabe lab at the University of Würzburg developed several impurity profiling methods for gentamicin sulfate using capillary electrophoresis, micellar electrokinetic chromatography (MEKC), nuclear magnetic resonance spectroscopy, and multivariate analysis [18–23]. Batches containing the aminoglycoside sisomicin (4,5-dehydrogentamicin C_{1a}; Figure 2) could be related to the ones that had caused the deaths. Hence, sisomicin was recognized as a lead impurity: Batches containing sisomicin were contaminated with more impurities of a higher quantity. The assessed batches of gentamicin sulfate were divided into two major groups: a sisomicin-containing group responsible for the deaths and a sisomicin-free group without linkage to the adverse effects.

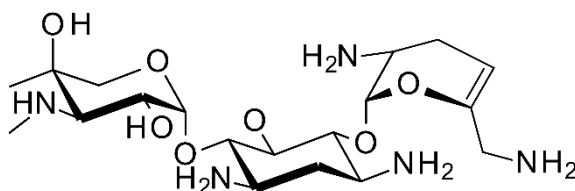


Figure 2 Sisomicin

In 2016, anaphylactic reactions including tachypnea, tachycardia, sweating, and shivering were reported owing to the application of gentamicin sulfate to horses. Later, humans were also affected, with one fatality reported. The reactions were caused by elevated levels of histamine in the drug substance, which occurred after the manufacturer had changed his supplier of fish peptone, a raw material required for the fermentative production of gentamicin. The levels of histamine produced with the new supplier's fish peptone were distinctly higher than those in the batches produced before, that is, about 100 ppm versus max. 12 ppm, because the new supplier had not stored the fish under suitable conditions [24]. Hence, microorganisms like *M. morganii* or *K. pneumoniae*, which grow during spoilage of fish, decarboxylated free histidine to

histamine [25]. Moreover, *M. purpurea*, which is used for the production of gentamicin, can produce histamine from histidine by its enzyme aromatic L-amino acid decarboxylase as well [26].

As a consequence, the manufacturer changed the supplier and the European Medicines Agency defined limits for histamine in both fish peptone and gentamicin sulfate, that is, 16 ppm, as no adverse reactions had been observed with batches complying with this limit [27]. After this, the General Monograph “Products of Fermentation” in the European Pharmacopoeia (PhEur) was revised. In earlier versions, the raw materials were required to be “of suitable quality for the intended purpose” [28]. Since the implementation of PhEur 9.6, the levels of free histidine in fish peptones must be considered to prevent the formation of histamine during fermentation processes [29]. Another revision, published in PhEur 10.4 and effective since 04/2021, states the following: “It must be demonstrated that the process or processes chosen reduce to a minimum or remove [...] histamine and other biogenic amines from fish and fishery products used in raw materials” [30].

In this study, histamine was quantified using liquid chromatography (LC) and mass spectrometric (MS) detection in 30 gentamicin batches that had been analyzed earlier in the context of the deaths in the United States. In addition, the lead impurity sisomicin was quantified by means of normalization to assess whether the contamination with sisomicin and its accompanying impurities, respectively, is linked to elevated contents of histamine. The aim of the work was to determine whether the deaths in the 1990s were caused by histamine instead of the hypothesized endotoxins.

3.1.2 Results and Discussion

3.1.2.1 Quantification of histamine in gentamicin sulfate

The quantification of histamine was performed according to a method provided by Sandoz Canada Inc. [31]. The 30 batches were analyzed using a hydrophilic interaction liquid chromatography (HILIC) column of unbound silica with a mixture of ammonium formate and acetonitrile (ACN) as the mobile phase and MS detection in multiple reaction monitoring (MRM) mode. Quantification was performed by external calibration (Figure 3) in the range of 1-250 ng/ml, equivalent to 0.2-50 ppm histamine. As described in the original method, a quadratic calibration curve was obtained, which is in line with previous reports on histamine quantification [32]. System suitability according to the original method requires a relative standard deviation of below 15%

at the calibration level of 100 ng/ml (20 ppm) and a recovery of 70-130% at the calibration level of 125 ng/ml (25 ppm) [31]. The relative standard deviation at 20 ppm was found to be 4.78% and the recovery at 25 ppm was 101.9% (± 3.8). Moreover, the recovery at the calibrator below the 16 ppm limit, that is, 10 ppm, was determined to be 107.8% ($\pm 6.3\%$).

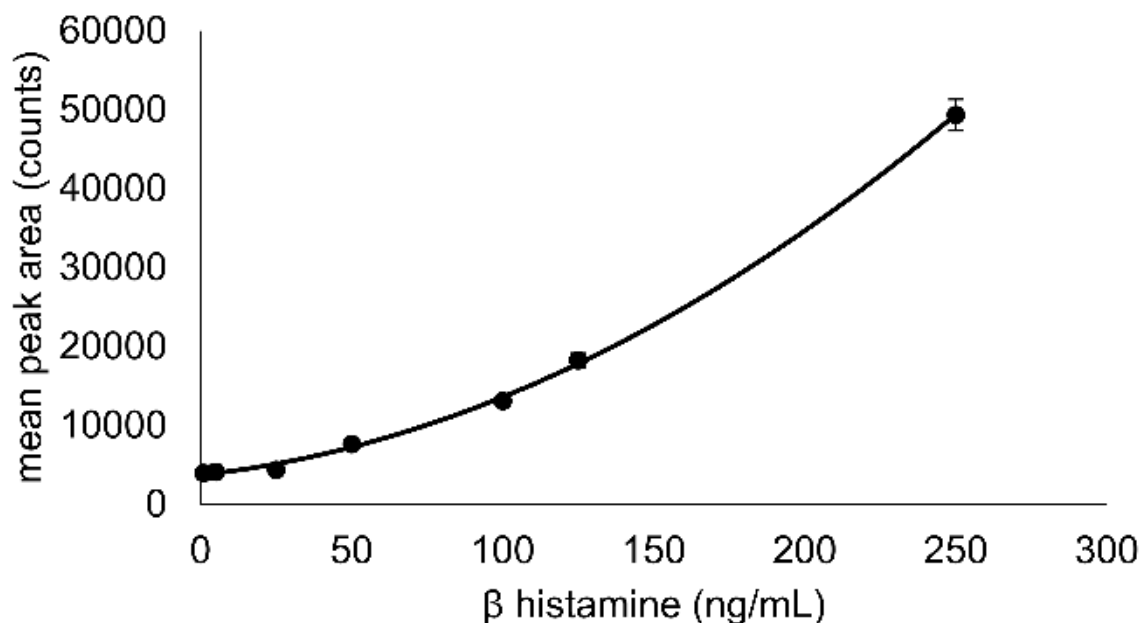


Figure 3 External calibration for histamine by quadratic regression ($n = 3, \pm 1$ SD, $y = 0.5591x^2 + 43.1342x + 3675.9810; R^2 = .9993$)

The content of histamine could be quantified in 6 of the 30 tested samples and ranged from 3.4 to 11.5 ppm (Table 1). All other batches showed contamination with histamine, but at a level below the quantification limit of 0.2 ppm. Exemplary chromatograms of G22 (11.5 ppm) and G24 (≤ 0.2 ppm) are shown in Figure 4. The neutral loss of ammonia, represented by the transition of m/z 112 \rightarrow 95, was the most favored fragmentation reaction of histamine and yielded higher peak areas than the formation of the imidazolyl radical (m/z 112 \rightarrow 68; Figure 5). The detection limit of the more sensitive transition (m/z 112 \rightarrow 95) is lower than 0.25 ng/ml, equivalent to 0.05 ppm (signal-to-noise ratio, 12.9 ± 2.1).

Table 1 Content of histamine and assignment to groups defined in previous studies of gentamicin sulfate

Sample	Histamine (ppm)	Sisomicin
G02	≤ 0.2	-
G04	≤ 0.2	-
G05	≤ 0.2	X
G06	≤ 0.2	-
G07	≤ 0.2	-
G08	≤ 0.2	-
G09	≤ 0.2	-
G10	≤ 0.2	-
G11	3.4	-
G12	≤ 0.2	X
G13	≤ 0.2	-
G14	≤ 0.2	X
G15	≤ 0.2	-
G16	≤ 0.2	X
G18	≤ 0.2	X
G20	≤ 0.2	X
G21	≤ 0.2	X
G22	11.5	X
G23	≤ 0.2	-
G24	≤ 0.2	-
G25	≤ 0.2	X
G26	≤ 0.2	X
G27	8.9	-
M1	3.9	n/a
M2	≤ 0.2	X
M3	≤ 0.2	-
M4	≤ 0.2	-
M5	8.7	X
M6	7.8	X
M7	≤ 0.2	-

Abbreviations: n/a, assignment to documentation ambiguous, X, sisomicin-containing group, -, sisomicin-free group.

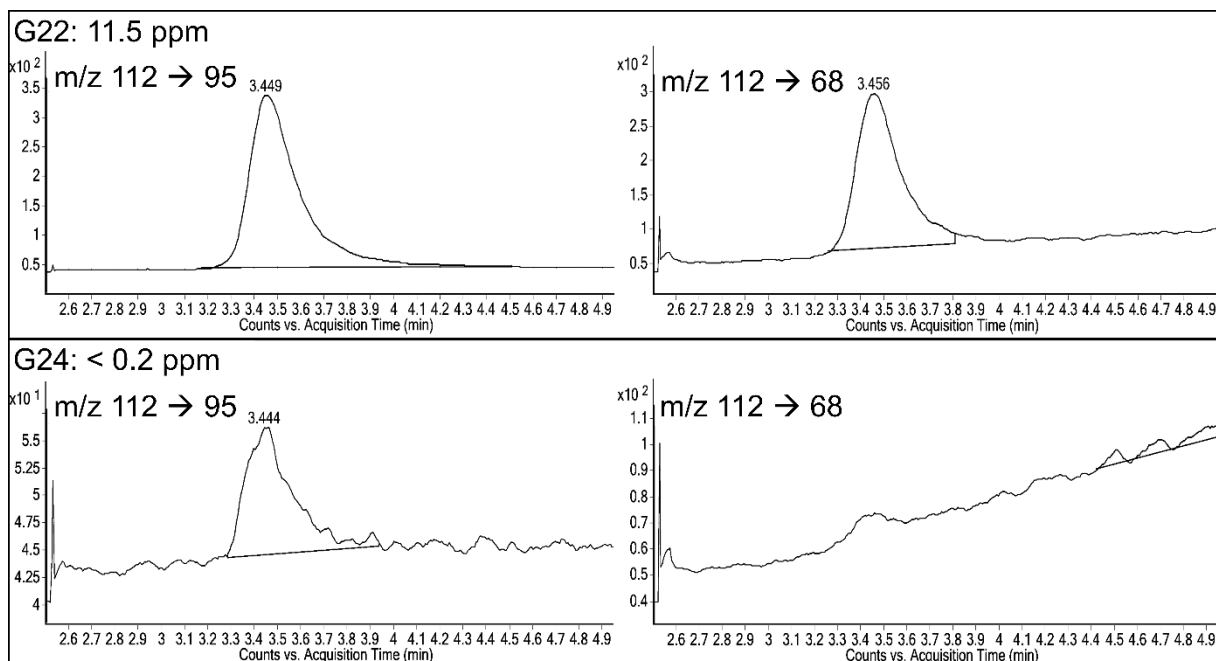


Figure 4 Characteristic extracted ion chromatograms for m/z 112→95 and m/z 112→68 of two gentamicin samples: G22, which is contaminated with 11.5 ppm histamine, and G24, which shows a peak below the quantification limit (like all samples with histamine contents below 0.2 ppm)

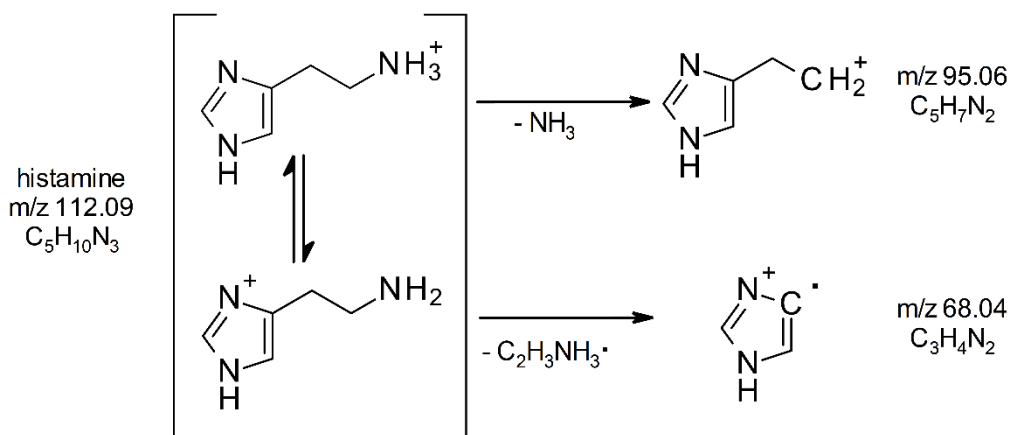


Figure 5 Fragmentation reactions of histamine monitored for quantification

3.1.2.2 Contamination with the lead impurity sisomicin

To check the correlation of the contamination with histamine and sisomicin, a relative quantification of sisomicin was performed. A HILIC (zwitterionic) method for the chromatographic separation of aminoglycosides suitable for MS detection was applied with slight modifications [33]. A quantification by means of normalization is appropriate in this case as the analytes' structures (cf. Figures 1 and 2) are closely related and thus are conjectured to show very similar ionization efficiencies [34]. Samples G02,

G05, G11, G22, and M5 were selected for the measurements considering their histamine content and presumed sisomicin contamination according to the documentation (cf. Table 1).

As reported in previous studies, the analyzed gentamicin samples could be divided into two groups: one contaminated with sisomicin and one showing significantly lower amounts of the lead impurity (Figure 6). As expected, elevated levels of the lead impurity occurred in the batches reported to contain sisomicin and many other impurities, in concordance with previous studies (MEKC) [21]. G05 contained sisomicin, but no histamine, and G11 vice versa. G22 and M5 contained both contaminants. Taken together, there is no link between the occurrence of histamine and sisomicin.

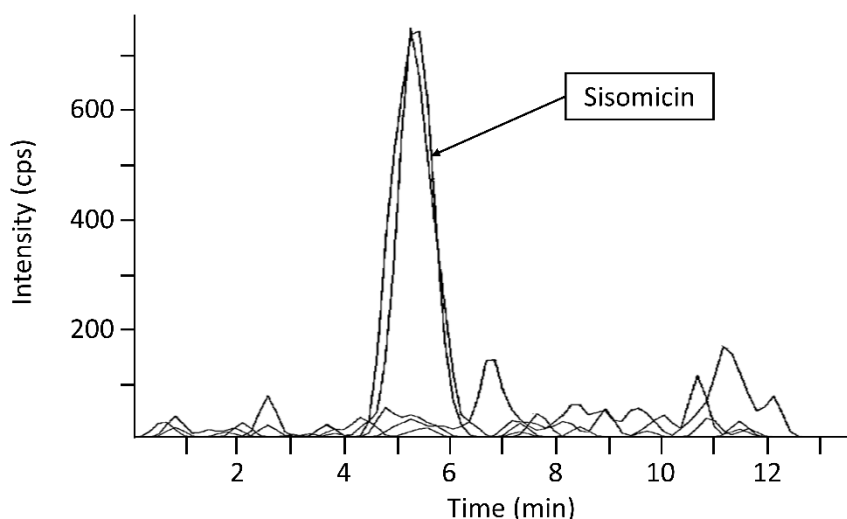


Figure 6 Overlay of exemplary extracted ion chromatograms of the sisomicin-containing group and the sisomicin-free group

3.1.3 Conclusion

Two main conclusions can be drawn from our studies with regard to the “old” batches: Since the concentrations of maximal 11.5 ppm of histamine detected are below the limit of 16 ppm, the occurrence of anaphylactic reactions upon application of these batches is unlikely. However, the limit of 16 ppm, which refers to the maximum single dose of 160 mg of gentamicin, results in a maximum intake of 4.3 μg of histamine and is regarded “not sufficiently below the quantity of histamine which is known to cause hypotension (7 μg)” [24]. Thus, a stricter limit is recommended to ensure the absence of anaphylactic reactions. The fact that the content of sisomicin in the batches is not

related to the histamine contamination strengthens the conclusion that histamine was not the causative agent of the deaths in the United States in 1998.

The occurrence of histamine in gentamicin sulfate illustrates the relevance of raw material quality in the production of drug substances. The change in the General Monograph “Products of Fermentation” of the PhEur was implemented to prevent the emergence of histamine in the drugs affected by the monograph by controlling the contamination of the raw material with free histidine and is now even more rigid, requiring suitable purification processes regarding biogenic amines from fishery products [29,30]. The fish peptone already contained histamine instead of its amino acid precursor [27], which shows that testing for histidine alone could be insufficient. Instead, control of both free histidine and histamine is necessary to consequently ensure appropriate quality of fish peptones. Moreover, similar events with other biogenic amines like serotonin and noradrenaline might be possible if the respective amino acids tryptophan and tyrosine were present in a fermentation broth together with bacteria capable of amino acid decarboxylation and hydroxylation. Especially with intravenous application, serious adverse events like the serotonin syndrome, elevated blood pressure, and tachycardia could result [35,36]. Thus, raw materials and bacterial strains must be selected considering possible degradation products of biomolecules.

3.1.4 Experimental

3.1.4.1 Materials and instrumentation

The quantification of histamine was performed using a modular Agilent 1200 LC system, equipped with an online degasser, a binary pump, and a column oven (Agilent Technologies). A Kinetex HILIC 50 × 2.1 mm, 2.6 μm, 100 Å (Phenomenex) column was used. The system was coupled to an Agilent 6460 TripleQuad LC/MS using electrospray ionization (ESI).

For the relative quantification of sisomicin, a modular Agilent 1100 LC system, equipped with an online degasser, a binary pump, and a diode array detector, was used with a VDSpher PUR 100 HILICZ, 150 × 2.1 mm, 5 μm (VDS optilab) column. The system was coupled to an Agilent LC/MSD Trap SL equipped with an ESI source.

Thirty samples (Table 1) of gentamicin sulfate provided by the Federal Institute of Drugs and Medical Devices for previous works were reused for this study. Histamine dihydrochloride as well as MS grade ACN and water were purchased from Sigma-

Aldrich. Ultrapure water was produced by a water purification system from Merck Millipore.

3.1.4.2 Quantification of histamine

Chromatographic separation was performed using a HILIC column of unbound silica (Kinetex HILIC). Mobile phase A was aqueous 25 mM ammonium formate and mobile phase B was a mixture of mobile phase A and ACN (30 + 70). The LC gradient and flow were adapted to the dimensions of the HILIC column used [37]. The gradient started with 100% B, which was decreased to 25% within 6 min. The system was cleaned and re-equilibrated by flushing the column with 100% B for 9 min. The flow rate was set to 0.2 ml/min and was directed to the mass spectrometer between 2.5 and 5 min (retention time of histamine: 3.5 min). The injection volume was set to 1 μ l. The ESI parameters were applied according to the original method (gas temperature, 350 °C; gas flow, 10 l/min; nebulizer, 40 psi; sheath gas temperature, 400 °C; sheath gas flow, 11 l/min; voltage, 5000 V; fragmentor, 135; collision energy, 25 V). Tandem MS (MS/MS) data were acquired in MRM mode. The neutral losses of ammonia (m/z 112 \rightarrow 95) and an aminoethyl radical (m/z 112 \rightarrow 68) were monitored (Figure 5). The sum of the peak areas in the extracted ion chromatograms (XIC) of both transitions was used for the quantification by means of a quadratic regression model.

10.35 mg of histamine dihydrochloride was weighed and dissolved in 25 ml of 0.01 M HCl (β = 414 μ g/ml equivalent to 250 μ g/ml of the free base). Seven standard solutions in the range of 1–250 ng/ml were prepared by dilution of the stock solution for the external calibration. The solutions were injected in triplicate in the order of increasing concentration.

For sample preparation, 25.0 mg of each sample was weighed and dissolved in 5.0 ml of 0.01 M HCl to reach a concentration of 5 mg/ml gentamicin sulfate. The solutions were transferred to chromatographic vials and analyzed using the method stated above.

3.1.4.3 Analysis of the lead impurity sisomicin

A published method suitable for the chromatographic separation of aminoglycosides using HILIC with a zwitterionic stationary phase (VDSpher PUR 100 HILIC-Z) was applied with slight modifications [33]. Mobile phase A consisted of 5 M ammonium acetate + 0.2% formic acid in a mixture of 5% water and 95% ACN. Mobile phase B contained the same buffer salts in 95% water and 5% ACN. After an isocratic step of

2.7 min at 100% B, mobile phase B was decreased to 10% within 2.2 min and held for 6.1 min to clean the column thoroughly. The system was re-equilibrated by flushing the column for 3 min with the start conditions. The injection volume was set to 5 μ l, and the flow rate was 0.8 ml/min. The ESI and MS/MS parameters were set considering the LC flow rate: dry temperature, 350 °C; nebulizer, 70 psi; dry gas, 12 l/min, skimmer, 40 V; and fragmentation amplitude, 0.6. The $[M+H]^+$ species for the main components of gentamicin (C_1 m/z 478, C_{1a} m/z 450, $C_2/C_{2a}/C_{2b}$ m/z 464) and sisomicin (m/z 448) were isolated and fragmented. The evaluation was performed based on the XICs for the most abundant fragment ion of m/z 322 for all aminoglycosides, which emerges upon cleavage of a glycosidic bond (neutral loss of the amino sugar purpurosamine bearing R1–R3, displayed on the right side in Figure 1).

Five gentamicin samples were selected considering their histamine contamination (see Section 3.1.2.1) and their characteristics based on the documentation of previous works of the Holzgrabe lab [18–22]. Solutions with a concentration of 100 μ g/ml of the gentamicin sulfate samples were created by dissolving 10 mg in 100.0 ml of a mixture of mobile phases A and B (3 + 8) and injected in triplicate.

Acknowledgements

The authors thank the Federal Institute of Drugs and Medical Devices (Bonn, Germany) for providing the samples of gentamicin sulfate and for helpful information. Open Access funding enabled and organized by Projekt DEAL.

Conflicts of interests

The authors declare that there are no conflicts of interests.

Author contributions

Jonas Wohlfart: Methodology, formal analysis, investigation, writing – original draft.

Ulrike Holzgrabe: Conceptualization, writing – review and editing, supervision, project administration.

3.1.5 References

- [1] M. J. Weinstein, G. M. Luedemann, E. M. Oden, G. H. Wagman, J. P. Rosselet, J. A. Marquez, C. T. Coniglio, W. Charney, H. L. Herzog, J. Black, *J. Med. Chem.* **1963** 6 463. DOI: 10.1021/jm00340a034
- [2] *European Pharmacopoeia 10.0*, Council of Europe, Strasbourg, France **2020**, Monograph: Gentamicin Sulfate
- [3] M. J. Weinstein, G. H. Wagman, E. M. Oden, J. A. Marquez, *J. Bacteriol.* **1967** 94, 789. DOI:10.1128/jb.94.3.789-790.1967
- [4] Hexal AG, Fachinformation: Gentamicin 40 HEXAL® SF, 40 mg/1 ml Inj.lsg., https://www.hexal.biz/praeparate/dokumente/fi/2019_08_gentahxsfinj_fi-1564031231.pdf, **2018** (accessed 29 June 2021)
- [5] National Center for Biotechnology Information, Gentamicin, <https://pubchem.ncbi.nlm.nih.gov/compound/3467>, **2020** (accessed 15 February 2021)
- [6] U. Holzgrabe, G. Scriba in *Kommentar zum Europäischen Arzneibuch*, (Eds: F. Bracher, P. Heisig, P. Langguth, E. Mutschler, G. Rücker, T. Schirmeister, G. Scriba, E. Stahl-Biskup, R. Troschütz), Wissenschaftliche Verlagsgesellschaft mbH **2016** Stuttgart, Germany
- [7] H. Lüllmann, K. Mohr, M. Wehling, L. Hein in *Pharmakologie und Toxikologie*, Georg Thieme Verlag KG, Stuttgart, Germany **2016**, chapter 25.1.2
- [8] Organon Healthcare GmbH, Fachinformation (Zusammenfassung der Merkmale der Arzneimittel) Diprogenta Creme/Salbe, <https://www.fachinfo.de/suche/fi/001757>, **2018** (accessed 29 June 2021)
- [9] Ursapharm Arzneimittel GmbH, Fachinformation Dexta-Gentamicin Kombipackung, <https://www.fachinfo.de/suche/fi/003724>, **2014** (accessed 29 June 2021)
- [10] K. M. Krause, A. W. Serio, T. R. Kane, L. E. Connolly, *Cold. Spring. Harb. Perspect. Med.* **2016** 6. DOI: 10.1101/cshperspect.a027029
- [11] A. Forge, J. Schacht, *Audiol. Neurotol.* **2000** 5, 3. DOI: 10.1159/000013861
- [12] J. A. Krieger, L. Duncan, *N. Engl. J. Med.* **1999** 340, 1122. DOI: 10.1056/nejm199904083401417
- [13] M. Z. Ali, M. B. Goetz, *Clin. Infect. Dis.* **1997** 24, 796. DOI: 10.1093/clinids/24.5.796
- [14] T. C. Bailey, J. R. Little, B. Littenberg, R. M. Reichley, W. C. Dunagan, *Clin. Infect. Dis.* **1997** 24, 786. DOI: 10.1093/clinids/24.5.786
- [15] J. M. Prins, H. R. Buller, P. Speelman, E. Kuijper, R. Tange, *The Lancet* **1993** 341, 335. DOI: 0.1016/0140-6736(93)90137-6
- [16] C. Peterson, N. Bendaaa, M. Veza, L. Mascola, R. Murthy, C. Pegues, E. Fontanilla, R. Shane, M. Kwong, R. Deamer, W. Schwarz, D. Pon, B. Young, M. Glick, K. Gibbs, C. Plata, R. Harder, M. Zellers, N. Boghossian,

- T. Breschini, S. Chang, K. Heinzmann, J. Rosenberg, S. Waterman, *Morb. Mortal. Wkly* **1998** 47, 877.
- [17] M. A. West, W. Heagy, *Crit. Care Med.* **2002** 30, 64.
- [18] R. Deubner, U. Holzgrabe, *J. Pharm. Biomed. Anal.* **2004** 35, 459. DOI: 10.1016/j.jpba.2004.01.015
- [19] U. Holzgrabe, S. Laug, F. Wienen in: *Capillary Electrophoresis* (Ed: P. Schmitt-Kopplin), Springer-Verlag GmbH, Heidelberg, Germany **2008**, chapter 30.
- [20] K.-D. Kühn, C. Weber, S. Kreis, U. Holzgrabe, *J. Pharm. Biomed. Anal.* **2008** 48, 612. DOI: 10.1016/j.jpba.2008.05.041
- [21] F. Wienen, U. Holzgrabe, *Electrophoresis* **2003** 24, 2948. DOI: 10.1002/elps.200305529
- [22] W. Winter, R. Deubner, U. Holzgrabe, *J. Pharm. Biomed. Anal.* **2005** 38, 833. DOI: 10.1016/j.jpba.2005.01.051
- [23] F. Wienen, R. Deubner, U. Holzgrabe, *Pharmeuropa* **2003** 15, 273.
- [24] European Medicines Agency, CHMP Assessment report Procedure no: EMEA/H/A-5(3)/1468 INN/active substance: gentamicin (solution for infusion/solution for injection), https://www.ema.europa.eu/en/documents/referral/assessment-report-article-53-procedure-gentamicin_en.pdf, **2018** (accessed 08 July 2021).
- [25] S. L. Taylor, J. E. Stratton, J. A. Nordlee, *J. Toxicol.: Clin. Toxic.* **1989** 27, 225. DOI: 10.3109/15563658908994420
- [26] The UniProt Consortium, *Nucl. Acids. Res.* **2019** 47, 506. DOI: 10.1093/nar/gky1049
- [27] Fujian Fukang Pharmaceutical Co., Ltd, Investigation Report of Adverse Effects of Gentamicin Sulfate **2017**
- [28] *European Pharmacopoeia* 8.0, Council of Europe, Strasbourg, France **2014**, General Monograph: Products of Fermentation
- [29] *European Pharmacopoeia* 9.6, Council of Europe, Strasbourg, France **2019**, General Monograph: Products of Fermentation
- [30] *European Pharmacopoeia* 10.4, Council of Europe, Strasbourg, France **2021**, General Monograph: Products of Fermentation
- [31] Sandoz Canada Inc., Determination of Residual Histamine in Gentamicin by LC-MS/MS, unpublished data, provided by Federal Institute of Drugs and Medical Devices, Bonn, Germany **2017**
- [32] S. Millán, M. Carmen Sampedro, N. Unceta, M. Aranzazu Goicolea, R. J. Barrio, *Anal. Chim. Acta* **2007** 584, 145. DOI: 10.1016/j.aca.2006.10.042
- [33] R. Oertel, V. Neumeister, W. Kirch, *J. Chromatogr. A.* **2004** 1058, 197. DOI: 10.1016/j.chroma.2004.08.158
- [34] K. R. Chalcraft, R. Lee, C. Mills, P. Britz-McKibbin, *Anal. Chem.* **2009** 81, 2506. DOI: 10.1021/ac802272u
- [35] E. Sampson, J. Warner, *Br. J. Gen. Pract.* **1999** 49, 867.

- [36] H. Lüllmann, K. Mohr, M. Wehling, L. Hein in *Pharmakologie und Toxikologie*, Georg Thieme Verlag KG, Stuttgart, Germany **2016**, chapter 10.3.1
- [37] D. Guillarme, D. Nguyen, S. Rudaz, J. L. Veuthey, *Eur. J. Pharm. Biopharm.* **2008** 68, 430. DOI: 10.1016/j.ejpb.2007.06.018

3.2 The nitrosamine contamination of drugs, part 3: Quantification of 4-Methyl-1-nitrosopiperazine in rifampicin capsules by LC-MS/HRMS

Jonas Wohlfart, Oliver Scherf-Clavel, Martina Kinzig, Fritz Sörgel, Ulrike Holzgrabe

Reprinted with Permission from

Journal of Pharmaceutical and Biomedical Analysis 203 (2021) 114205

Abstract

Upon emergence of nitrosamines in various drugs, e.g. in valsartan, metformin and ranitidine, 4-methyl-1-nitrosopiperazine (MeNP) was found in rifampicin in August 2020. Rifampicin is used, amongst others, for post-exposure prophylaxis of leprosy. The occurrence of MeNP can be explained by the synthesis, because 1-amino-4-methylpiperazine is concomitantly used with the organic oxidizing reagent isoamyl nitrite. According to a method reported by the FDA, the quantification of MeNP in rifampicin capsules was performed by LC–MS/HRMS. A significant contamination with MeNP was found in all samples, ranging from 0.7 to 5.1 ppm, and exceeding the acceptable intake limit proposed by the FDA up to 32-fold. However, the severity of a possible leprosy infection outweighs the risks, which are concomitant with the intake of a single dose of rifampicin for post-exposure prophylaxis. Nevertheless, the extent of contamination is alarming, and countermeasures are needed to minimize public health risks. The presence of nitrosamines in rifampicin illustrates the need for better strategies in impurity profiling and compendial testing once again.

3.2.1 Introduction

The semi-synthetic antibiotic rifampicin was first introduced in Italy in 1968 and shortly afterwards in many other countries worldwide [1]. It is mainly used for the treatment and prevention of tuberculosis and other infectious diseases, e.g. leprosy, in combination with other antimycobacterial substances [2]. Physicians in service of international non-governmental organizations use rifampicin as single doses of 600 mg (adults), 450 mg (adolescents) and 300 mg (children) for post-exposure prophylaxis of leprosy in healthy individuals who have had close contact to leprosy patients.

Since the detection of N-nitrosodimethylamine in valsartan containing drugs in 2018 [3,4], nitrosamine impurities have been subject of intensive investigations. Hence, similar nitrosamines were found in various other sartans [5], but also in other drugs, e.g. ranitidine [6]. In August 2020, the US Food and Drug Administration (FDA) became aware of the nitrosamine contamination of the antimycobacterial drugs rifampicin and rifapentine, which are part of the *World Health Organization Model List of Essential Medicines* [7]. Depending on the substituents of the piperazine moiety, 4-methyl-1-nitrosopiperazine (MeNP, Fig. 1) was found in rifampicin, while 4-cyclopentyl-1-nitrosopiperazine (CPNP) was detected in rifapentine [8].

The occurrence of MeNP can be explained by the production pathway. The synthesis of rifampicin requires a fermentation product of *Amycolatopsis mediterranei*, i.e. rifamycin B, which is converted to rifamycin S or rifamycin SV in ventilated, aqueous solutions [9]. The following reaction with formaldehyde and a lower alkyl-, cycloalkyl-, carboxyalkyl- or hydroxyalkylamine [10] gives Mannich bases of rifamycin SV (see Fig. 1). Any of these Mannich bases is oxidized by means of a weak oxidizing agent like alkyl nitrites (isoamyl nitrite) or lead tetraacetate to form 3-formyl rifamycin SV. Eventually, the conversion with 1-amino-4-methylpiperazine (AMP) yields rifampicin [11]. The potential of the formation of MeNP is high for two reasons: 1) Alkyl nitrites can hydrolyze to free nitrites [12], which can react with AMP to MeNP [13]. 2) Hydrazine derivatives like AMP can be oxidized to nitrosamines by aerial oxygen, also forming MeNP [14]. The current monograph of rifampicin in the European Pharmacopoeia (PhEur)10th edition states two related substances, being the oxidation products quinone and N-oxide of rifampicin [15]. Additionally, the compendial monograph requires testing of the pH value, drying loss and sulfated ash, but does not consider side-products such as nitrosamines.

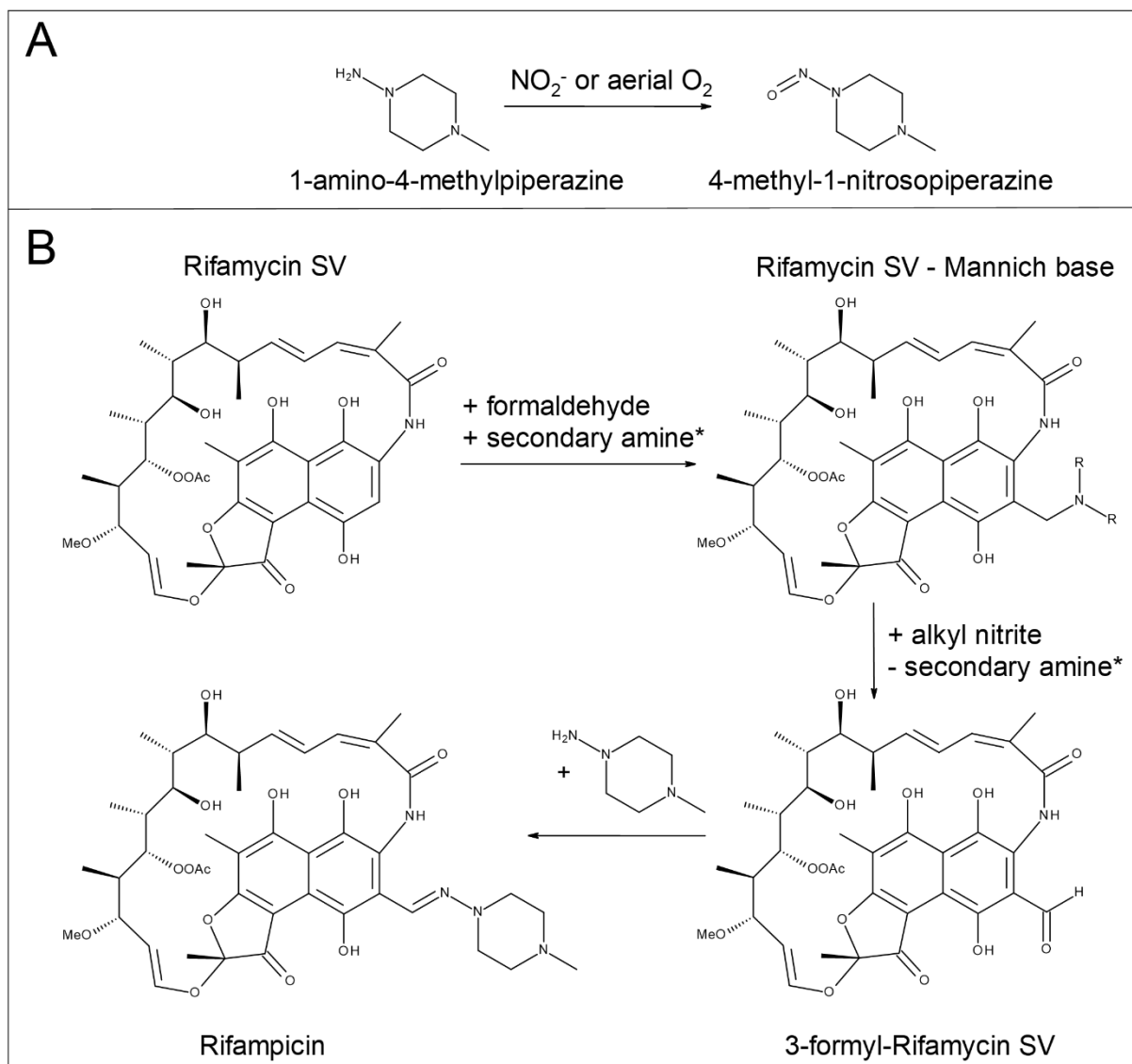


Figure 1 Formation of 4-methyl-1-nitrosopiperazine from 1-amino-4-methylpiperazine (A) during the synthesis of rifampicin: Mannich reaction of rifamycin SV, subsequent oxidation (e.g. alkyl nitrite) and reaction with 1-amino-4-methylpiperazine (B)
*lower alkyl, cycloalkyl-, or hydroxyalkylamine.

Like other nitrosamines, MeNP is considered of being potentially carcinogenic [16]. In consequence, acceptable intake limits of 0.16 ppm and 0.10 ppm were stated by the FDA for MeNP and CPNP, respectively [8]. However, batches showing amounts below 5 ppm MeNP and 20 ppm CPNP were not generally withdrawn from the market but are subject to case-by-case decisions in order to prevent shortages of such important, lifesaving drugs. The FDA published a method for the identification and quantification of MeNP and CPNP in drug substance and drug product based on LC-ESI-MS/HRMS [17]. In this study, 15 rifampicin-containing medicinal products of four different

manufacturers were analyzed regarding their possible contamination with MeNP using the FDA-method with minor modifications.

3.2.2 Experimental

3.2.2.1 **Materials and instrumentation**

The medicinal products were purchased on local markets (Brazil, Comoros, India, Nepal & Tanzania) and contained rifampicin in doses of 150–600 mg (Table S1). MeNP (95 % m/m) was purchased from Enamine (Kiev, Ukraine). MS-grade methanol (MeOH), water, ammonium formate and ammonia solution (25 % m/V) were purchased from Sigma-Aldrich (Taufkirchen, Germany).

Chromatography was performed on an Agilent Infinity II system (Waldbronn, Germany) consisting of a quaternary pump, a thermostatted autosampler and a thermostatted column compartment. An InfinityLab Poroshell 120 PhenylHexyl (2.7 μm , 4.6 x 100 mm) column was used for chromatographic separation (Agilent, Waldbronn, Germany). The LC-system was coupled to a Sciex X500R QTOF mass spectrometer (Concord, Ontario, Canada) equipped with a Turbo VTM Ion Source (ESI). Automatic calibration of the mass spectrometer was performed using the provided tuning solution for ESI (Sciex, Concord, Ontario, Canada).

For sample preparation, a Fisher Scientific vortex mixer (Schwerte, Germany), a Heidolph overhead shaker (Schwabach, Germany) and a Beckman Coulter centrifuge (Krefeld, Germany) were used. Sample filtration was performed using Rotilabo (PVDF, 0,22 μm , \varnothing 13 mm) syringe filters (Roth, Karlsruhe, Germany).

3.2.2.2 **Sample preparation**

For each analysis, a single capsule was opened and suspended in a defined volume of MeOH (150 mg: 5. mL, 300–600 mg: 10.0 mL). Subsequently, the samples were vortexed for 60 s and shaken for 40 min using the overhead shaker at 100 rpm. After centrifugation for 15 min at 3000 rpm (2095 x g) the supernatant was filtered into vials, discarding the first milliliter. If necessary, the samples were diluted with MeOH to reach a final concentration of 30 mg/mL rifampicin. Three capsules per batch and blank samples (MeOH without rifampicin capsule) were prepared.

3.2.2.3 **Preparation of standard solutions**

10 mg MeNP (95% m/m) were weighed and dissolved in 100.0 mL MeOH to reach a concentration of 100 $\mu\text{g/mL}$. This stock solution was diluted (100 μL ad 100.0 mL in

volumetric flask) with MeOH to obtain a stock standard preparation (SSP) with a concentration of 100 ng/mL. The working standard preparation (WSP) with a concentration of 3 ng/mL was created by dilution of the SSP (750 μ L ad 25.0 mL in volumetric flask) with MeOH.

Three sets of five or six solutions were prepared by dilution of SSP and the stock solution to cover the range of concentrations detected in the samples (50–200 ng/mL, 5–30 ng/mL, 10–150 ng/mL). These were used for linear regression models replacing the one-point calibration required by the FDA-method.

3.2.2.4 LC-ESI-MS/HRMS

Mobile phase A was an aqueous buffer of 10 mM ammonium formate (pH 9.00), adjusted with ammonia solution (25% m/V), while mobile phase B was MeOH. The gradient, which was adapted to the dimensions of the used column [18], started with 40% of mobile phase B for 6 min. The ratio of mobile phase B was raised to 100% over 8.5 min and held for 6.5 min. For re-equilibration the column was flushed with 40% B for 7 min. The flow rate was set to 0.5 mL/min and was directed to the mass spectrometer between 2 and 5 min (retention time of MeNP: 3.4 min). The injection volume was 3 μ L.

The parameters for the MS/HRMS experiment were optimized by flow-injection using positive polarity (Gas1: 60 psi, Gas2: 55 psi, Curtain gas: 20 psi, Ionspray voltage: 4000 V, Temperature: 650 °C, Declustering potential: 40 V, Collision energy: 10 V).

WSP was injected six-fold for one-point calibration and for checking the system suitability at the beginning of each injection sequence and additionally every six samples. The solutions for linear regression were injected in duplicate in order of rising concentration. Automatic calibration of the mass spectrometer was performed every five injections.

3.2.3 Results and discussion

The content of the nitrosamine MeNP was determined by the LC–MS/HRMS method. As described by the FDA-method, the reaction of the $[M+H]^+$ of MeNP (m/z 130.1) to its most intense fragment (neutral loss of $NO\cdot$) with m/z 100.0995 (\pm 0.0037 Da) was monitored (see Fig. 2). Typical extracted ion chromatograms of m/z 100.0995 \pm 0.0037 Da are shown in Fig. 3.

Results – The nitrosamine contamination of drugs, part 3: Quantification of 4-Methyl-1-nitrosopiperazine in rifampicin capsules by LC-MS/HRMS

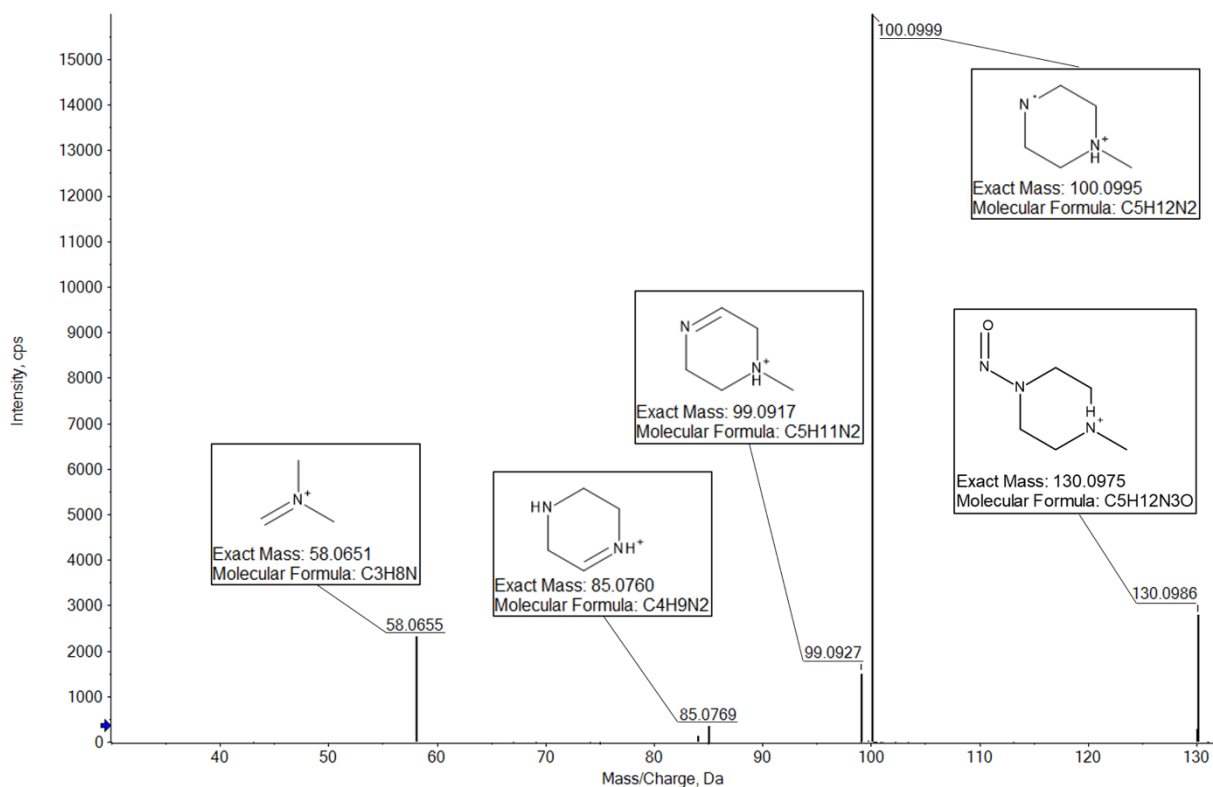


Figure 2 MS/HRMS spectrum of MeNP and assignment of fragments.

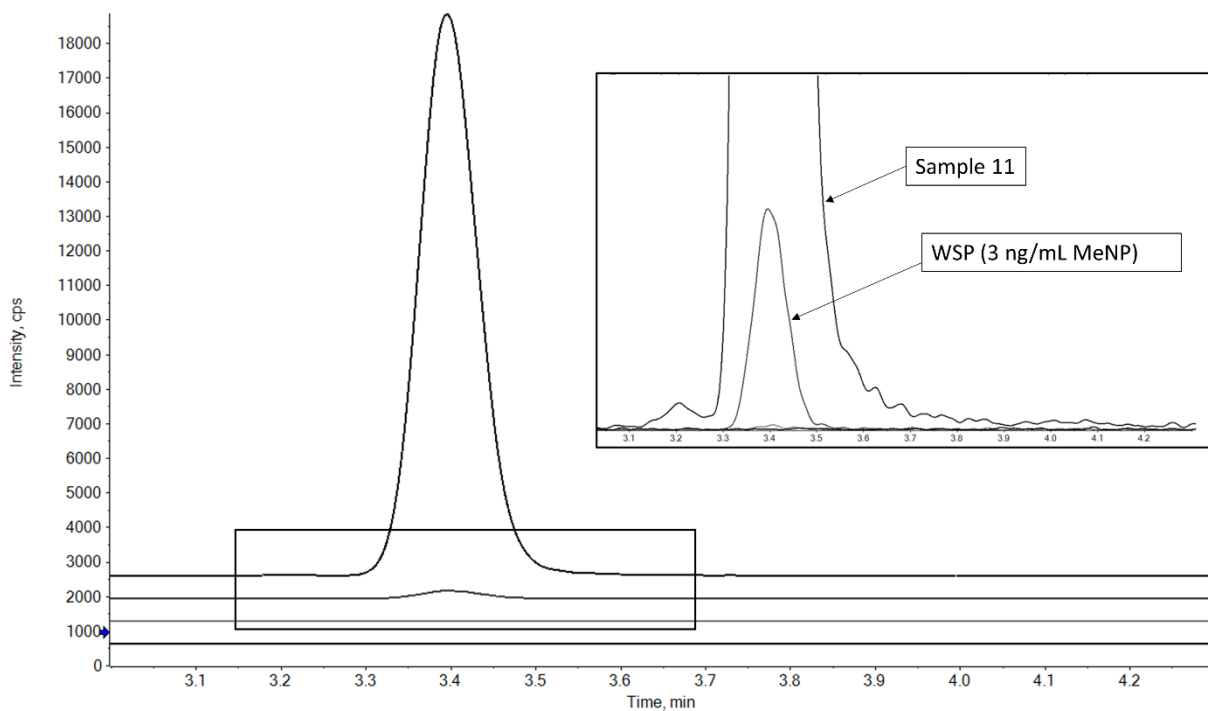


Figure 3 Extracted ion chromatograms of m/z 100.0995 \pm 0.0037 Da, top to bottom: RICIN 300 mg, WSP (3 ng/mL), blank sample (MeOH prepared like samples) and blank injection (MeOH)

3.2.3.1 System suitability and external calibration

The system suitability test, as demanded by the FDA-method, requires relative standard deviations of lower than 10% for the first six injections of WSP and lower than 15% for all injections of WSP. The samples were analyzed in three sequences due to different arrival times. The measured relative standard deviations fulfil the requirements in all sequences: 4.35%, 4.85% and 9.95% (first six injections) and 6.71%, 7.65% and 14.9% (all injections), respectively. The calibration curves and residual plots proved suitability of a linear regression model for the quantification of MeNP (Fig. S1). The calibration functions were as follows: $y = 600.4x - 12426.1$ (50-200 ng/mL, $R^2 = 0.994$), $y = 740.1x - 913.3$ (5-30 ng/mL, $R^2 = 0.996$) and $y = 225.7x - 1356.2$ (10-150 ng/mL, $R^2 = 0.990$) with $y =$ peak area in counts and $x =$ MeNP concentration in ng/mL.

3.2.3.2 MeNP contamination of rifampicin samples

All samples showed a relevant contamination with MeNP, ranging from 0.7 to 5.1 ppm, equivalent to 22-152 ng/mL (Fig. 4).

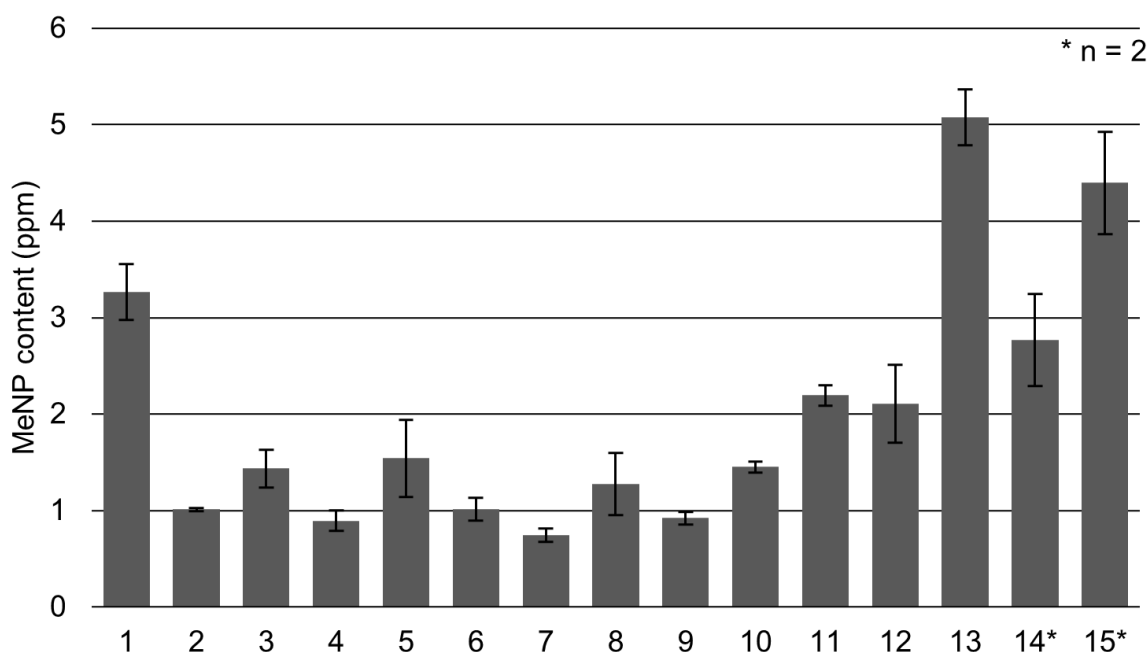


Figure 4 Content of MeNP in rifampicin capsules ($n = 3$, ± 1 sdv).

First, the evaluation was performed by means of one-point calibration as described in the FDA-method. Applying this calibration, the MeNP concentration of sample 13 was found to be 7.7 ± 0.5 ppm and thus, exceeded the indicated linearity range of 0.017-6.67 ppm (equivalent to 0.5-200 ng/mL) of the original method. Hence, an external

calibration by linear regression was performed to quantify MeNP correctly. Here, the MeNP concentration was found to be 5.1 ± 0.3 ppm (equivalent to 152.4 ± 8.8 ng/mL), thus falling in the range of linearity of the original method. This indicates that one-point calibration led to an overestimation of the MeNP concentration, which can be explained by the great difference between the peak areas of MeNP in the rifampicin samples and WSP (see Fig. 3). In addition, the linear range of the QTOF mass spectrometer and its ion source may differ from the linear range of the system described in the FDA-method which makes use of a hybrid quadrupole-Orbitrap instrument. In consequence, all samples were evaluated using linear regression models.

Two additional modifications of the described method were performed due to differing equipment: the use of an overhead shaker instead of a mechanical wrist action shaker and centrifugation for 15 min at 3000 rpm (2095 x g) instead of 10 min at 4000 rpm (relative centrifugal force not given in method description). However, these modifications are not expected to reduce the overall method's robustness, accuracy, or sensitivity.

The content of MeNP in sample 13 exceeds the acceptable intake limit of 0.16 ppm by far (32-fold). Moreover, the upper limit for a case-by-case decision of 5 ppm is exceeded slightly. Also, all other samples exceed the acceptable intake limit, but show levels of below 5 ppm MeNP. The risk-benefit balance needs to be assessed carefully for all samples. The risk of an avoidable leprosy infection must be weighed against the risks concomitant with the intake of a drug contaminated with nitrosamines. Regarding the severity of a possible leprosy infection, the nitrosamine intake of a single dose of rifampicin is considered negligible and might be acceptable in the opinion of the regulatory authorities [19].

The samples were produced by four different manufacturers. The MeNP contents show clear differences. Whereas the manufacturers M1 and M3 have delivered rifampicin batches with a low MeNP content in average, rifampicin of manufacturers M2 and M4 contain very high amounts, which even pass the content allowed. As the production methods and precise conditions are not known to public – they are only described in the drug master files – a reliable explanation for the difference cannot be given. The use of different synthetic routes, raw materials and purification processes influences the concentration of nitrosamines in the products. Yet, it might not be feasible to produce rifampicin entirely free of MeNP, as the important reactant AMP can be

oxidized to MeNP easily [14]. This illustrates the importance of effective purification processes and compendial testing of the drug substance.

3.2.3.3 Regulatory considerations

The occurrence of nitrosamines in rifampicin shows that the compendial monograph of the PhEur 10th edition is not suitable to guarantee the safety of the tested drug substance [15]. Monographs in the European Pharmacopoeia usually consider impurities related with a single synthesis route of the drug substance and hence control only the impurities related to this specific procedure. In particular, the monograph includes the test for related substances of rifampicin (HPLC-UV, $\lambda = 254$ nm), covering the oxidation products rifampicin quinone and rifampicin N-oxide, as well as testing of pH-value, loss on drying and sulfated ash. Here, the synthesis route considered in the monograph development might not have shown potential to form MeNP or this potential was not considered and thus, not recognized. Thus, it is necessary to improve the synthesis assessment, e.g. by detailed reaction matrices [20]. Yet, it might be impossible to develop a complete impurity profile based solely on the synthesis procedure. Hence, the combination of targeted analytics for expected impurities and untargeted approaches based on highly sensitive mass spectrometric detection (*MS/MS^{ALL}, general unknown comparative screening*) could complement conventional strategies of impurity profiling and increase the safety of medicines [21].

The contamination with nitrosamines was only discovered due to the search for nitrosamines in various drugs as a consequence of the 2018 valsartan scandal. Hence, it is necessary to implement specific tests for MeNP in rifampicin or to extend the just published monograph “N-nitrosamines in active substances” (PhEur chapter 2.5.46) for the MeNP quantification [22].

3.2.4 Conclusion

In general, the parameters of methods intended for the application in different laboratories and thus, different equipment, should be easily transferable and robust. Even though the system suitability requirements were met in this work, correct quantification of MeNP was not possible with the intended one-point calibration, but only with linear regression. Furthermore, the centrifugation parameters of the original method are stated in rpm. They should be given as relative centrifugal force (RCF), which is also favored by PhEur, to ensure an easy transfer of the method to laboratories with different equipment [23].

The detection of MeNP and CPNP in rifampicin and rifapentine, respectively, shows that the follow-up of the valsartan scandal is still going on. It illustrates that a thorough and comprehensive search for nitrosamine impurities is necessary and might be the only way to detect these potential carcinogens in other drugs as well.

CRedit authorship contribution statement

Jonas Wohlfart: Methodology, Formal analysis, Investigation, Writing - original draft.

Oliver Scherf-Clavel: Writing - review & editing, Supervision. **Martina Kinzig:**

Resources, Writing - review & editing, Supervision. **Fritz Sörgel:** Resources, Writing -

review & editing, Supervision. **Ulrike Holzgrabe:** Conceptualization, Writing- review &

editing, Supervision, Project administration.

Declaration of Competing Interest

The authors report no declarations of interest.

Acknowledgements

We thank AB Sciex (Concord, Ontario, Canada) and IBMP (Heroldsberg, Germany) for the possibility to use the LC-MS system.

3.2.5 References

- [1] P. Sensi, History of the Development of Rifampin, *Rev. Infect Dis* 5 (1983) 402-406.
- [2] Rifampin Uses, Side Effects & Warnings. Drugs.com, 2020 (accessed: 4th January 2021) <https://www.drugs.com/mtm/rifampin.html>.
- [3] Valsartan: chargenbezogener Rückruf valsartanhaltiger Arzneimittel, deren Wirkstoff von dem chinesischen Hersteller Zhejiang Huahai Pharmaceutical produziert wurde. Bundesinstitut für Arzneimittel und Medizinprodukte, 2018 (accessed: 4th January 2021) <https://www.bfarm.de/SharedDocs/Pressemitteilungen/DE/2018/pm5-2018.html>.
- [4] F. Sörgel, M. Kinzig, M. Abdel-Tawab, C. Bidmon, A. Schreiber, S. Ermel, J. Wohlfart, A. Besa, O. Scherf-Clavel, U. Holzgrabe, The contamination of valsartan and other sartans, part 1: New findings, *J Pharm Biomed Anal* 172 (2019) 395-405
- [5] FDA Updates and Press Announcements on Angiotensin II Receptor Blocker (ARB) Recalls. U.S. Food & Drug Administration, 2018 (accessed: 4th January 2021) <https://www.fda.gov/drugs/drug-safety-and-availability/fda-updates-and-press-announcements-angiotensin-ii-receptor-blocker-arb-recalls-valsartan-losartan>.
- [6] FDA Updates and Press Announcements on NDMA in Zantac (ranitidine). U.S. Food & Drug Administration, 2020 (accessed: 4th January 2021) <https://www.fda.gov/drugs/drug-safety-and-availability/fda-updates-and-press-announcements-ndma-zantac-ranitidine#:~:text=Glenmark%20Pharmaceutical%20Inc.,FDA%20has%20advised%20companies%20to%20recall%20their%20ranitidine%20if%20testing,conduct%20their%20own%20laboratory%20testing>.
- [7] World Health Organization Model List of Essential Medicines, World Health Organization, 2019, 21st List.
- [8] FDA works to mitigate shortages of rifampin and rifapentine after manufacturers find nitrosamine impurities. U.S. Food & Drug Administration, 2020 (accessed: 11th December 2020) <https://www.fda.gov/drugs/drug-safety-and-availability/fda-works-mitigate-shortages-rifampin-and-rifapentine-after-manufacturers-find-nitrosamine>.
- [9] K. Hartke, H. Hartke, M. Wichtl, Rifamycin-Na, Kommentar zum Europäischen Arzneibuch 54 (2016).
- [10] N. Maggi, P. Sensi, Mannich Bases of Rifamycin SV, US3349082, USA, 1967.
- [11] N. Maggi, P. Sensi, Derivatives of Rifamycin SV, US3342810A, USA, 1964.
- [12] P. García-Santos, E. Calle, S. González-Mancebo, J. Casado, Kinetics of the aminolysis and hydrolysis of alkyl nitrites: Evidence for an orbital controlled mechanism, *Chem Mon* 127 (1996) 997-1003.
- [13] L. A. Carpino, Synthesis and Oxidation of 2-Amino-2,3-dihydro-1H-benz[de]isoquinoline and 1,2,3,4-Tetrahydronaphtho[1,8-de][1,2]diazepine and Related Cyclic 1,2-Dibenzylhydrazines, *J Am Chem Soc* 85 (1963) 2144-2149.
- [14] G. Lunn, E. B. Sansone, A.W. Andrews, Aerial oxidation of hydrazines to nitrosamines, *Environ Mol Mutagen* 17 (1991) 59-62.

- [15] Rifampicin, European Directorate for the Quality of Medicines & HealthCare, European Pharmacopoeia 10.0, 2021.
- [16] 1-methyl-4-nitrosopiperazine, European Chemicals Agency, 2020, Notified Classification and labelling according to CLP criteria.
- [17] LC-ESI-HRMS Method for the Determination of MNP in Rifampin and CPNP in Rifapentine Drug Substance and Drug Product, U.S. Food & Drug Administration, 2020 (accessed: 4th January 2021), <https://www.fda.gov/media/142092/download>.
- [18] D. Guillarme, D. Nguyen, S. Rudaz, J.L. Veuthey, Method transfer for fast liquid chromatography in pharmaceutical analysis: Application to short columns packed with small particle. Part II: Gradient experiments, *Eur J Pharm Biopharm* 68 (2008) 430-440.
- [19] Interim advice on the use of rifampicin for post-exposure prophylaxis (PEP), in light of recent information on nitrosamine impurities in rifampicin, ILEP International Federation of Anti-Leprosy Associations, 2020 (accessed: 7th April 2021) <https://ilepfederation.org/interim-advice-on-the-use-of-rifampicin-for-post-exposure-prophylaxis-peg-in-light-of-recent-information-on-nitrosamine-impurities-in-rifampicin/>.
- [20] A. Leistner, S. Haerling, J. Kreher, I. Becker, D. Jung, U. Holzgrabe, Risk assessment report of potential impurities in cetirizine dihydrochloride, *J Pharm Biomed Anal* 189 (2020) 113425.
- [21] O. Scherf-Clavel, M. Kinzig, A. Besa, A. Schreiber, C. Bidmon, M. Abdel-Tawab, J. Wohlfart, F. Sörgel, U. Holzgrabe, The contamination of valsartan and other sartans, Part 2: Untargeted screening reveals contamination with amides additionally to known nitrosamine impurities, *J Pharm Biomed Analysis* 172 (2019) 278-284.
- [22] Ph.Eur. Commission adopts a new general chapter for the analysis of N-nitrosamine impurities, European Directorate for the Quality of Medicines & HealthCare, 2020 (accessed: 22nd January 2021) <https://www.edqm.eu/en/news/ph-eur-commission-adopts-new-general-chapter-analysis-n-nitrosamine-impurities>.
- [23] General notices, European Directorate for the Quality of Medicines & HealthCare, European Pharmacopoeia 10.0, 2021.

3.2.6 Supplementary Information

Table S1 Overview of analyzed medicinal products

Sample	Medicinal Product	Manufacturer	Batch	Expiry date
1	R-Cin 150 mg	M1: Aurangabad, India	A901562	02/2021
2	R-Cin 300 mg		A902392	04/2021
3	R-Cin 300 mg		A904729	08/2021
4	R-Cin 300 mg		A906202	11/2021
5	R-Cin 450 mg		A001154	02/2022
6	R-Cin 450 mg		A904772	08/2021
7	R-Cin 600 mg		A902151	04/2021
8	R-Cin 600 mg		A903128	05/2021
9	R-Cin 600 mg		A904941	08/2021
10	R-Cin 300 mg		A002155	03/2022
11	R-Cin 450 mg		A001759	03/2022
12	R-Cin 600 mg		A001523	03/2022
13	RICIN 300 mg	M2: Bangkok, Thailand	181040	09/2021
14	LQFEx Rifampicina 300 mg	M3: Brazil	200725	07/2022
15	Rifampicin 300 mg	M4: Mumbai, India	ERE42001B	12/2021

Results – The nitrosamine contamination of drugs, part 3: Quantification of 4-Methyl-1-nitrosopiperazine in rifampicin capsules by LC-MS/HRMS

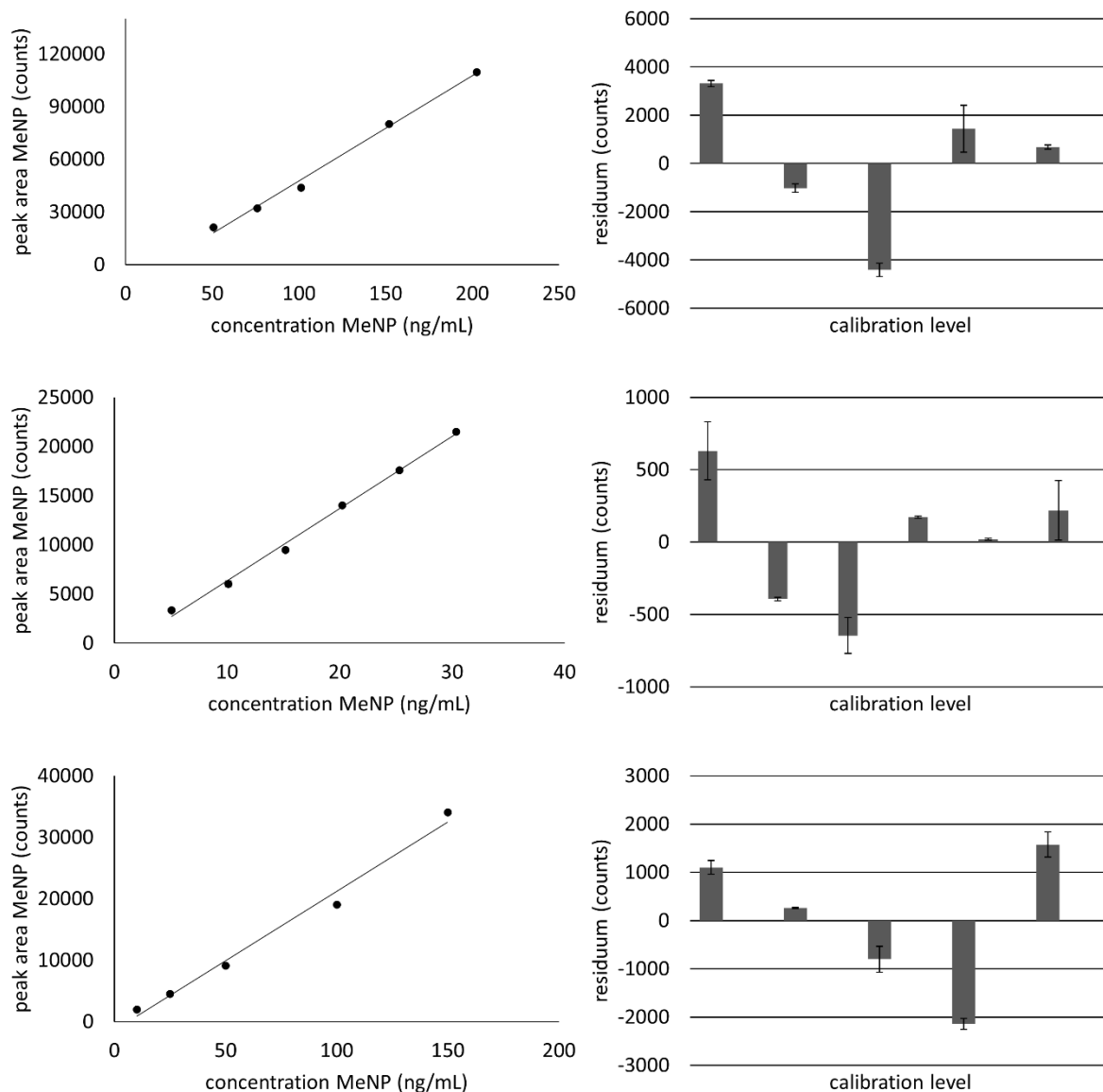


Figure S1 calibration curves and residual plots
top: $y = 600.4x - 12426.1$ ($R^2 = 0.994$), middle: $y = 733.6x - 994.2$ ($R^2 = 0.996$),
down: $y = 225.7x - 1356.2$ ($R^2 = 0.990$)

3.3 Analysis of Naproxen-PEG-Esters in Soft Gel Capsule Formulations

Jonas Wohlfart, Ulrike Holzgrabe

Unpublished Manuscript

3.3.1 Introduction

The nonsteroidal anti-inflammatory drug (NSAID) naproxen (Figure 1) is used in the therapy of inflammation- and pain-associated diseases, like acute and chronic osteoarthritis, rheumatoid arthritis, injuries, and dysmenorrhoea [1-3]. Both the free acid and the sodium salt are marketed in different formulations e.g. tablets, soft gel capsules, and suspensions [4-6].

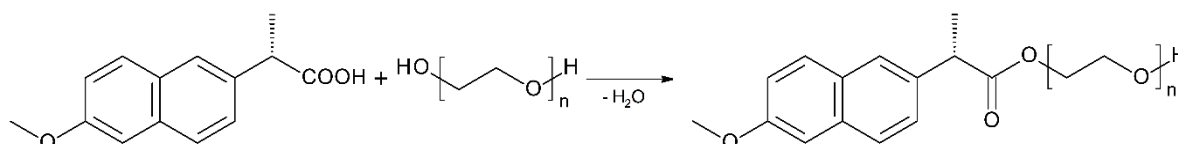


Figure 1 Esterification reaction of naproxen and PEG 600 (n = 10-14)

There are various classes of impurities in medicinal products like by-products of the synthesis of the active pharmaceutical ingredient (API), degradation products of the API, reaction products of the API with excipients and impurities thereof, etc., which are covered by respective guidelines published by the *International Council for Harmonisation of Technical Requirements for Pharmaceuticals for Human Use* (ICH) [7-9]. Several classes of excipients are known to hold the potential of contamination with reactive impurities, e.g. peroxides in polyethylene glycols (PEG) and their derivatives and reducing sugars in carbohydrates [10]. These impurities can lead to degradation of the API and to the formation of new impurities, which add to the API's impurity profile. Furthermore, reactions of APIs with excipients can occur when certain functional groups are present in the formulation. For example, the formation of esters from APIs containing carboxylic acid groups and excipients with free alcohol groups has been described for cetirizine and sorbitol/glycerol [11]. Other examples are the Maillard reaction of APIs with amine groups and reducing sugars, e.g. gabapentin and lactose [12], and Michael additions for APIs with amines and excipients containing Michael systems, e.g. sitagliptin and fumaric acid [13].

The formulation of marketed soft gel capsules containing the API naproxen (or naproxen sodium) and the excipient PEG 600 incorporates reactants for the formation

of ester impurities due to the potential incompatibility of the carboxylic acid of the API and the alcoholic group(s) of PEG 600 (Figure 1) [14]. In this work, naproxen-PEG-ester was synthesized as reference material for the development of a liquid chromatography (LC) method with UV detection. This method was applied in the analysis of stressed soft gel capsule formulations to determine the influence of the drug load, pH, and the water content on the formation of naproxen-PEG-esters (NPEG).

3.3.2 Experimental

3.3.2.1 **Materials and Instrumentation**

Naproxen, naproxen sodium, PEG 600, L(+)-lactic acid, NaOH 50% (m/V) for HPLC, potassium dihydrogen phosphate and acetonitrile (ACN) for HPLC (gradient grade) were purchased from Sigma-Aldrich (Taufkirchen, Germany) and phosphoric acid (85% m/V) from VWR (Darmstadt, Germany). The reagents required for synthesis and characterization of the synthesized impurity, i.e. dichloromethane, methanol, methanol-d₄, N,N-dimethylpyridin-4-amine, and 3-[[[(ethylimino)methylidene]amino]-N,N-dimethylpropan-1-amine hydrochloride were obtained from the University of Würzburg chemicals supply.

¹H and ¹³C nuclear magnetic resonance spectroscopy (NMR) was performed using a Bruker Avance III 400 MHz UltraShield spectrometer (Bruker Corporation, Billerica, Massachusetts, USA). LC-MS was performed on a Shimadzu LCMS-2020 Single Quadrupole system (Shimadzu, Duisburg, Germany) operated with a Synergy Fusion-RP column (4 μm, 80 Å, 4.6 x 150 mm, Phenomenex, Aschaffenburg, Germany).

The samples were prepared using an IKA RCT basic heated magnetic stirrer (Staufen, Germany) and a Metrohm pH-Meter 744 (Herisau, Switzerland), and thermally stressed in a Heraeus 6030 oven (Hanau, Germany).

Analysis of the samples was performed on an Agilent 1200 modular LC system equipped with quaternary pump, degasser, thermostatted column compartment and variable wavelength UV detector (Agilent Technologies, Waldbronn, Germany), operated with a DeactiSil ODS-3 (5 μm, 100 Å, 4.6 x 250 mm) column (ES Industries, West Berlin, New Jersey, USA).

3.3.2.2 **Synthesis of naproxen-PEG-ester**

250 mg of naproxen were dissolved in 25 mL of dichloromethane. 53 mg of N,N-dimethylpyridin-4-amine, 291 mg of 3-[[[(ethylimino)methylidene]amino]-N,N-

dimethylpropan-1-amine hydrochloride, and 2 g of PEG 600 were added under ice-cooling. The cool mixture was stirred for 10 min and for 4 h at room temperature. The product was purified by column chromatography (dichloromethane/methanol 9/1 v/v).

The product was characterized by NMR and LC-UV-MS. ^1H and ^{13}C NMR spectra were acquired from a solution of 10 mg/mL NPEG in methanol- d_4 . The LC-UV-MS analysis was performed applying a mobile phase of 0.1% (v/v) formic acid in water (A) and methanol (B). The gradient started with 5% B, which was raised to 90% within 8 min and held for 5 min. The injection volume was 20 μl and the eluent flow was 1 mL/min. The spectrophotometer wavelength was set to 254 nm and the mass spectrometer was operated with electrospray ionization in positive mode. The purity of the product was determined by peak area normalization.

3.3.2.3 Preparation of formulations

All formulations consisted of PEG 600, naproxen sodium, lactic acid, and water. An overview of the compositions is displayed in Table 1.

Table 1 Overview of prepared soft gel capsule formulations

Formulation	A	B	C	D	E	F	G
naproxen sodium (g)	7.10	5.46	5.51	5.52	5.52	5.68	5.73
PEG 600 (g)	15.06	17.28	15.91	17.36	17.74	17.81	18.01
lactic acid (g)	1.52	1.19	1.97	1.19	1.19	1.22	1.23
molar ratio lactic acid/naproxen	0.60	0.61	1.00	0.60	0.60	0.60	0.60
water (g)	1.30	1.05	1.68	1.04	0.52	0.26	0.13
% drug load (m/m)	26.0	20.0	20.1	20.1	20.2	20.8	20.8

The required amount of PEG 600 was weighed into a polypropylene tube and heated to 60 °C. While stirring, naproxen sodium and lactic acid were added, respectively. Finally, water was added, and the suspensions were stirred at 60 °C until the system was clear (maximal 3 h). After cooling to room temperature and centrifugation (10 min at 4000 rpm), five aliquots of each 25 mg of the supernatant were weighed and dissolved in 10.0 mL of a mixture of mobile phase A and B (30/70 v/v) and analyzed by means of LC-UV (see section 2.4). Subsequently, the formulations were stressed at 60 °C for 7 d. Samples of the supernatant were prepared and analyzed as described

above. If a precipitate was present, 25 mg (n = 5) were weighed after centrifugation and decantation, and analyzed accordingly.

3.3.2.4 Determination of naproxen-PEG-ester amounts

Mobile phase A was composed of a 20 mM phosphate buffer, adjusted to pH 3 with potassium dihydrogen phosphate and phosphoric acid, and mobile phase B was ACN. The gradient started with 40% B, which was raised to 50% within 20 min and held for 5 min. Re-equilibration was achieved by flushing the column with the starting conditions for 4 min. The flow was set to 1.5 mL/min and the injection volume was 25 µL. After every sample injection, 3 x 100 µL of isopropyl alcohol were injected. Blank runs were performed every 5 sample injections.

UV detection was performed at 272 nm and the amount of NPEG was determined by peak area normalization. Five samples of every formulation (cf. Table 1, formulation A-G) were analyzed.

3.3.3 Results and Discussion

Different naproxen soft gel capsule formulations were prepared and thermally stressed (7 d at 60 °C) to determine influences on the formation of NPEG. The samples were analyzed by an LC-UV method and NPEG was quantified by means of peak area normalization. The LC-UV system required rinsing of the injector after every sample injection. This is due to the high viscosity of PEG 600. To guarantee the absence of peaks in blank injections, 3 x 100 µL of isopropyl alcohol were injected after every sample injection to clean the injector.

All samples were analyzed before applying the stress conditions to show the absence of NPEG in the native formulations. The respective chromatograms did not show a peak for NPEG in any formulation. Thus, the influences discussed in the following are due to the stress test conditions only. The results of samples A and B were compared to determine the influence of the drug load on the formation of NPEG. The impact of the lactic acid concentration was investigated by comparison of sample B with sample C. Formulations D-G were studied to determine the influence of the water concentration and contained 4.1%, 2.1%, 1.0% and 0.5% of water, respectively (cf. Table 1).

3.3.3.1 Characterization of the synthesized naproxen-PEG-ester

A summary of the characteristics is given in Table 2. The ^1H and ^{13}C NMR spectra of the synthesized NPEG (Figure 2) were referenced to the solvent signal, and are displayed in Figure 3 and Figure 4, respectively [14].

Table 2 Characteristics of the synthesized NPEG

Visual appearance	Brownish, pasty solid
Molecular formula	$\text{C}_{14}\text{H}_{13}\text{O}_3(\text{C}_2\text{H}_4\text{O})_n\text{H}$ ($n = 10-14$)
Molecular weight	670.8-847.0 g/mol
Reaction control	$R_f = 0.61$ (silica gel, dichloromethane:MeOH 9:1)
Purity	97%
^1H NMR (CD_3OD , δ [ppm], J [Hz])	7.73-7.12 (6H, m, $\text{C}^3\text{-H}$), 4.20 (2H, t, $^3J = 4.6$, $\text{C}^5\text{-H}_2$), 3.88 (4H, s, $\text{C}^7\text{-H}_3$, q, $^3J = 7.0$, $\text{C}^8\text{-H}$), 3.58 (50H, m, $\text{C}^4\text{-H}_{2n}$), 1.53 (3H, d, $^3J = 7.2$, $\text{C}^9\text{-H}$)
^{13}C NMR (CD_3OD , δ [ppm])	174.7 (C^1), 157.8 (C^2), 135.8-105.4 (9C^3), 70.2 (C^4), 63.9 (C^5), 60.9 (C^6), 54.5 (C^7), 45.2 (C^8), 17.7 (C^9)

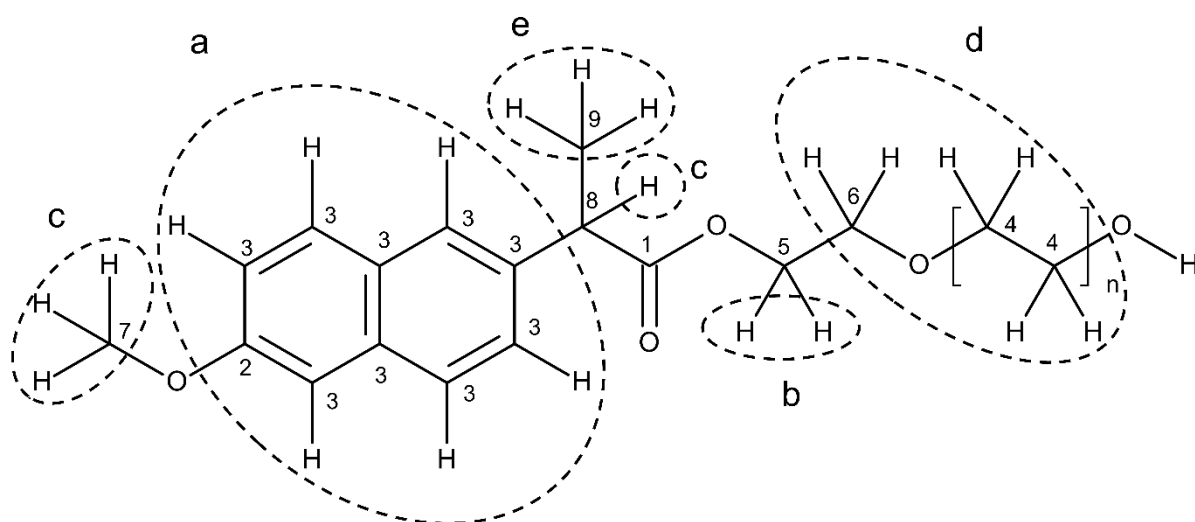


Figure 2 Structure of NPEG ($n = 10-14$) and assignment of atoms to signals in ^1H (letters) and ^{13}C NMR (numbers) (cf. Figures 3 and 4, respectively) [15, 16]

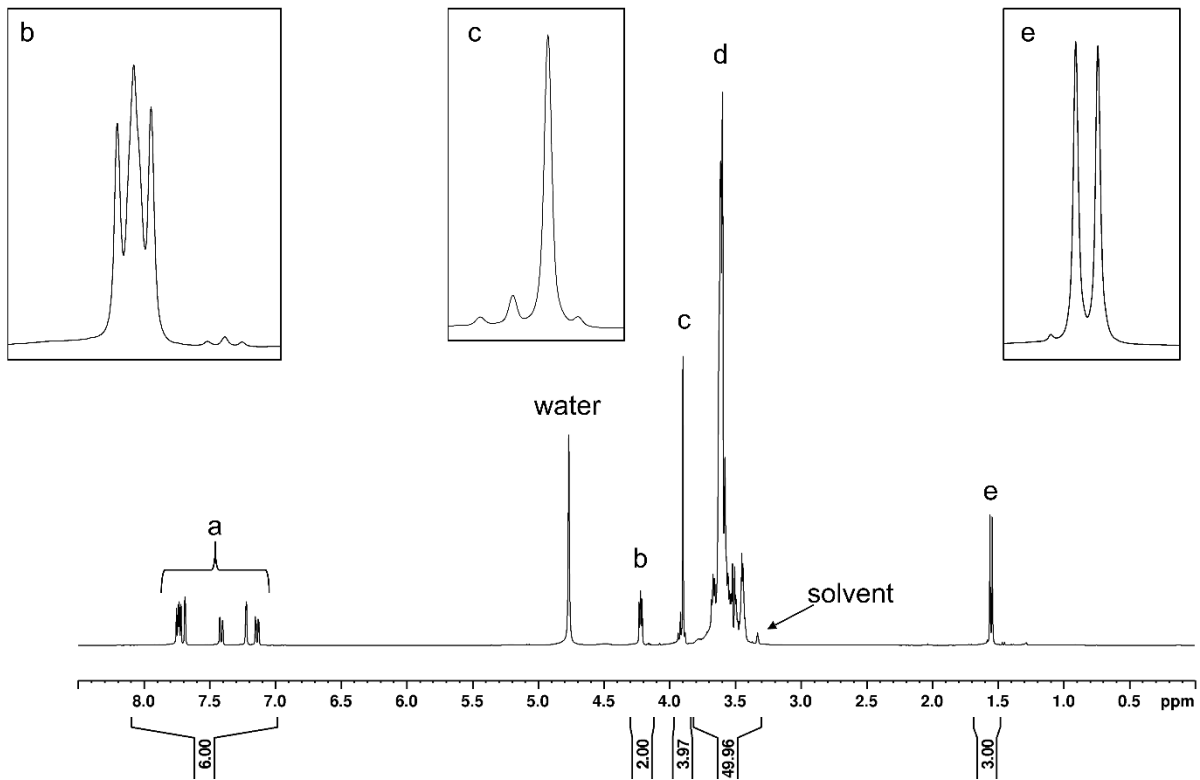


Figure 3 ^1H NMR of NPEG and signal assignment (cf. Figure 2)

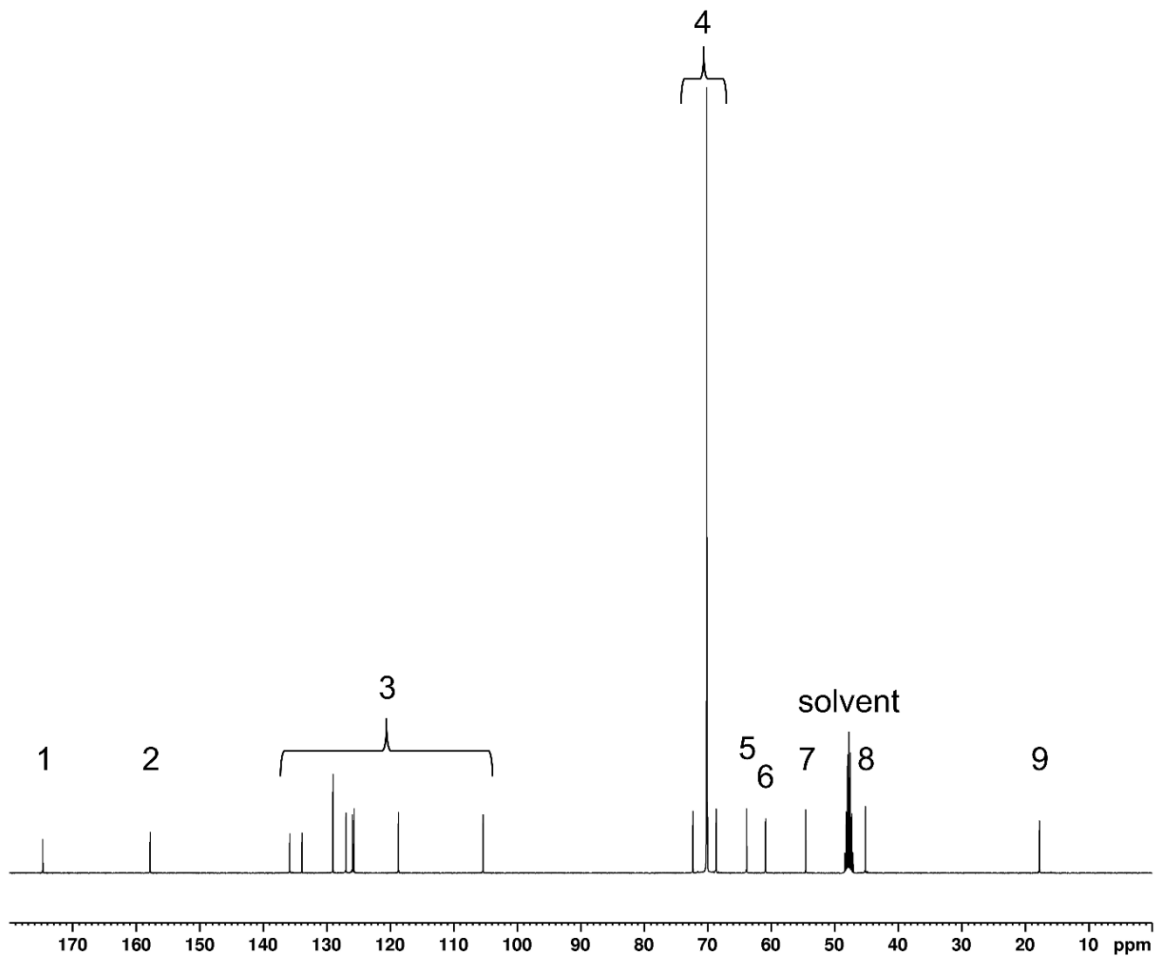


Figure 4 ^{13}C NMR of NPEG and signal assignment (cf. Figure 2)

The UV chromatogram is displayed in Figure 5. The corresponding mass spectrum (Figure 6) shows $[M+H]^+$ species of NPEG with 10-14 ethylene glycol monomers (m/z 671.3: $n = 10$; m/z 715.3: $n = 11$; m/z 759.4: $n = 12$; m/z 803.4: $n = 13$ and m/z 847.4: $n = 14$) and $[M+2H]^{2+}$ species (m/z 402.3: $n = 13$ and m/z 424.3: $n = 14$).

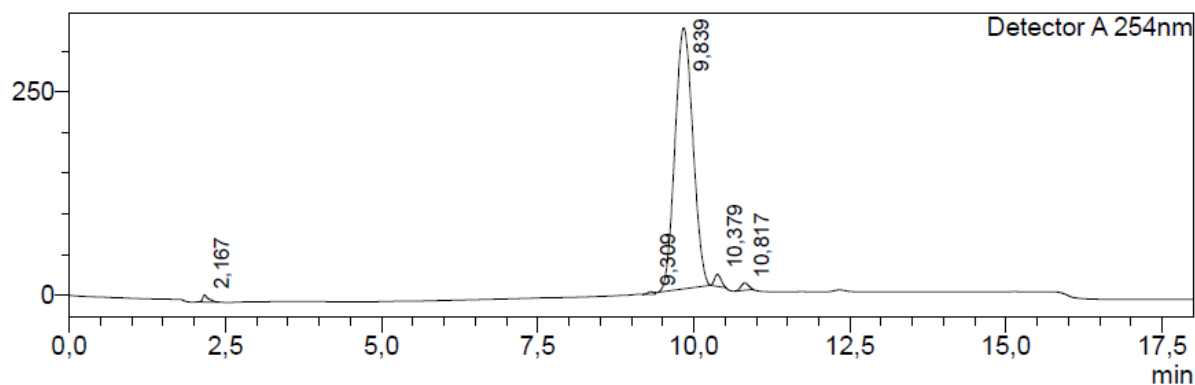


Figure 5 UV chromatogram ($\lambda = 254$ nm) of the synthesized naproxen-PEG-ester

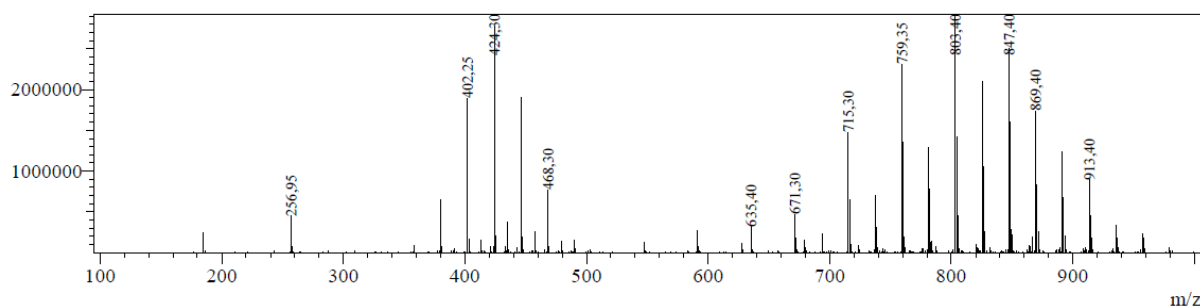


Figure 6 Mass spectrum of the synthesized NPEG (cf. Figure 2)

3.3.3.2 Influence of the drug load

Samples A and B were analyzed to investigate the influence of the drug load on the formation of NPEG. During preparation of the samples and their storage at 60 °C, both formulations were clear. However, after cooling to room temperature, a precipitate became visible in formulation A, which had the higher drug concentration of 26% (m/m). In contrast, sample B with a drug load of 20% (m/m) remained clear after cooling. The relative peak area of naproxen after injection of the precipitate was 99.87% ($\pm 0.01\%$), indicating that the precipitate consisted of naproxen only. Apparently, the system with a drug load of 26.0% (formulation A) was supersaturated, which lead to precipitation of the API.

The amount of NPEG in sample A was lower than sample B (Figure 7), which can be explained by the presence of the precipitate. Naturally, if a fraction of the API is bound in a precipitate, the amount available for reactions with excipients is lower than in a

system with a completely dissolved API. Furthermore, the amount of the precipitate needs to be considered when evaluating the NPEG concentration, as the relative peak area is calculated with regard to the dissolved ratio of the API only. The absolute amount of precipitate was not determined in this study but given the fact that the solid did not contain NPEG, the relative amount of NPEG considering the overall amount of naproxen in the formulation is even lower than indicated by the LC-UV analysis.

3.3.3.3 Influence of lactic acid and water concentration

The molar ratio of lactic acid and naproxen was 0.6 and 1.0 in formulations B and C, respectively. The amount of NPEG was higher in sample C, which contained a higher quantity of lactic acid (cf. Figure 7). As the condensation of a carboxylic acid (here: naproxen) and an alcohol (here: PEG 600) is an acid catalyzed reaction, the observed effect is plausible from a chemical point of view [18].

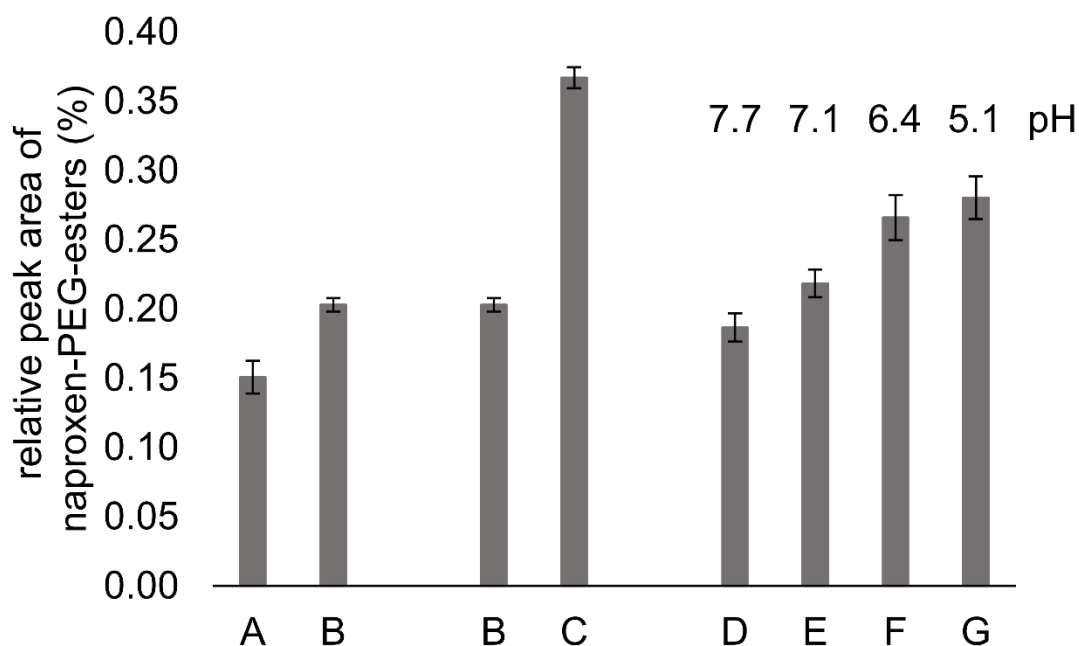


Figure 7 Comparison of naproxen-PEG-ester amounts in the analyzed formulations

Formulations D-G were analyzed to determine the influence of the water concentration – they contain water contents in the range from 4.1-0.5%. The NPEG content in the respective samples increased with decreasing water concentration (cf. Figure 7 and Figure 8). This can be explained by *Le Chatelier's Principle*: a lower amount of water shifts the equilibrium towards the product side in condensation reactions [19].

However, the observed effect is not only due to the water concentration but is reinforced by the pH of the formulations. Determination of the pH of formulations D-G

showed that a more acidic milieu results when lower water concentrations are used. As the ester formation is an acid catalyzed reaction, both the low pH value and the low water concentration can contribute to the increased ester formation.

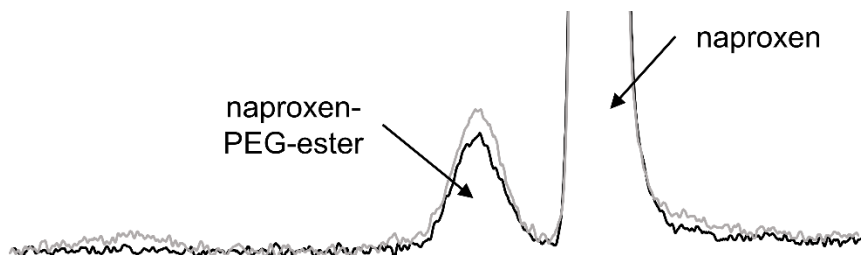


Figure 8 Overlaid chromatograms of formulations E (black, $0.22 \pm 0.01\%$ naproxen-PEG-ester) and G (grey, $0.28 \pm 0.02\%$ naproxen PEG-ester) containing 2.1% and 0.5% water, respectively. The lower water content of formulation G leads to elevated concentrations of naproxen-PEG-esters when compared to formulation E.

3.3.4 Conclusion

The example of NPEG formation in soft gel capsule formulations illustrates that excipients need to be selected carefully considering the potential of API-excipient interactions/reactions. Moreover, the impurities of excipients and APIs need to be considered besides the reactivity of the API and the excipients itself [10].

The formation of NPEG follows simple chemical rules and can be influenced by variations of the formulation. As can be predicted from the nature of the reaction – an acid catalyzed condensation – the pH value and the water concentration have a significant impact on the extent of the ester formation.

With a maximum daily dose of 1250 mg naproxen [2], the qualification threshold according to the effective ICH guideline is 0.2% [20]. The contents of NPEG in the analyzed formulations varied from 0.15% to 0.37%. The impurity must be controlled at a content below the qualification threshold or further information needs to be acquired to estimate the toxicological potential of NPEG. However, as esters are common and frequently used linkers in prodrugs, it is plausible that NPEG will be cleaved *in vivo*, releasing the API naproxen [21]. Ester prodrugs of naproxen and other NSAIDs have been described in the literature [22]. Moreover, an ester of the NSAID ibuprofen and PEG 400 has been assessed as a potential prodrug offering a prolonged duration of action and reduced toxicity in comparison to ibuprofen alone [23]. Hence, it is unlikely that NPEG triggers negative effects, but it may have pharmacokinetic implications.

3.3.5 References

- [1] P.A. Todd, S. P. Clissold, Naproxen. A reappraisal of its pharmacology, and therapeutic use in rheumatic diseases and pain states, *Drugs* 40 (1990) 91-137
- [2] Aristo Pharma GmbH, Fachinformation Naproxen Aristo 500 mg Tabletten, <http://fachinformation.srz.de/pdf/aristo/naproxenaristo500mgtabletten.pdf>, 2018 (accessed 16th August 2021)
- [3] Naproxen in: European Pharmacopoeia 10.0, Council of Europe, Strasbourg, France, 2020
- [4] Naproxen sodium in: European Pharmacopoeia 10.0, Council of Europe, Strasbourg, France, 2020
- [5] Bayer Consumer Health, ALEVE, <https://www.aleve.com/>, 2021 (accessed 16th August 2021)
- [6] Vidal MMI Germany GmbH, Naproxen, https://www.gelbe-liste.de/wirkstoffe/Naproxen_1806, 2021 (accessed 16th August 2021)
- [7] International Council for Harmonisation of Technical Requirements for Pharmaceuticals for Human Use, ICH Topic Q3A (R2) Impurities in new Drug Substances, 2006
- [8] International Council for Harmonisation of Technical Requirements for Pharmaceuticals for Human Use, ICH Topic Q1A (R2) Stability Testing of new Drug Substances and Products, 2003
- [9] International Council for Harmonisation of Technical Requirements for Pharmaceuticals for Human Use, ICH guideline Q3C (R6) on impurities: guideline for residual solvents, 2019
- [10] K. Zhang, J. D. Pellett, A. S. Narang, Y. J. Wang, Y. T. Zhang, Reactive impurities in large and small molecule pharmaceutical excipients—A review, *Trends Anal Chem* 101 (2018) 34-42
- [11] H. Yu, C. Cornett, J. Larsen, S. H. Hansen, Reaction between drug substances and pharmaceutical excipients: formation of esters between cetirizine and polyols, *J Pharm Biomed Anal* 53 (2010) 745-750
- [12] F. Monajjemzadeh, D. Hassanzadeh, H. Valizadeh, M. R. Siahi-Shadbad, J. S. Mojarrad, T. A. Robertson, M. S. Roberts, Detection of gabapentin-lactose Maillard reaction product (Schiff's Base): Application to solid dosage form preformulation/Part 2, *Pharm Ind* 73(2) (2011) 376-382
- [13] A. Gumieniczek, A. Berecka, T. Mroczek, K. Wojtanowski, K. Dabrowska, K. Stepień, Determination of chemical stability of sitagliptin by LC-UV, LC-MS and FT-IR methods, *J Pharm Biomed Anal* 164 (2019) 789-807
- [14] Bayer Consumer Health, Aleve Liquid Gels, <http://labeling.bayercare.com/omr/online/aleve-liquid-gels.pdf>, 2021 (accessed 16th August 2021)
- [15] G. R. Fulmer, A. J. M. Miller, N. H. Sherden, H. E. Gottlieb, A. Nudelman, B. M. Stoltz, J. E. Bercaw, K. I. Goldberg, NMR Chemical Shifts of Trace Impurities: Common Laboratory Solvents, Organics, and Gases in Deuterated Solvents Relevant to the Organometallic Chemist, *Organom* 29 (2010) 2176-2179

- [16] DrugBank, ¹H NMR Spectrum (DB00788) Naproxen, https://go.drugbank.com/spectra/nmr_one_d/1802, 2020 (accessed 14th September 2021)
- [17] ChemicalBook, Naproxen (22204-53-1) ¹³C NMR, https://www.chemicalbook.com/SpectrumEN_22204-53-1_13CNMR.htm, 2017 (accessed 14th September 2021)
- [18] Chapter 14: Carbonsäurederivate in: T. Schirmeister, C. Schmuck, P. R. Wich, Beyer/Walter | Organische Chemie, 25th edition, S. Hirzel Verlag, Stuttgart, Germany, 2015
- [19] Chapter 17: Das chemische Gleichgewicht, in C. E. Mortimer, U. Müller, Chemie – Das Basiswissen der Chemie, Georg Thieme Verlag KG, Stuttgart, Germany, 2019
- [20] International Council for Harmonisation of Technical Requirements for Pharmaceuticals for Human Use, Impurities in New Drug Products Q3B (R2), 2006
- [21] J. Rautio, H. Kumpulainen, T. Heimbach, R. Oliyai, D. Oh, T. Järvinen, J. Savolainen, Prodrugs: design and clinical applications, *Nat Rev Drug Discov* 7 (2008) 255-270
- [22] A. M. Qandil, Prodrugs of nonsteroidal anti-inflammatory drugs (NSAIDs), more than meets the eye: a critical review, *Int J Mol Sci* 13 (2012) 17244-17274
- [23] A. Nayak, A. Jain, In vitro and in vivo study of poly (ethylene glycol) conjugated ibuprofen to extend the duration of action, *Sci Pharm* 79 (2011) 359-374

3.4 Impurity Profiling of Bisoprolol Fumarate by Liquid Chromatography-High-Resolution Mass Spectrometry: A Combination of Targeted and Untargeted Approaches using a Synthesis Reaction Matrix and General Unknown Comparative Screening

Jonas Wohlfart, Elisabeth Jäckel, Oliver Scherf-Clavel, Dirk Jung, Martina Kinzig, Fritz Sörgel, Ulrike Holzgrabe

Reprinted with Permission from

Journal of Chromatography Open 1 (2021) 100012

Abstract

Several examples of the emergence of unexpected impurities in medicinal products in the past, e.g. the 2018 valsartan scandal, disclosed the need for sophisticated approaches in impurity profiling. Advanced techniques in mass spectrometry offer the possibility to detect impurities in untargeted approaches complementing the targeted search for potential impurities. In this study, a combination of targeted and untargeted approaches using LC-MS/HRMS was applied in creating an impurity profile of bisoprolol fumarate. In the targeted approach, a reaction matrix was used to predict potential impurities, which were searched for in addition to the related substances stated in the *European Pharmacopoeia*. For the untargeted analytics, *general unknown comparative screening* was performed to detect unexpected impurities. To cover a maximum range of detectable analytes, two complementary mobile phases, i.e. buffered to acidic and basic pH, were combined with four mass spectrometric ionization conditions, i.e. *electrospray ionization* and *atmospheric pressure chemical ionization* in both positive and negative mode. *Information-dependent acquisition* was used to generate MS and MS/MS data in a single run. The targeted and the untargeted approach revealed the presence of 18 and 17 impurities, respectively. The plausibility of proposed/elucidated structural formulae was checked by *in silico* fragmentation and assignment of characteristic fragments/neutral losses. Quantification of the impurities was performed with respect to the internal standard metoprolol. The analyzed batches showed contents of up to 0.05% of single impurities. A thorough procedure for the development of a complete impurity profile for drug substances was demonstrated. To ensure a maximum of patient safety, the described approach is prototypical and should

be implemented during drug development and after relevant changes in manufacturing processes.

3.4.1 Introduction

Bisoprolol is a cardio-selective beta blocker used for the treatment of heart diseases like hypertension and coronary heart disease [1]. Given the fact that millions of people take this medication permanently, a thorough control of the impurities present in the medicinal products is essential to ensure a maximum patient safety [2]. At least 44 manufacturers across the world produce the active pharmaceutical ingredient (API) for a variety of generic medicinal products [3, 4]. Thus, it is likely that there are different methods of synthesis used for producing commercial batches and each pathway and production plant is associated with a distinct impurity profile.

The synthesis route (Figure 1) of bisoprolol fumarate applied by Arevipharma (Radebeul, Germany) starts off with the condensation of 4-hydroxybenzyl alcohol (1) with 2-isopropoxyethanol, catalyzed by p-toluenesulfonic acid (PTSA). The resulting ether (2) reacts with epichlorohydrin under basic conditions to form an oxirane derivative (3). Upon nucleophilic attack and ring-opening of the oxirane by isopropylamine, the free base of bisoprolol (4) is formed. The reaction with fumaric acid yields the API bisoprolol fumarate (5) [5]. Alternative methods for the preparation of bisoprolol follow a similar pathway [6, 7].

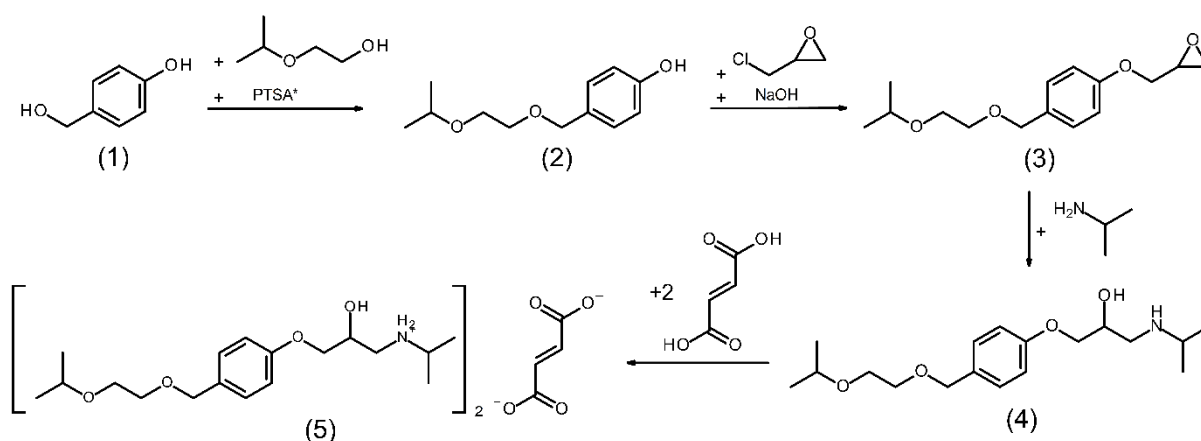


Figure 1 Synthesis of bisoprolol fumarate (*PTSA = p-toluenesulfonic acid)

To control present and possible impurities in APIs, the International Council for Harmonisation of Technical Requirements for Pharmaceuticals for Human Use (ICH) guideline Q3A (R2) states thresholds/procedures for detected impurities and requests an appraisal of the synthesis procedure to recognize any potential formation of

mutagenic impurities [8]. The concept of structural alerts is used to avoid certain functional groups being known to hold mutagenic potential (e.g. nitrosamines) or the risk of forming reactive metabolites [9]. Examples for such groups, which might be relevant for bisoprolol fumarate from the synthesis shown in Figure 1, include alkenes, halogenated compounds and oxiranes [10]. However, the occurrence of structural alerts in APIs cannot be avoided at all costs since these features might be necessary for the pharmacodynamic activity. For example, double bonds and aromatics, which are essential parts of many pharmacophores, can be converted to hydroxylated metabolites via reactive intermediates such as oxiranes [11, 12]. However, these moieties can be considered as non-mutagenic when they occur in the same chemical environment as in the API, if the latter tested negative in a bacterial mutagenicity test according to the effective ICH guideline M7 (R1) for mutagenic impurities [13]. Here, impurities are divided into five classes to define actions and acceptable intake limits, depending on the impurity (chemical structure and carcinogenicity data) and the maximum daily dose of the API. Besides experimental toxicity tests, the toxicologic potential of molecules can be estimated by a variety of computer-based approaches [14-16]. To complete an impurity profile of an API, stress tests have to be performed according to ICH guideline Q1A (R2) in order to find degradation and side products [17]. Residual solvents and elemental impurities have to be considered as well [18, 19].

API manufacturers, market authorization holders and regulatory authorities can only control impurities they are aware of, which makes the appraisal of the synthesis a crucial step in the development of an impurity profile. In addition to the impurities emerging from the synthesis route, side reactions of the reactants, reagents and their impurities, and potential degradants need to be considered. The assessment can be supported by automated, standardized procedures like reaction matrices considering starting materials, reactants, solvents, their impurities and related reaction products [20]. However, even the best techniques and expertise might not be able to predict all relevant impurities occurring in an API. The 2018 valsartan scandal is just one of many examples illustrating that current strategies in impurity profiling are insufficient when it comes to the assessment of impurities, which are not structurally related to the respective API [21]. To enable the detection of unexpected impurities, targeted analytics can be complemented with untargeted mass spectrometric (MS) approaches like MS/MSALL, sequential window acquisition of all theoretical fragments (SWATH),

information dependent acquisition (IDA) and general unknown comparative screening (GUCS) [22].

In MS/MS^{ALL}, IDA and SWATH, a simultaneous acquisition of MS and tandem MS (MS/MS) data is achieved within a single analysis. While specific precursor ions are selected for fragmentation by predefined criteria in IDA, all precursors are fragmented in MS/MS^{ALL} and SWATH [23, 24]. Besides chemometric evaluation procedures [25], GUCS is an option to handle complex data by comparing the samples of interest with a control sample [26]. Thus, evaluation is simplified by accentuating distinctive features and eliminating irrelevant signals. The MS and MS/MS data of relevant signals can be used for the identification of compounds, e.g. by comparing fragment spectra to spectral libraries [27]. However, spectral libraries might not cover all compounds present in a sample. Then, the molecular formula and the structure of the respective compound must be determined based on exact mass and fragmentation rules, which can be supported by *in silico* fragmentation based on e.g. machine-learning and quantum chemistry [28-30].

The *European Pharmacopoeia* (PhEur) controls 15 related substances of bisoprolol fumarate by means of liquid chromatography (LC) with spectrophotometric detection at 225 nm, using an octadecylsilyl stationary phase and gradient elution with phosphoric acid in water and acetonitrile (ACN) [31]. The method applied in the *Japanese Pharmacopoeia* is similar but makes use of an octylsilyl stationary phase and does not state specified impurities [32]. The *United States Pharmacopoeia* test on chromatographic purity makes use of ion-pair chromatography applying an octylsilyl column, isocratic elution with water/ACN 65/35 + heptafluorobutyric acid, dimethylamine and formic acid (FA), a detection wavelength of 273 nm and does also not specify any impurity [33].

In this study, an impurity profile of the API bisoprolol fumarate was established by means of LC-HRMS (high resolution mass spectrometry). An untargeted approach using IDA and GUCS was combined with a targeted search for potential impurities (PI) derived from a detailed reaction matrix. The plausibility of proposed/elucidated structural formulae was checked by *in silico* fragmentation and assignment of characteristic fragments/neutral losses. Furthermore, the detected impurities were quantified with respect to the internal standard (IS) metoprolol.

3.4.2 Experimental

3.4.2.1 **Materials and instrumentation**

Five batches of bisoprolol fumarate (batches A-E), metoprolol succinate and [4-(oxiran-2-ylmethoxy)phenyl]methanol (PI 1.31) were provided by Arevipharma (Radebeul, Germany). Bisoprolol fumarate *chemical reference substance* (CRS) Y0000812 was purchased from the European Directorate for the Quality of Medicines and HealthCare (EDQM, Strasbourg, France). Bisoprolol impurities C and Q were purchased from LGC (Teddington, United Kingdom). MS-grade water, methanol (MeOH), ACN, ammonium formate, FA and ammonium hydrogen carbonate were purchased from Sigma-Aldrich (Taufkirchen, Germany). Epichlorohydrin for synthesis was purchased from Merck (Darmstadt, Germany), 4-(hydroxymethyl)phenol $\geq 99.0\%$ from Biesterfeld Spezialchemie (Hamburg, Germany) and potassium carbonate $\geq 99\%$ from Acros Organics (Geel, Belgium).

The development of the LC method was performed on an Agilent 1100 modular system (Waldbronn, Germany, delay volume 1.12 mL) consisting of a binary pump, a thermostatted autosampler, a thermostatted column compartment and a diode array detector applying three wavelengths (210, 254 and 271 nm). The following columns were used: Kinetex XB-C18 100 Å (5 μm , 4.6 x 100 mm, Phenomenex, Torrance, USA), InfinityLab Poroshell 120 Phenyl Hexyl (2.7 μm , 4.6 x 100 mm, Agilent, Waldbronn, Germany), Symmetry Shield RP8 (3.5 μm , 3.0 x 100 mm, Waters, Eschborn, Germany).

All LC-MS measurements were performed on an Agilent Infinity II system (Waldbronn, Germany, delay volume 0.58 μL) consisting of a quaternary pump, a thermostatted autosampler and a thermostatted column compartment with the Kinetex C18 column. The LC system was coupled to a Sciex X500R QTOF mass spectrometer (Concord, Ontario, Canada) equipped with a Turbo VTM Ion Source with *electrospray ionization* (ESI) or *atmospheric pressure chemical ionization* (APCI) probe. Automatic calibration of the mass spectrometer was performed using specific tuning solutions for ESI and APCI, respectively (Sciex, Concord, Ontario, Canada). LC-MS data was acquired and evaluated using Sciex OS 1.6 software (Concord, Ontario Canada).

3.4.2.2 **Sample preparation**

10.0 mg bisoprolol fumarate were dissolved and diluted to 10.0 mL with water and then further diluted with water to reach a concentration of 100 $\mu\text{g/mL}$.

Samples spiked with metoprolol succinate were prepared by adding 10 μ L of a 100 μ g/mL metoprolol succinate stock solution to the respective bisoprolol fumarate sample prior to dilution of the sample. The final concentration of the IS was 10 ng/mL.

Calibration solutions of impurities C, Q and metoprolol succinate with concentrations of 1, 5, 10, 15, 20, 30 and 40 μ g/mL were prepared from a mixed stock solution containing 1 μ g/mL of each of the three compounds.

10 g of 4-(hydroxymethyl)phenol were dissolved in 403 mL butan-2-one. After addition of 33.4 g potassium carbonate and 15.8 mL epichlorohydrin, the mixture was heated up to 80 °C for 42 h and filtered. The filtrate was washed with acetone and purified by column chromatography (silica gel, ethyl acetate/dichloromethane 2/1 v/v) to give 7.6 g of PI 1.31 ([4-(oxiran-2-ylmethoxy)phenyl]methanol). The product was characterized by 1 H NMR (500 MHz, chloroform-d, data not shown). 10.0 mg of the product were dissolved in a mixture of ACN/water (80/20 v/v) and diluted with water to the final concentration of 10 μ g/mL.

3.4.2.3 LC-HRMS

3.4.2.3.1 Impurity profiling

Chromatographic separation was performed applying either acidic or basic conditions. The acidic buffer consisted of 5 mM ammonium formate + 0.032% FA (pH 3.5), while the basic buffer was 10 mM ammonium hydrogen carbonate (pH 8.0). The buffer salts were dissolved in (A) water or (B) a mixture of ACN, MeOH and water (47.5/47.5/5, v/v). The gradient started after an initial isocratic step of 3% B for 3 min. B was raised to 100% within 8 min and held at 100% B for 9 min. The flow rate was set to 1.0 mL/min and the injection volume was 5 μ L. The thermostatted autosampler was set to 8 °C. The injection system was flushed thoroughly after every injection by applying MeOH + 0.1% (v/v) FA as needle wash medium (20 s). Additionally, the column was flushed by a rinsing gradient (flow 1.5 mL/min, start with 3% B, after 1 min raise to 100% B within 2.6 min and hold for 1.7 min), followed by re-equilibration.

MS detection was performed applying four IDA methods, i.e. ESI and APCI in both positive and negative polarity, respectively, with generic source parameters with regard to the used LC flow (Table 1) [34].

The samples were analyzed using eight LC-HRMS variants combining each of the four MS methods with acidic and basic chromatography conditions, respectively. All

samples were injected five-fold per method variant, resulting in 240 sample injections in total. The order of injections of each of the eight subsets was randomized. Blank runs (water) and automatic mass calibration of the mass spectrometer with respective tuning solutions for ESI or APCI were performed every five runs.

A solution of the synthesized (see section 2.2) PI 1.31 was injected to the system applying the described method with the acidic buffer and positive mode ESI.

Table 1 MS parameters and IDA criteria

Parameter	ESI+	ESI-	APCI+	APCI-
Gas 1		50		30
Gas 2		50		n/a
Temperature (°C)		550		400
Spray Voltage (V)	5500	-4500		n/a
Nebulizer current (µA)		n/a	3	-3
Mass range (Da)		50 - 1000		
Curtain gas		20		
CAD gas		7		
Declustering Potential ± spread (V)	70 ± 30	-70 ± 30	60 ± 20	-60 ± 20
TOF MS				
Accumulation time (s)		0.25		
Collision energy ± spread (V)	10 ± 0	-10 ± 0	10 ± 0	-10 ± 0
IDA				
Accumulation time (s)		0.1		
Collision energy ± spread (V)	35 ± 15	-35 ± 15	35 ± 15	-35 ± 15
Maximum candidate ions		10		
Intensity threshold (counts/s)		10		
Dynamic background subtraction		True		

3.4.2.3.2 Quantification of impurities

Quantification was performed applying acidic LC conditions and ESI in positive polarity as described in section 2.3.1. Standard solutions and spiked samples were injected in

triplicates. Blank runs (water) and automatic mass calibration of the mass spectrometer were performed every five runs.

3.4.2.4 Evaluation

3.4.2.4.1 Impurity profiling

The expected *mass-to-charge ratios* (m/z) of the 15 related substances stated in the monograph of bisoprolol fumarate in the PhEur [31], and PIs derived from the reaction matrix (see Supplementary Information) were used to generate *extracted ion chromatograms* (XIC) of the $[M+H]^+$ or $[M-H]^-$ species from positive and negative mode measurements, respectively. Moreover, an automated, untargeted peak finding process was performed in GUCS, where a peak area ratio > 10 (sample/blank) triggered inspection of the respective signal.

Molecular formulae were verified or developed based on the precursor m/z (mass error < 5 ppm) and respective isotope patterns (intensity tolerance: 20%). The structures of presumed impurities were verified by automated comparison of experimental fragment spectra with *in silico* fragment spectra. A plausibility of 90% was considered as verification, indicating that 90% of the total peak area in the fragment spectrum can be explained by *in silico* fragments with a mass error below 15 ppm. Furthermore, a library of characteristic fragments and neutral losses was created.

3.4.2.4.2 Quantification of impurities

Molar response factors (RF) of impurities C and Q with respect to the IS metoprolol were calculated as the ratio of the slopes of the respective linear regression curves [35]. Correction factors (CF) were calculated as reciprocal values of the respective RFs. The content of impurities was calculated using the following equation:

$$\text{Content (ppm)} = \frac{\text{Peak Area}_{\text{Imp}}}{\text{Peak Area}_{\text{IS}}} * \frac{c_{\text{IS}} * M_{\text{Imp}}}{10^9 * \beta_{\text{API}}} * CF$$

with c_{IS} = molar concentration of the IS (mol/L), M_{Imp} = molar mass of the impurity (g/mol), CF = correction factor and β_{API} = concentration of bisoprolol fumarate ($\mu\text{g/mL}$).

The contents of all impurities were calculated with respect to the IS metoprolol. A CF of 1.27 was applied for all impurities containing one basic nitrogen atom according to section 3.4. Impurities with two basic nitrogen atoms were quantified in two ways: Firstly, based on $[M+2H]^{2+}$ with respect to the IS metoprolol (CF: 1.15 according to section 3.4) and secondly, based on $[M+H]^+$ with respect to impurity C, which then

acted as an alternative IS. The concentrations of impurity C and Q were determined in all batches using linear regression models (impurity C: $y = 1558.1x + 143.0$, $R^2 = 0.993$; impurity Q: $y = 4471.9x + 9043.6$, $R^2 = 0.998$).

3.4.3 Results & Discussion

3.4.3.1 Method development

The aim of the method development was to detect a maximum of possible compounds with different physicochemical properties: impurities reported in the reaction matrix and unexpected impurities. Hence, different column types and mobile phases were tested in preliminary LC-UV measurements varying the chromatographic selectivity. The width of the bisoprolol signal, which naturally represents the largest peak in the chromatogram, was the main criterion in the selection of stationary and mobile phases to decrease the risk of co-elution of impurities with the API and thus minimize ion suppression (Table 2) [36].

Table 2 Peak characteristics of fumarate and bisoprolol using different columns and mobile phases (acidic: 0.1% FA pH 2.6, basic: 10 mM ammonium hydrogen carbonate pH 8.0) in preliminary LC-UV experiments

Column	Medium	Organic modifier	Width (min)		No. of impurity peaks
			fumarate	bisoprolol	
Kinetex XB-C18	Acidic	MeOH	0.13	0.31	10
		ACN	0.12	0.24	9
	Basic	MeOH	0.08*	0.19	2
		ACN	0.08*	0.32	8
Poroshell Phenyl Hexyl	Acidic	MeOH	0.12	0.42	7
		ACN	0.09	0.33	8
	Basic	MeOH	0.08*	0.19	5
		ACN	0.08*	0.20	5
Symmetry Shield RP8	Acidic	MeOH	0.14	0.36	2
		ACN	0.18	0.80	2
	Basic	MeOH	0.08*	0.34	5
		ACN	0.08*	0.34	7

* not separated from injection peak

The tested columns were selected because an adequate retention of bisoprolol could be expected for all of them, which was the case for all stationary phases. Testing of further columns could be a possibility to extend the versatility of the approach, which was not pursued because satisfactory results were reached with the applied selection. Eventually, the Kinetex XB-C18 column was selected for all further experiments.

An acidic mobile phase enhances ionization of basic analytes in positive mode MS [37]. However, also acidic impurities might be present, requiring negative mode MS. As a consequence, a basic buffer of 10 mM ammonium hydrogen carbonate (pH 8.0) was applied to enable negative mode measurements in addition to the acidic buffer (pH 3.5) [38]. The use of two different buffers furthermore allows for the distinction of in-source fragments and adducts from independent signals as co-elution of two different substances in both the acidic and the basic method is unlikely. MeOH produced sharper peaks when using an acidic medium while ACN performed better when applying the basic buffer (cf. Table 2). Hence, a mixture of the organic modifiers was applied in the final methods.

In impurity profiling, a high concentration of the API is necessary to make the detection of impurities with low contents possible [39]. However, peak broadening and carry-over effects limit the sample concentration in many cases. Here, a concentration of 100 µg/mL bisoprolol fumarate and an injection volume of 5 µL were selected, limited by carry-over. The whole system required rinsing after every injection to guarantee the absence of peaks in impurity XICs. This was achieved by application of MeOH + 0.1% FA as needle wash medium (20 s) after every injection as well as a rinsing gradient. The order of injections was randomized to eliminate errors due to fluctuations in sensitivity or other random errors. These actions were taken to guarantee the highest possible grade of data integrity.

The analyses were performed with both ESI and APCI to enable the detection of polar and nonpolar substances [40]. With the focus on the detection of unknown impurities, it was not considered reasonable to optimize the ionization parameters for a specific analyte. In contrast, generic parameters were selected with respect to the LC flow to address a wide variety of substances (cf. Table 1) [34]. The detection of basic and acidic impurities is possible due to the use of both positive and negative mode. IDA was chosen over other SWATH and MS/MS^{ALL} techniques because the acquired fragment spectra generally show a higher purity and are thus less susceptible to

interferences from co-eluting substances [41]. However, the acquisition of certain fragment spectra had to be repeated due to an inappropriate collision energy, or because no fragment spectra had been acquired during IDA. This was especially the case for impurities of a very low amount.

Finally, it is worth mentioning that in LC-MS it is good practice to direct the LC flow towards the mass spectrometer during a short period of time only, e.g. when an analyte to be quantified elutes from the system. However, in this study the LC flow was directed towards the qTOF throughout the analysis to detect all eluting molecules, as the sample matrix was most simple (API in water) and thus, no pollution of the MS was expected. Naturally, this cannot be transferred to the analysis of e.g. drug products and chemically stressed samples, where it might be beneficial to protect the MS from contamination with high amounts of excipients and stressing agents, respectively.

3.4.3.2 Structure confirmation methods (targeted approach)

Both MS and MS/MS data were used to identify the PIs derived from the reaction matrix. The respective molecular formulae were confirmed based on the MS data by comparing the experimental exact m/z (mass error < 5 ppm) and the isotope pattern with the respective theoretical properties (Figure 2). However, with rising molecular masses more than one molecular formula might be possible within the mass error of the used mass spectrometer. This problem can be overcome to some extent by considering the isotopic pattern. For the accurate determination of the exact mass and the subsequent molecular formula, a periodically calibrated instrument at maximum resolution power is needed [42]. Therefore, automatic mass calibration of the mass spectrometer by direct infusion of respective tuning solutions was implemented within the sample sequences to maintain a mass error below 5 ppm over the entire mass range and measurement period.

The structures of the proposed impurities were confirmed by *in silico* fragmentation. Here, structural formulae are subjected to fragmentation according to pre-defined rules and the resulting *in silico* fragment spectra are compared with the experimental MS/MS data [43]. The obtained *in silico* plausibility gives the percentage of the MS/MS signal intensity which can be explained by theoretical fragments. This step again requires HRMS data for the determination of molecular formulae of fragment ions. In addition to the automated *in silico* fragmentation, characteristic fragments and neutral losses were used to identify recurrent moieties (Table 3). For example, the fragment I with an

m/z of 116.1070 is characteristic for the basic side chain of bisoprolol, the tropylium cation (fragment F) indicates a benzylic substructure [44, 45], and the neutral loss of j ($C_5H_{12}O_2$) is an indicator for a 2-isopropoxyethoxy moiety.

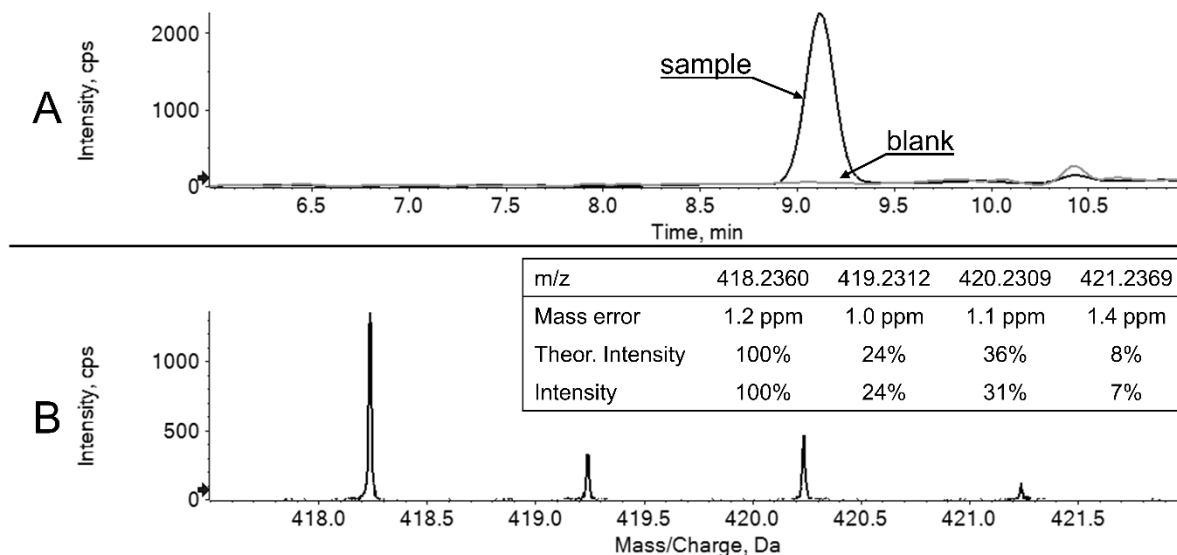
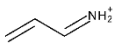
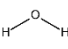
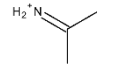
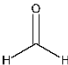
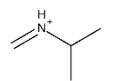
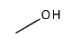
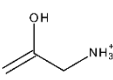
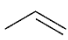
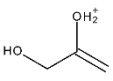
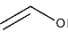
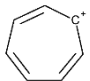
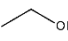
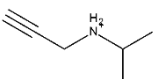
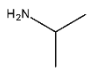


Figure 2 Overlaid XICs of m/z 418.2360 of a sample and a blank injection (A) and confirmation as $[C_{21}H_{37}ClNO_5]^+$, PI 2.19 by exact mass and isotope characteristics (B)

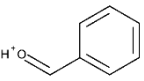
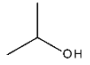
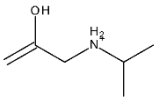
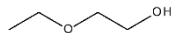
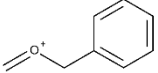
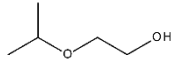
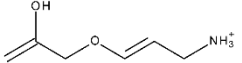
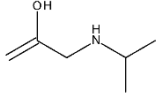
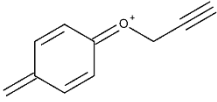
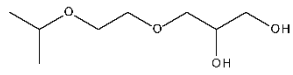
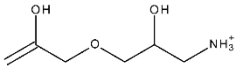
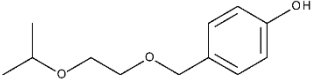
18 impurities were detected using the targeted approach based on the related substances stated in the PhEur and the PIs derived from the reaction matrix (Table 4). The respective molecular formulae were verified in all cases and 9 of the structures could be confirmed by *in silico* fragmentation (plausibility > 90%). All detected substances showed the highest intensity in the data acquired by the acidic LC method and detection in positive mode ESI. Thus, the presented results refer to this method version only.

Results – Impurity Profiling of Bisoprolol Fumarate

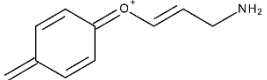
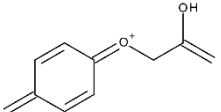
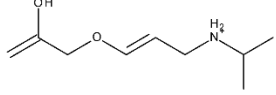
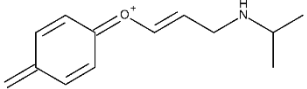
Table 3 Proposed structures of characteristic fragments and neutral losses

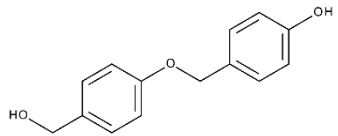
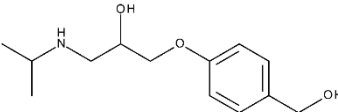
Fragments				Neutral losses			
#	m/z	Molecular formula	Proposed structure	#	m/z	Molecular formula	Proposed structure
A	56.0495	[C ₃ H ₆ N] ⁺		a	18.0106	H ₂ O	
B	58.0651	[C ₃ H ₈ N] ⁺		b	30.0106	CH ₂ O	
C	72.0808	[C ₄ H ₁₀ N] ⁺		c	32.0262	CH ₃ OH	
D	74.0600	[C ₃ H ₈ NO] ⁺		d	42.0470	C ₃ H ₆	
E	75.0441	[C ₃ H ₇ O ₂] ⁺		e	44.0262	C ₂ H ₄ O	
F	91.0542	[C ₇ H ₇] ⁺		f	46.0419	C ₂ H ₅ OH	
G	98.0964	[C ₆ H ₁₂ N] ⁺		g	59.0735	C ₃ H ₉ N	

Results – Impurity Profiling of Bisoprolol Fumarate

Fragments				Neutral losses			
#	m/z	Molecular Formula	Proposed structure	#	m/z	Molecular Formula	Proposed structure
H	107.0491	[C ₇ H ₇ O] ⁺		h	60.0575	C ₃ H ₈ O	
I	116.1070	[C ₆ H ₁₄ NO] ⁺		i	90.0681	C ₄ H ₁₀ O ₂	
J	121.0648	[C ₈ H ₉ O] ⁺		j	104.0837	C ₅ H ₁₂ O ₂	
K	130.0863	[C ₆ H ₁₂ NO ₂] ⁺		k	115.0997	C ₆ H ₁₃ NO	
L	145.0648	[C ₁₀ H ₉ O] ⁺		l	178.1205	C ₈ H ₁₈ O ₄	
M	148.0968	[C ₆ H ₁₄ NO ₃] ⁺		m	210.1256	C ₁₂ H ₁₈ O ₃	

Results – Impurity Profiling of Bisoprolol Fumarate

Fragments			
#	m/z	Molecular Formula	Proposed structure
N	162.0913	[C ₁₀ H ₁₂ NO] ⁺	
O	163.0754	[C ₁₀ H ₁₁ O ₂] ⁺	
P	172.1332	[C ₉ H ₁₈ NO ₂] ⁺	
Q	204.1383	[C ₁₃ H ₁₈ NO] ⁺	

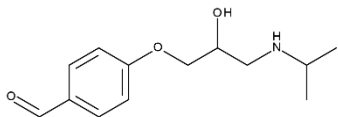
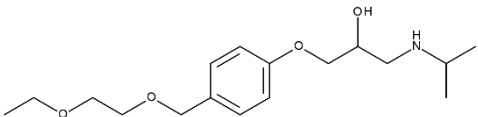
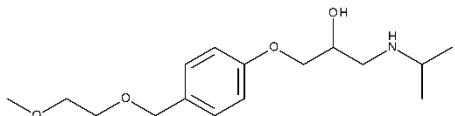
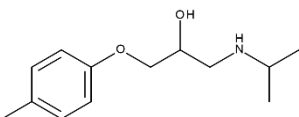
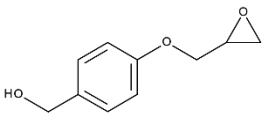
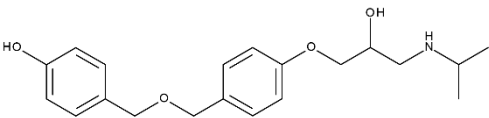
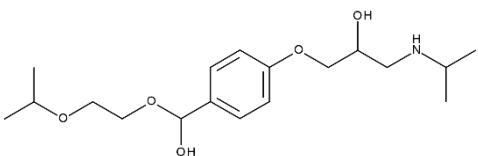
Neutral losses			
#	m/z	Molecular Formula	Proposed structure
n	230.0943	C ₁₄ H ₁₄ O ₃	
o	239.1521	C ₁₃ H ₂₁ NO ₃	

Results – Impurity Profiling of Bisoprolol Fumarate

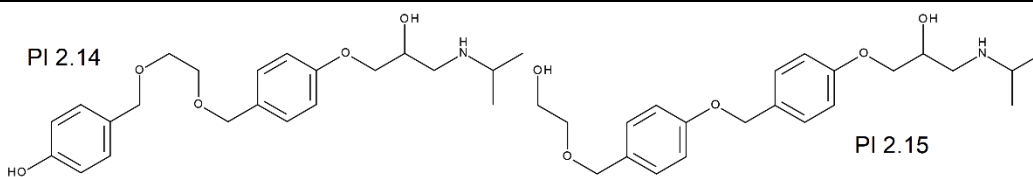
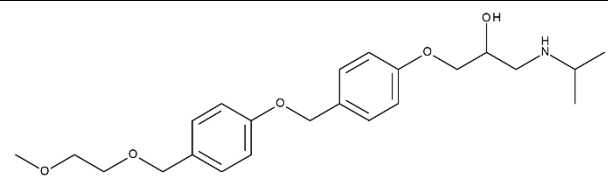
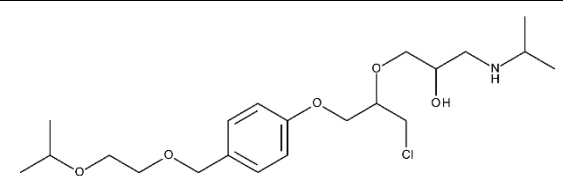
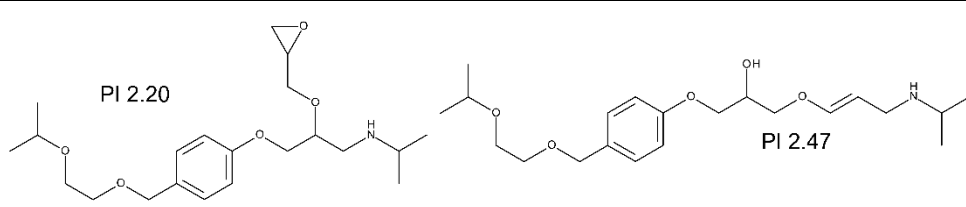
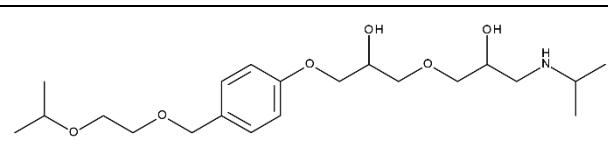
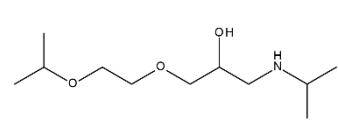
Table 4 Molecular and structural formulae of detected impurities with respective *in silico* plausibility, characteristic fragments and neutral losses (cf. Table 3). The given structures are proposals and not experimentally verified.

Name	Structure	<i>in silico</i> plausibility (%)	Fragments	Neutral losses
Impurity A (C ₁₃ H ₂₁ NO ₃)		90.9	A, B, C, D, F, G, H, I, L, N, O	-a -d -(a+g) -(2a+d)
Impurity C (C ₂₅ H ₃₈ N ₂ O ₄)		99.2	A, B, C, D, G, H, I, L, O	-k
Impurity D (C ₂₆ H ₄₀ N ₂ O ₅)		94.7	A, B, C, D, G, H, I, L, N, O, Q	-d -o
Impurity E (C ₁₈ H ₂₉ NO ₃)		96.2	E, F, H, L	-g
Impurity G (C ₁₉ H ₃₃ NO ₅)		99.2	A, B, C, D, E, F, G, H, I, J, L, N, O, Q	-(a+b+j)
Impurity K (C ₁₈ H ₂₉ NO ₅)		91.0	A, C, D, G, H, I	-a -(a+k) -(d+j) -(a+d+j) -(h+k)

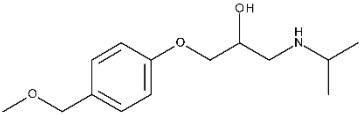
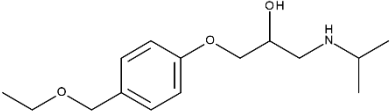
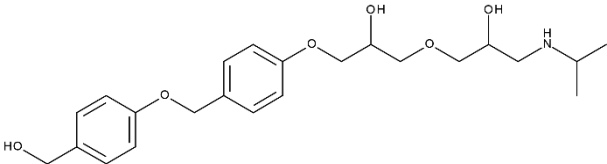
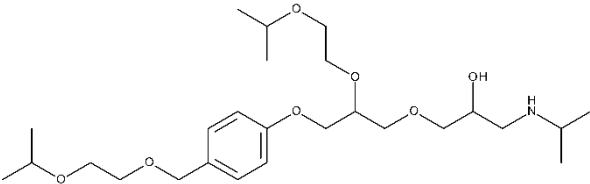
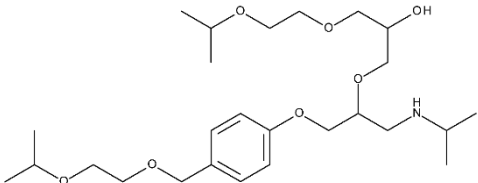
Results – Impurity Profiling of Bisoprolol Fumarate

<p>Impurity L (C₁₃H₁₉NO₃)</p> 	73.1	A, B, C, D, I, J	-a -d
<p>Impurity N (C₁₇H₂₉NO₄)</p> 	98.5	A, B, C, D, F, G, H, I, J, L, N, O, Q	-a -i -(a+i)
<p>Impurity Q (C₁₆H₂₇NO₄)</p> 	53.8 (verified by spiking)	A, B, D, I, L	n/a
<p>Impurity R (C₁₃H₂₁NO₂)</p> 	78.3	A, B, C, D, F, G, H, I, J	-a -d -(a+g)
<p>PI 1.31 (C₁₀H₁₂O₃)</p> 	37.4 (falsified by spiking)	n/a	n/a
<p>PI 2.1 (C₂₀H₂₇NO₄)</p> 	76.2	A, B, C, D, I	n/a
<p>PI 2.2 (C₁₈H₃₁NO₅)</p> 	98.0	A, B, C, D, E, F, G, I, J, O	-j

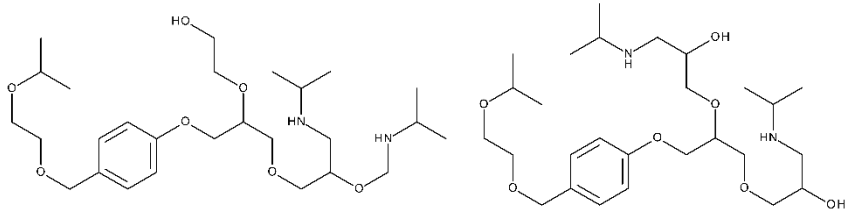
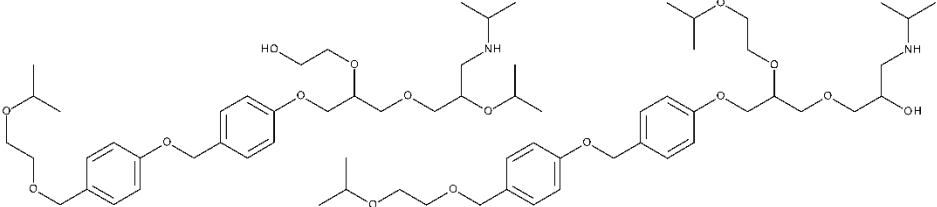
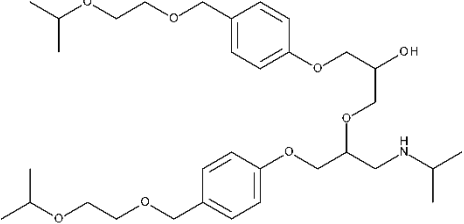
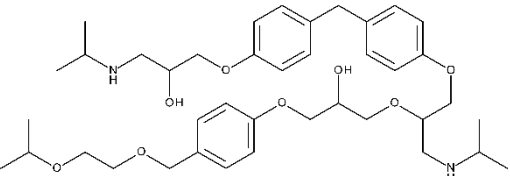
Results – Impurity Profiling of Bisoprolol Fumarate

<p>PI 2.14 / PI 2.15 (C₂₂H₃₁NO₅)</p>		<p>65.4 (both)</p>	<p>C, D, I, L</p>	<p>n/a</p>
<p>PI 2.16b (C₂₃H₃₃NO₅)</p>		<p>80.0</p>	<p>D</p>	<p>n/a</p>
<p>PI 2.19 (C₂₁H₃₆ClNO₅)</p>		<p>89.5</p>	<p>A, C, D, F, G, I, J</p>	<p>-a -j</p>
<p>PI 2.20 or PI 2.47 (C₂₁H₃₅NO₅)</p>		<p>96.2 (both)</p>	<p>A, C, D, G, I, K, L, P</p>	<p>-j -m</p>
<p>PI 2.46 (C₂₁H₃₇NO₆)</p>		<p>68.9</p>	<p>A, F, K, M</p>	<p>-m</p>
<p>U1 (C₁₁H₂₅NO₃)</p>		<p>88.0</p>	<p>A, C, D, G, I</p>	<p>-a -d -h -(2d)</p>

Results – Impurity Profiling of Bisoprolol Fumarate

U2 (C ₁₄ H ₂₃ NO ₃)		91.0	A, B, C, D, F, G, H, I, J, L, N, O	-(a+c+d)
U3 (C ₁₅ H ₂₅ NO ₃)		98.0	A, B, C, D, F, G, H, I, L, N, Q	-a -d -(a+f) -(a+g)
U4 (C ₂₃ H ₃₃ NO ₆)		91.4	A, C, D, G, H, I, L, P	-n
U5 (C ₂₆ H ₄₇ NO ₇)		95.0	A, B, C, E, G, I, K, L, P	-j -(d+j) -m -(d+m) -(2d+m) -(d+h+m) -(j+m)
U6 (C ₂₆ H ₄₇ NO ₇)		96.1	A, B, C, D, E, F, G, H, J, L, N, Q	-j -l -m -(d+m) -(j+l) -(2d+m)

Results – Impurity Profiling of Bisoprolol Fumarate

<p>U7 (C₂₇H₅₀N₂O₇)</p>		<p>98.9 / 96.8</p>	<p>A, B, C, D, F, G, H, I, J, K, L, M, P</p>	<p>-(a+k) -(a+d+k) -(a+d+e+k) -m -(d+m) -(e+m) -(a+d+j+k) -(k+m) -(a+k+m)</p>
<p>U8 (C₃₃H₅₃NO₈)</p>		<p>97.0 / 92.8</p>	<p>A, B, C, D, E, F, G, H, I, J, K, L, O, P</p>	<p>-a -m -(d+m) -(e+m) -(d+e+m)</p>
<p>U9 (C₃₃H₅₃NO₈)</p>		<p>91.3</p>	<p>A, C, D, E, F, G, H, J, K, L, N, P, Q</p>	<p>-m -(d+e+m)</p>
<p>U10 (C₄₀H₆₀N₂O₈)</p>		<p>92.2</p>	<p>A, C, F, G, I, L</p>	<p>-j -m -(a+m)</p>

Discrimination between closely related substances cannot be achieved in all cases. The structures of the impurities were not proven experimentally and hence, constitutional isomers to the structures given in Table 4 need to be considered. For example, PI 2.20 and PI 2.47 are constitutional isomers. In this case, the *in silico* fragmentation for the two molecules fit the experimental MS/MS data equally well (Figure 3). However, the plausibility to occur in the API can be compared considering other factors, e.g. the point of possible emergence in the synthesis and the impurity's reactivity. In specific, isopropylamine and other nucleophiles are used in excess upon the synthesis and are conjectured to react with any oxirane moieties, which lowers the chance of the presence of PI 2.20 [46]. The distinct differentiation between potentially mutagenic and harmless substances should be the major objective of *in silico* fragmentation, as different rules apply for these kinds of impurities. Hence, it might not be necessary to determine the definite constitution of impurities in some cases if the consequences are the same for both isomers.

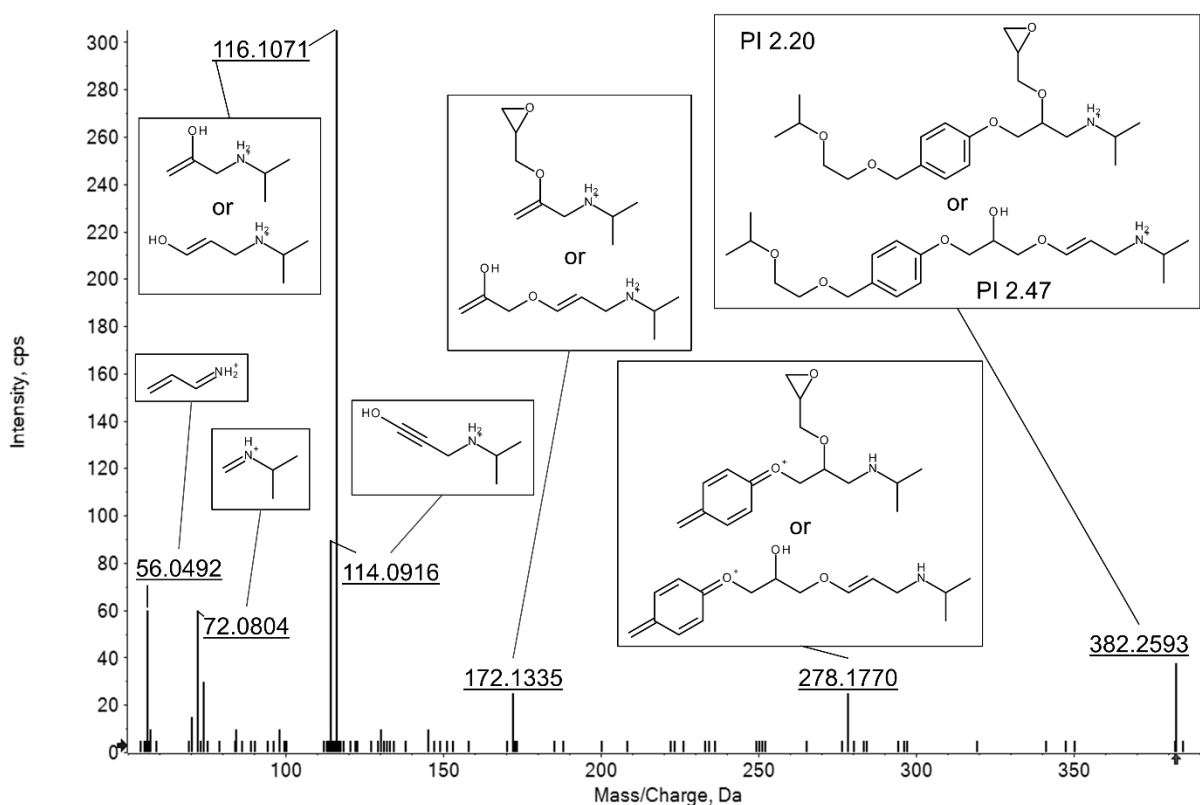


Figure 3 Fragment spectrum and assignment of signals to potential fragments of PI 2.20 and PI 2.47

3.4.3.3 Structure elucidation (untargeted approach)

Based on an untargeted peak finding procedure, GUCS was performed to detect signals, which occur in samples but not in blank injections (peak area ratio > 10). New

impurities were elucidated using the same information as described above: Molecular formulae based on exact mass and isotopic ratio, and structural formulae based on *in silico* fragmentation and assignment of characteristic fragments and neutral losses (cf. Table 3).

The untargeted approach yielded 17 additional signals. Plausible structural formulae could be derived for U1-U10, depicted in Table 4. U11-U17 are low concentrated isomers of other impurities (U11+U12: impurity N, U13+U14: impurity K, U15: PI 2.2, U16: impurity G and U17: PI 2.46). They produced additional signals with low intensities in respective XICs, making a reasonable evaluation difficult and preventing the establishment of structures. Negative mode measurements did not show any signals except fumarate and some fragments of bisoprolol, indicating the absence of acidic impurities.

Upon elucidation of the structures of impurities, not only the plausibility of the fragment spectra, but also the synthetic plausibility of the molecules was considered. In most cases, the structures given in Table 4 are plausible from both angles. However, some impurities' structures fit the experimental MS/MS data well but appear unlikely from the view of the synthesis procedure (cf. Figure 1). For example, the fragment spectra of U7 and U8 show the neutral loss of (e+m), corresponding to C₂H₄O and C₁₂H₁₈O₃, respectively (cf. Table 3), which implies the existence of a cleavable 2-hydroxyethyl moiety. Such impurities can be explained only by reactions of possible impurities of starting materials, which appear in low amounts. Thus, they take part in side reactions less likely than the reactants itself and respective impurities are less likely to occur in the final API. In contrast, molecules with an isopropoxyethoxy moiety (j) appear more plausible from the synthesis perspective but cannot explain the observed neutral loss.

3.4.3.4 Quantification of impurities

Considering the large number of detected impurities, the preparation of standard substances for the quantification of every impurity is impractical and very time-consuming. Furthermore, normalization to the bisoprolol peak is not reasonable in LC-MS due to detector saturation. Hence, quantification was performed by means of an IS as a straightforward alternative for the assessment of multiple analytes in a single run. An IS with similar physicochemical properties and thus, similar ionization efficiency was selected, i.e. metoprolol succinate. The ionization efficiency of analytes in ESI depends on the ratio of ionized molecules, determined by the basicity (pK_a) as well as

the affinity towards the drop surface, determined by polarity, distribution coefficient and molecular weight [47]. Metoprolol succinate was chosen as an IS because it shows the same chemical environment for the basic nitrogen as the detected impurities. Moreover, with metoprolol being smaller than most impurities, higher ionization efficiencies can be expected for larger impurities (higher lipophilicity), which leads to an overestimation of the analytes' contents and thus minimizes the risk of missing relevant compounds. This assumption can be extended to the alternative IS impurity C as it is the smallest of all impurities containing two basic nitrogen atoms.

The molar CFs of impurities C and Q with respect to the IS (Figure 4) were calculated from the slopes of respective linear regression curves (Figure 5). The response of the $[M+H]^+$ species of impurity C is distinctly lower than for metoprolol and impurity Q. This is due to the presence of two basic nitrogen atoms in impurity C, which leads to the formation of double charged species $[M+2H]^{2+}$ and lowers the intensity of $[M+H]^+$.

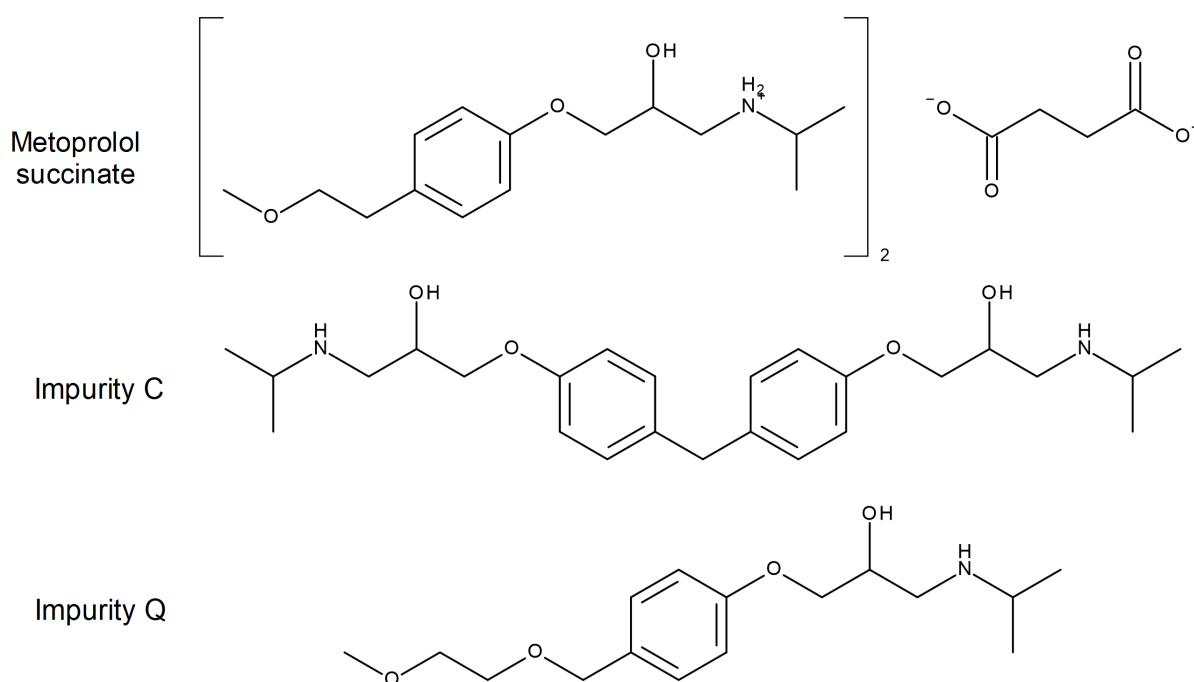


Figure 4 Structural formulae of metoprolol succinate, impurity C and impurity Q

Results – Impurity Profiling of Bisoprolol Fumarate

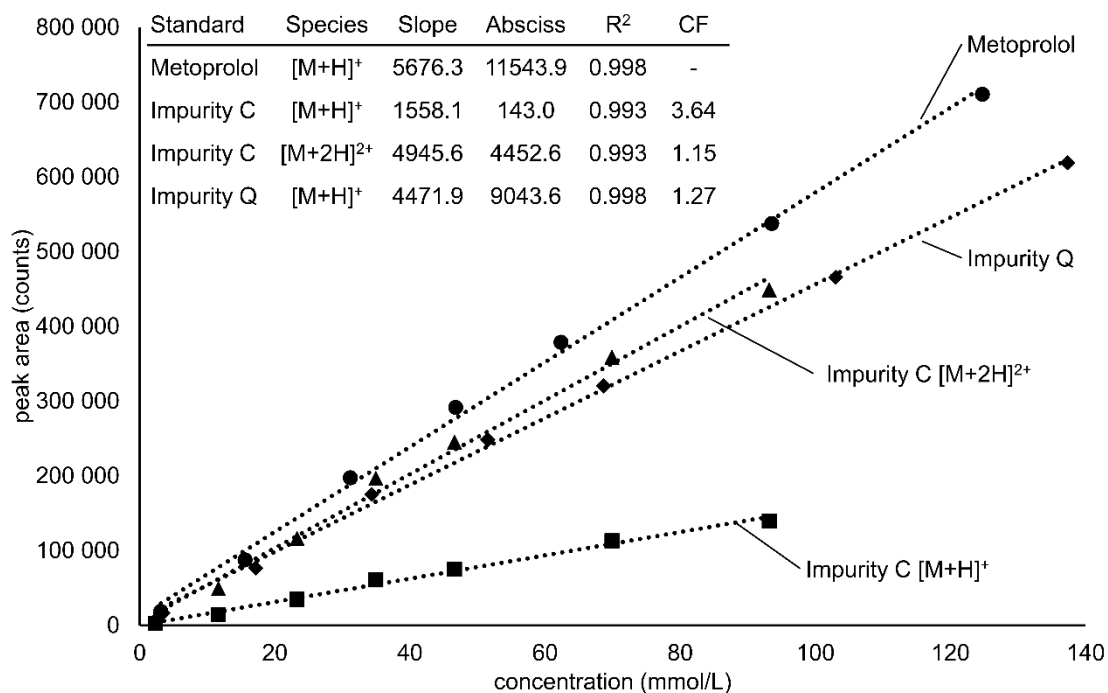
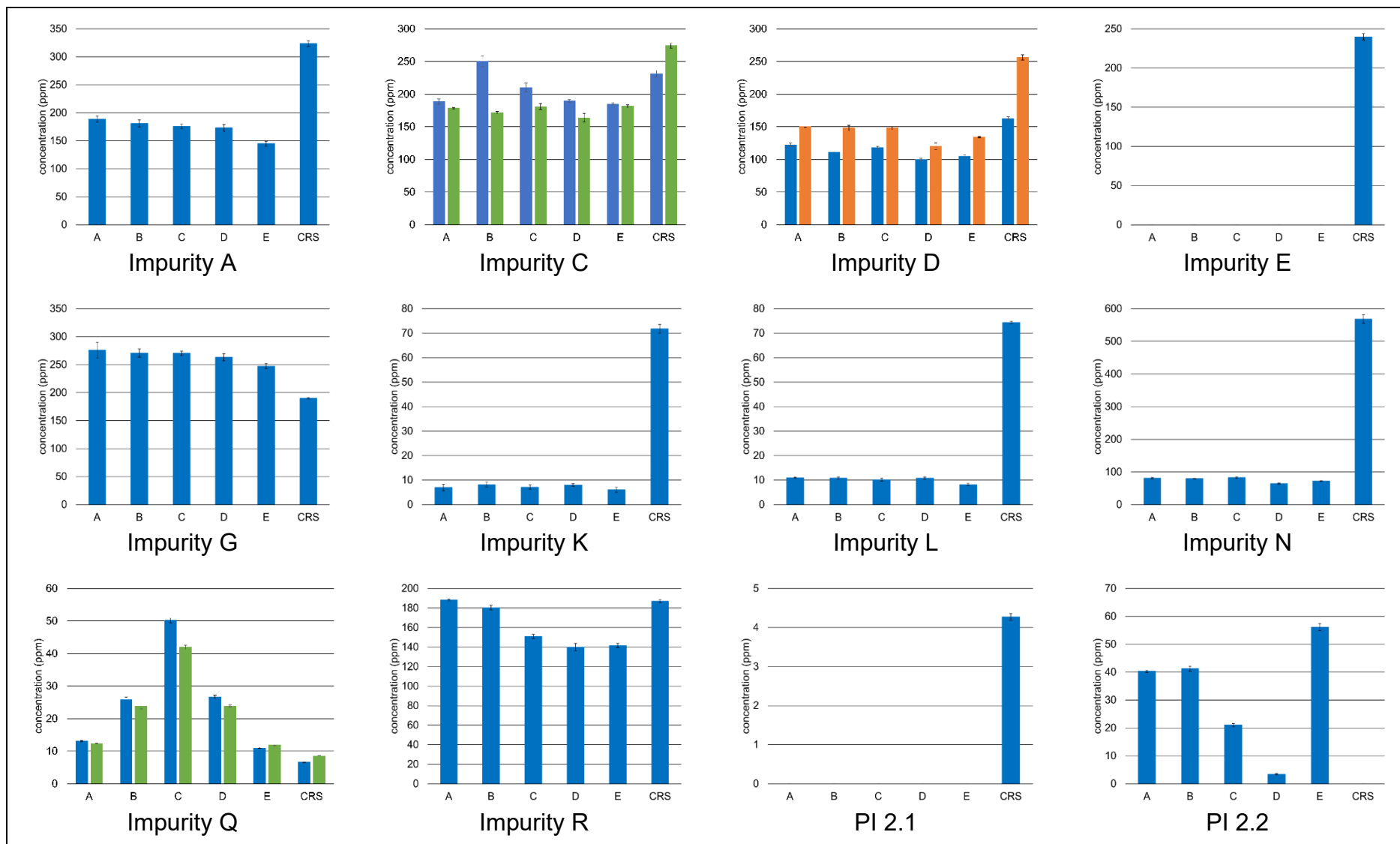


Figure 5 Linear regression curves of metoprolol, impurity Q and impurity C (single and double charged) (CF = correction factor)

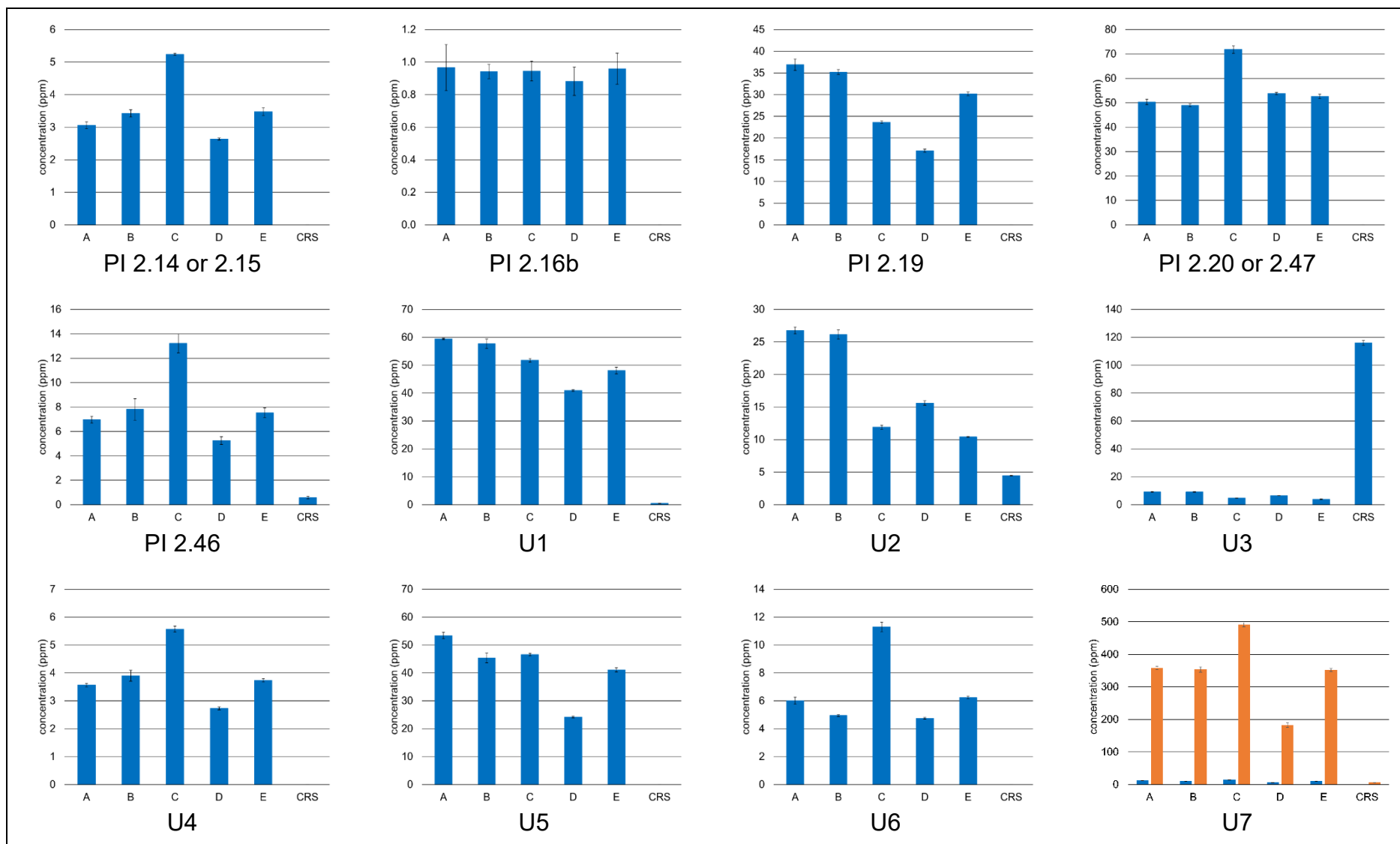
The maximum concentrations of related substances, PIs and new impurities in Arevipharma batches were 0.026% of impurity G, 0.007% of PI 2.47, and 0.049% of U7, respectively. The highest contamination of the CRS was impurity N with 0.047%. Thus, all impurities are below or at the reporting threshold of 0.05% according to ICH Q3A (R2) for both CRS and the Arevipharma batches [8]. An overview of all quantification results is depicted in Table 5.

Results – Impurity Profiling of Bisoprolol Fumarate

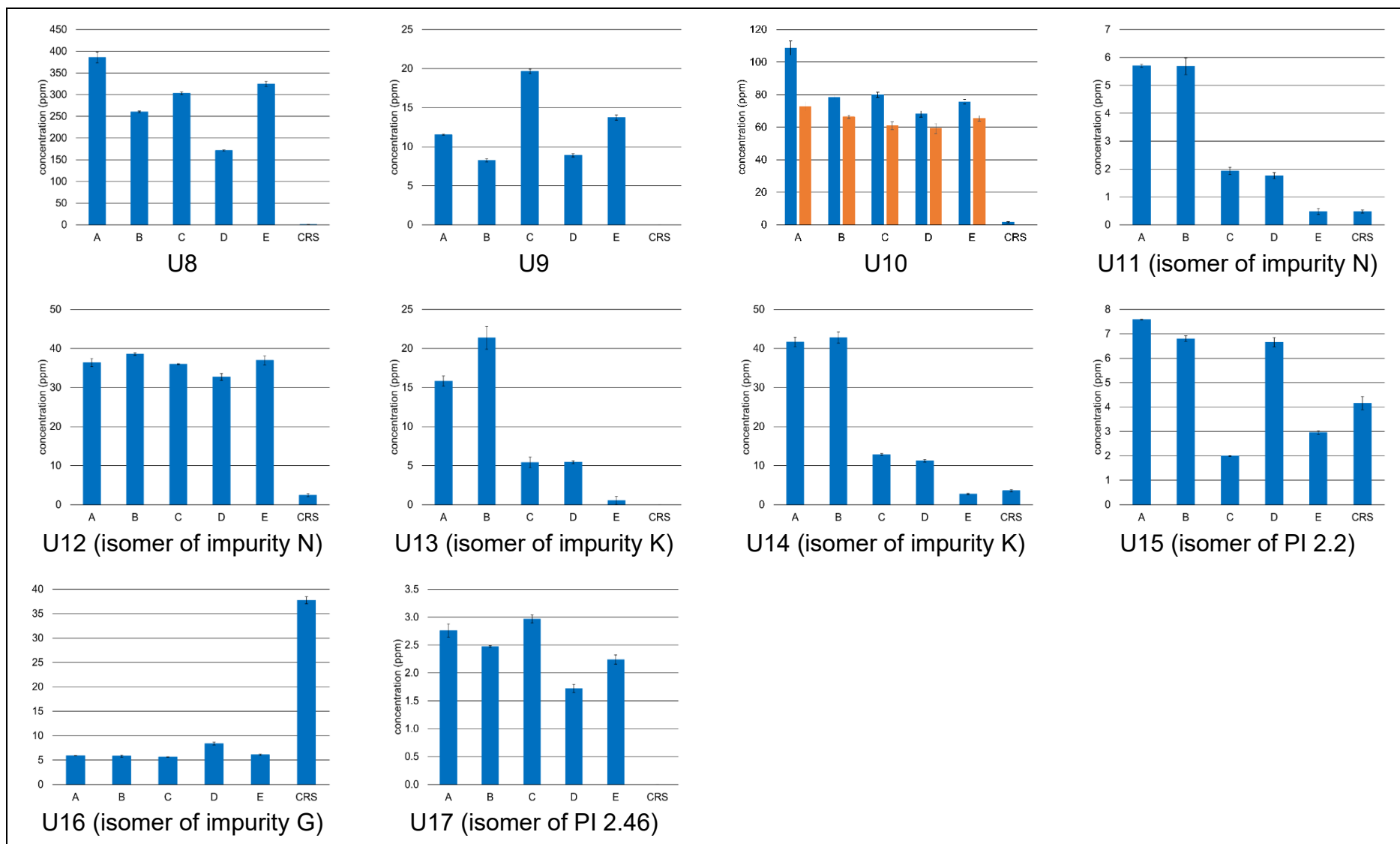
Table 5 Contents of all impurities in the analyzed batches (blue: IS metoprolol, green: external calibration, orange: IS impurity C), n = 3, ± 1 sdv



Results – Impurity Profiling of Bisoprolol Fumarate



Results – Impurity Profiling of Bisoprolol Fumarate



The concentrations of the PhEur impurities C and Q were determined considering the IS, and additionally by linear regression. For impurity Q, both evaluation methods yielded similar results (cf. Table 5). Thus, usage of the IS metoprolol is reasonable for the quantification of impurities with one basic nitrogen atom. In contrast, quantification of the double basic impurity C with the IS method led to overestimation of the concentration when compared to the linear regression (cf. Table 5). However, overestimation of impurity contents is acceptable because it decreases the risk of overlooking relevant substances.

Impurities with two basic nitrogen atoms were quantified in two ways. Firstly, metoprolol was used as IS considering the double charged species $[M+2H]^+$ of the impurity with a correction factor of 1.15 (cf. Figure 5). Secondly, impurity C was used as an alternative standard after determination of its content by linear regression. Here, the $[M+H]^+$ species was considered. Thus, quantification of double basic impurities was performed considering both the single (IS: impurity C) and the double charged species (IS: metoprolol). The higher of the two calculated concentrations was considered in the evaluation.

The highest content was found for U7, which contains two basic nitrogen atoms and was thus quantified with respect to the $[M+2H]^{2+}$ species (IS: metoprolol) and the $[M+H]^+$ species (IS: impurity C). In contrast to all other double basic impurities, the $[M+H]^+$ species of U7 is more abundant than the $[M+2H]^{2+}$ (cf. Figure 5). Hence, an overestimation of the content results when using $[M+H]^+$ (0.049%), while usage of $[M+2H]^{2+}$ (0.001%) leads to significant underestimation and the “true” content lies somewhere between these values.

It is well-known that the impurity profile of an API depends on the respective synthesis pathway [48], which is mirrored in the amounts of the impurities (cf. Table 5). The concentrations of the impurities differ significantly between the Arevipharma batches and the CRS in most cases. As can be expected, PhEur related substances occur in higher concentrations in the CRS while PIs are present mostly in the Arevipharma batches. 12 out of the 35 detected impurities occur only in bisoprolol fumarate of one origin, i.e. either in Arevipharma batches or in CRS.

3.4.3.5 Structural alerts

The only impurities carrying structural alerts which are not part of the bisoprolol molecule, are the alkene in impurity E, the haloalkane PI 2.19 and the oxiranes of PIs

1.31 and PI 2.20 [9, 10]. PI 1.31 was synthesized to check whether the detected compound is in fact the suspected molecule as the *in silico* plausibility was 37.4% only. Injection of the synthesized substance did not give a peak for the expected m/z of 181.0859 for $[M+H]^+$, but two peaks for the $[M+H-H_2O]^+$ species (m/z 163.0754). The retention times differed from the signal detected in the bisoprolol fumarate samples: 7.04 and 9.23 min (PI 1.31) vs. 8.41 min (impurity in samples). Thus, the substance detected at m/z 181.0859 is not PI 1.31. Due to the low signal intensity, an alternative structure could not be developed.

Obviously, the oxirane moiety is too labile for detection applying the described method. Hence, the presence of PI 2.20 is unlikely compared to PI 2.47. More specific analytics might be necessary for the detection of oxirane containing impurities.

Concluding, the only detected impurity with a structural alert present in the Arevipharma batches is PI 2.19, which is present at a maximal concentration of 37 ppm (equivalent to 0.004%). Impurity E is only present in CRS (0.024%).

3.4.4 Conclusion

The detection of impurities in both the targeted and the untargeted evaluation demonstrates the suitability and necessity of the combined approach. The reaction matrix proved its capability to generate PIs relevant for the total impurity profile. However, not all present impurities could be predicted, as additional compounds were detected in the untargeted approach. Hence, a combination of these procedures is recommended to generate an impurity profile as comprehensive as possible. However, such an approach may not only be applied during drug development, but also after changes of production methods and modifications in the supply chain.

Naturally, impurities of APIs as analyzed in this study, are a major contribution to the overall impurity profile of a medicinal product. However, impurities of excipients as well as interaction/reaction products of the API with excipients and primary packaging materials (and impurities thereof) must be analyzed and controlled, too [49, 50]. Therefore, the presented approach might be useful for the analysis of finished drug products as well.

With the aim of maximizing the number of detectable analytes, different LC and MS conditions were applied. Yet, there are many more possibilities to extend the versatility of the approach like different stationary phases, detection methods, sample

preparation etc. Thus, the presented method is a compromise between straightforwardness and time/cost investment.

Upon the establishment of new impurity structures, both MS/MS information and the synthetic pathway of the API were considered. For the latter, reactants, solvents, and catalysts were regarded. However, also impurities of the reagents used can participate in side reactions and contribute to the API's impurity profile. Hence, the establishment of impurity profiles of all substances used is necessary to reach a most comprehensive overview of possible side reactions.

The synthesis assessment described (Supplementary Information) is based on detailed information: synthesis route, used reagents, reactants, raw materials, catalysts and their impurities, purification processes, and possible degradants of intermediate impurities. Only manufactures can create such a detailed synthesis assessment, which should go along with the production process. The data should be reported to buyers of the APIs, market authorization holders and, of course, regulatory authorities.

In this work, only the synthesis procedure applied by Arevipharma was considered, and only samples from this manufacturer and CRS were analyzed. Hence, the described impurity profile is valid for this specific product only. However, many different manufacturers produce the API bisoprolol fumarate, presumably applying different synthetic conditions and routes. A comparison of the impurity profiles of APIs produced from different manufacturers could be an interesting advancement of this study but is only possible with detailed information regarding the applied synthetic conditions. However, the establishment of a reaction matrix and a targeted/untargeted analysis should be performed for each and every drug synthesis.

Funding

This research did not receive any specific grant from funding agencies in the public, commercial, or not-for-profit sectors.

Acknowledgements

The authors thank AB Sciex (Concord, Ontario, Canada) and IBMP (Heroldsberg, Germany) for the possibility to use the LC-MS system.

CRediT authorship contribution statement

Jonas Wohlfart: Methodology, Formal Analysis, Investigation, Writing – Original Draft.

Elisabeth Jäckel: Conceptualization, Resources, Writing – Review & Editing. **Oliver**

Scherf-Clavel: Methodology, Writing – Review & Editing. **Dirk Jung:** Resources,

Supervision, Project administration, Funding acquisition. **Martina Kinzig:** Resources.

Fritz Sörgel: Resources. **Ulrike Holzgrabe:** Conceptualization, Writing – Review &

Editing, Supervision, Project administration.

3.4.5 References

- [1] Merck KGaA, Fachinformation (Zusammenfassung de Merkmale des Arzneimittels) Concor 5 mg/10 mg Filmtabletten. <https://www.fachinfo.de/suche/fi/003991>, 2020 (accessed 28 June 2021).
- [2] Barmer, Barmer Arzneimittelreport 2020. <https://www.barmer.de/blob/254084/b1fa6438da1c611b757a7b74b982f62a/data/dl-barmer-arzneimittelreport.pdf>, 2020 (accessed 28 June 2021).
- [3] LePro PharmaCompass OPC Private Limited, Bisoprolol fumarate. <https://www.pharmacompass.com/active-pharmaceutical-ingredients/bisoprolol-fumarate>, 2021 (accessed 11th June 2021).
- [4] Vidal MMI Germany GmbH, Bisoprolol fumarat. https://www.gelbe-liste.de/wirkstoffe/Bisoprolol-fumarat_24876, 2021 (accessed 28 June 2021).
- [5] A. Kleemann, J. Engel, B. Kutscher, D. Reichert, Pharmaceutical Substances: Syntheses, Patents and Applications of the most relevant APIs, 5th edition, Georg Thieme Verlag KG, Stuttgart, Germany, 2009.
- [6] D. V. Soloviev, M. Matarrese, R. M. Moresco, S. Todde, T. A. Bonasera, F. Sudati, P. Simonelli, F. Magni. D. Colombo, A. Carpinelli, M. G. Kienle, F. Fazio, Asymmetric synthesis and preliminary evaluation of R and (S)-[^{11}C]-bisoprolol, a putative β_1 -selective adrenoreceptor radioligand, *Neurochem. Int.* 38 (2001) 169-180. [https://doi.org/10.1016/S0197-0186\(00\)00049-8](https://doi.org/10.1016/S0197-0186(00)00049-8).
- [7] Z. Fumin, Preparation method of chiral bisoprolol fumarate, Jiangsu Yuexing Pharmaceutical Co Ltd (2021), CN112194587A.
- [8] International Council for Harmonisation of Technical Requirements for Pharmaceuticals for Human Use, ICH Topic Q3A (R2) Impurities in new Drug Substances. <https://database.ich.org/sites/default/files/Q3A%28R2%29%20Guideline.pdf>, 2006 (accessed 28 June 2021).
- [9] A. F. Stepan, D. P. Walker, J. Bauman, D. A. Price, T. A. Baillie, A. S. Kalgutkar, M. D. Aleo, Structural Alert/Reactive Metabolite Concept as Applied in Medicinal Chemistry to Mitigate the Risk of Idiosyncratic Drug Toxicity: A Perspective Based on the Critical Examination of Trends in the Top 200 Drugs Marketed in the United States, *Chem. Res. Toxicol.* 24 (2011) 1345-1410. <https://doi.org/10.1021/tx200168d>.
- [10] S. D. Nelson, Metabolic activation and drug toxicity, *J. Med. Chem.* 25 (1982) 753-765. <https://doi.org/10.1021/jm00349a001>.
- [11] L. W. Wormhoudt, J. N. M. Commandeur, N. P. E. Vermeulen, Genetic Polymorphisms of Human N-Acetyltransferase, Cytochrome P450, Glutathione-S-Transferase, and Epoxide Hydrolase Enzymes: Relevance to Xenobiotic Metabolism and Toxicity, *Crit. Rev. Toxicol.* 29 (1999) 59-124. <https://doi.org/10.1080/10408449991349186>.
- [12] R. Snyder, C. C. Hedli, An overview of benzene metabolism, *Environ. Health Perspect.* 104 (1996) 1165-1171. <https://doi.org/10.1289/ehp.961041165>.
- [13] International Council for Harmonisation of Technical Requirements for Pharmaceuticals for Human Use, ICH guideline M7 (R1) on assessment and

- control of DNA reactive (mutagenic) impurities in pharmaceuticals to limit potential carcinogenic risk.
https://database.ich.org/sites/default/files/M7_R1_Guideline.pdf, 2015 (accessed 28 June 2021).
- [14] A. Nuez, R. Rodríguez, Current methodology for the assessment of ADME-Tox properties on drug candidate molecules, *Biotechnol. Apl.* 25 (2008) 97-110
- [15] H. Yang, J. Lie, Z. Wu, W. Li, G. Liu, Y. Tang, Evaluation of Different Methods for Identification of Structural Alerts Using Chemical Ames Mutagenicity Data Set as a Benchmark, *Chem. Res. Toxicol.* 30 (2017) 1355-1364
- [16] L. Coqin, S. J. Canipa, W. C. Drewe, L. Fisk, V. J. Gillet, M. Patel, J. Plante, R. J. Sherhod, J. D. Vessey, New structural alerts for Ames mutagenicity discovered using emerging pattern mining techniques, *Toxicol. Res.* 4 (2015) 46-56
- [17] International Council for Harmonisation of Technical Requirements for Pharmaceuticals for Human Use, ICH Topic Q1A (R2) Stability Testing of new Drug Substances and Products.
<https://database.ich.org/sites/default/files/Q1A%28R2%29%20Guideline.pdf>, 2003 (accessed 28 June 2021).
- [18] International Council for Harmonisation of Technical Requirements for Pharmaceuticals for Human Use, ICH guideline Q3C (R8) on impurities: guideline for residual solvents.
https://database.ich.org/sites/default/files/ICH_Q3C-R8_Guideline_Step4_2021_0422_1.pdf, 2019 (accessed 28 June 2021).
- [19] International Council for Harmonisation of Technical Requirements for Pharmaceuticals for Human Use, ICH Q3D (R1) on elemental impurities.
https://www.ema.europa.eu/en/documents/scientific-guideline/international-conference-harmonisation-technical-requirements-registration-pharmaceuticals-human-use_en-32.pdf, 2019 (accessed 6 July 2021).
- [20] A. Leistner, S. Haerling, J.-D. Kreher, I. Becker, D. Jung, U. Holzgrabe, 2020. Risk assessment report of potential impurities in cetirizine dihydrochloride, *J. Pharm. Biomed. Anal.* 189,113425. <https://doi.org/10.1016/j.jpba.2020.113425>.
- [21] F. Sörgel, M. Kinzig, M. Abdel-Tawab, C. Bidmon, A. Schreiber, S. Ermel, J. Wohlfart, A. Besa, O. Scherf-Clavel, U. Holzgrabe, The contamination of valsartan and other sartans, part 1: New findings, *J. Pharm. Biomed. Anal.* 172 (2019) 395-405. <https://www.doi.org/10.1016/j.jpba.2019.05.022>.
- [22] O. Scherf-Clavel, M. Kinzig, A. Besa, A. Schreiber, C. Bidmon, M. Abdel-Tawab, J. Wohlfart, F. Sörgel, U. Holzgrabe, The contamination of valsartan and other sartans, Part 2: Untargeted screening reveals contamination with amides additionally to known nitrosamine impurities, *J. Pharm. Biomed. Anal.* 172 (2019) 278-284. <https://doi.org/10.1016/j.jpba.2019.04.035>.
- [23] J. D. Whitman, K. L. Lynch, Optimization and comparison of information-dependent acquisition (IDA) to sequential window acquisition of all theoretical fragment ion spectra (SWATH) for high-resolution mass spectrometry in clinical toxicology, *Clin. Chem.* 65 (2019) 862-870.
<https://doi.org/10.1373/clinchem.2018.300756>.

- [24] M. Raetz, R. Bonner, G. Hopfgartner, SWATH-MS for metabolomics and lipidomics: critical aspects of qualitative and quantitative analysis, *Metabolomics* 16 (2020) 71. <https://doi.org/10.1007/s11306-020-01692-0>.
- [25] A. M. Knolhoff, J. A. Zweigenbaum, T. R. Croley, Nontargeted Screening of Food Matrices: Development of a Chemometric Software Strategy To Identify Unknowns in Liquid Chromatography–Mass Spectrometry Data, *Anal. Chem.* 88 (2016) 3617-3623. <https://www.doi.org/10.1021/acs.analchem.5b04208>.
- [26] F. L. Sauvage, N. Picard, F. Saint-Marcoux, J. M. Gaulier, G. Lachâtre, P. Marquet, General unknown screening procedure for the characterization of human drug metabolites in forensic toxicology: applications and constraints, *J. Sep. Sci.* 32 (2009) 3074-3083. <https://doi.org/10.1002/jssc.200900092>.
- [27] T. Bruderer, E. Varesio, A. O. Hidas, E. Duchoslav, L. Burton, R. Bonner, G. Hopfgartner, Metabolomic spectral libraries for data-independent SWATH liquid chromatography mass spectrometry acquisition, *Anal. Bioanal. Chem.* 410 (2018) 1873-1884. <https://www.doi.org/10.1007/s00216-018-0860-x>.
- [28] T. Kind, O. Fiehn, Advances in structure elucidation of small molecules using mass spectrometry, *Bioanal. Rev.* 2 (2010) 23-60. <https://www.doi.org/10.1007/s12566-010-0015-9>.
- [29] Y. Djoumbou-Feunang, A. Pon, N. Karu, J. Zheng, C. Li, D. Arndt, M. Gautam, F. Allen, D. S. Wishart, CFM-ID 3.0: Significantly Improved ESI-MS/MS Prediction and Compound Identification, *Metabol.* 9 (2019) 72. <https://doi.org/10.3390/metabo9040072>
- [30] C. A. Krettler, G. G. Thallinger, A map of mass spectrometry-based in silico fragmentation prediction and compound identification in metabolomics, *Brief. Bioinform.* 22 (2021) bbab073. <https://doi.org/10.1093/bib/bbab073>.
- [31] Bisoprolol Fumarate in: European Pharmacopoeia 10.0, Council of Europe, Strasbourg, France, 2020.
- [32] Bisoprolol Fumarate in: Japanese Pharmacopoeia 18, Pharmaceuticals and Medical Devices Agency, Tokyo, Japan, 2021.
- [33] Bisoprolol fumarate in: USP 43-NF 38, U.S. Food and Drug Administration, Silver Spring, Maryland, USA, 2020.
- [34] AB Sciex, Turbo VTM Ion Source Operator Guide (RUO-IDV-05-6147-B). <https://sciex.com/content/dam/SCIEX/pdf/customer-docs/operator-guide/turbo-v-operator-guide-en.pdf>, 2018 (accessed 28 June 2021).
- [35] Chapter 2.2.46 Chromatographic separation techniques in: European Pharmacopoeia 10.0, Council of Europe, Strasbourg, France, 2020
- [36] J.-P. Antignac, K. de Wasch, F. Monteau, H. De Brabander, F. Andre, B. Le Bizec, The ion suppression phenomenon in liquid chromatography–mass spectrometry and its consequences in the field of residue analysis, *Anal. Chimica Acta* 529 (2005) 129-136. <https://doi.org/10.1016/j.aca.2004.08.055>.
- [37] R. Kostianen, T. J. Kauppila, Effect of eluent on the ionization process in liquid chromatography–mass spectrometry, *J. Chromatogr. A* 1216 (2009) 685-699. <https://doi.org/10.1016/j.chroma.2008.08.095>.

- [38] A. Tan, J. C. Fanaras, 2019. Use of high-pH (basic/alkaline) mobile phases for LC–MS or LC–MS/MS bioanalysis, *Biomed. Chromatogr.* 33, e4409. <https://www.doi.org/10.1002/bmc.4409>.
- [39] S. Almeling, U. Holzgrabe, Use of evaporative light scattering detection for the quality control of drug substances: Influence of different liquid chromatographic and evaporative light scattering detector parameters on the appearance of spike peaks, *J. Chromatogr. A* 1217 (2010) 2163-2170. <https://www.doi.org/10.1016/j.chroma.2010.02.017>.
- [40] D. Brecht, F. Uteschil, O. J. Schmitz, 2020. Development of a fast-switching dual (ESI/APCI) ionization source for liquid chromatography/mass spectrometry, *Rapid Commun. Mass Spectrom.* 34, e8845. <https://www.doi.org/10.1002/rcm.8845>.
- [41] X. Zhu, Y. Chen, R. Subramanian, Comparison of Information-Dependent Acquisition, SWATH, and MSAll Techniques in Metabolite Identification Study Employing Ultrahigh-Performance Liquid Chromatography–Quadrupole Time-of-Flight Mass Spectrometry, *Anal. Chem.* 86 (2014) 1202-1209. <https://www.doi.org/10.1021/ac403385y>.
- [42] T. Reemtsma, Determination of molecular formulas of natural organic matter molecules by (ultra-) high-resolution mass spectrometry: Status and needs, *J. Chromatogr. A* 1216 (2009) 3687-3701. <https://doi.org/10.1016/j.chroma.2009.02.033>.
- [43] AB Sciex, LC-MS/MS analysis of emerging food contaminants. Identification of Artificial Colors and Dyes in Food Samples using LC-HR-MS/MS. https://sciex.com/content/dam/SCIEX/pdf/brochures/emerging_food_X500R_QT_OF_food_dyes.pdf, 2016 (accessed 17 August 2021).
- [44] P. Brown, Occurrence and timing of the rearrangement of benzyl ions to tropylium ions in the mass spectra of substituted benzyl phenyl ethers, *J. Am. Chem. Soc.* 90 (1968) 2694-2696.
- [45] J. H. Gross, Fragmentierung organischer Ionen und Interpretation von EI-Massenspektren, in: *Massenspektrometrie*, Springer Verlag GmbH, Heidelberg, Germany, 2013, pp. 273-379.
- [46] T. Schirmeister, C. Schmuck, P. Wich, 6.2.4 Ausgewählte Verbindungen - Derivate der Glycole, in: *Beyer/Walter: Organische Chemie 25*, S. Hirzel Verlag, Stuttgart, Germany, 2016, pp. 191-193.
- [47] M. Oss, A. Krueve, K. Herodes, I. Leito, Electrospray ionization efficiency scale of organic compounds, *Anal. Chem.* 82 (2010) 2865-2872. <https://doi.org/10.1021/ac902856t>.
- [48] S. Görög, M. Babjak, G. Balogh, J. Brik, A. Csehi, F. Dravec, M. Gasdag, P. Horvath, A. Lauko, K. Varga, Drug impurity profiling strategies, *Talanta* 44 (1997) 1517-1526. [https://doi.org/10.1016/S0039-9140\(96\)02179-0](https://doi.org/10.1016/S0039-9140(96)02179-0).
- [49] K. Zhang, J. D. Pellett, A. S. Narang, Y. J. Wang, Y. T. Zhang, Reactive impurities in large and small molecule pharmaceutical excipients – A review, *Trends Anal. Chem.* 101 (2018) 34-42. <https://doi.org/10.1016/j.trac.2017.11.003>.

- [50] International Council for Harmonisation of Technical Requirements for Pharmaceuticals for Human Use, Impurities in New Drug Products Q3B (R2). <https://database.ich.org/sites/default/files/Q3B%28R2%29%20Guideline.pdf>, 2006 (accessed 28 June 2021).

3.4.6 Supplementary Information

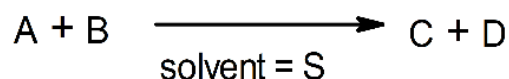
Identification of potential impurities and carryover considerations

To address the formation and fate of impurities in the whole manufacturing process of bisoprolol fumarate, it is necessary to evaluate all sources of potential impurities and transformations of the impurities via the process. Furthermore, the pathway of these compounds is considered over the whole process (synthesis & purification). Therefore, the impurity assessment is a two-stage process:

- Identification of potential impurities using a reaction matrix
- Carryover consideration to assign impurities that are likely to be present in the drug substance and further evaluation of their mutagenic potential (Hazard Assessment)

The identification of potential impurities is carried out by a reaction matrix, which contains starting materials, reagents, auxiliaries, intermediates, solvents and their impurities for each step of the process. Moreover, the chemical transformations of these potential impurities were examined under the process conditions. Each sub-step of the entire manufacturing process (reactions and purification steps) was considered to allow an in-depth evaluation.

A reaction matrix for the following exemplary reaction is given below:



	A	A1	A2	B	B1	C	D	S	I1	I2	I3
A	I1			I2	I...	I...	I...	I...	I...	I...	I...
B		I...	I...	I...		I...	I...			I...	I...
C		I...	I...		I...	I...	I...	I...			
D		I...	I...		I...		I...		I...	I...	I...
S		I...	I...		I...			I...	I...	I...	I...

In this matrix all used starting materials, reagents, auxiliaries, intermediates and solvents as well as their known and potential (concluded from their manufacturing process) impurities are listed in the first row. The first column is filled with all major compounds, and each intersect has been evaluated for potential reaction products.

In this context it is plausible to state that:

- a) It is unlikely that reactants (e.g. A) and their impurities (e.g. A1, A2) react with each other because of their co-existence in the starting material.
- b) It is unlikely that two impurities of starting materials or reagents (e.g. A1 + B1) react with each other due to their low concentrations. An exception of this rationale is solvent impurities because solvents are added in higher quantities.
- c) At a certain point, a further transformation of impurities into new species is unlikely due to incomplete conversions and decreasing concentrations of the required reactants (exception: solvents).

After evaluation of potential side products, all identified compounds are assessed regarding reactive groups, which can cause consecutive reactions. All “reactive” impurities are added to the first row and their interactions with the major compounds are considered until no “reactive” impurities are existent.

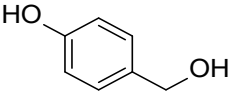
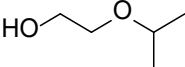
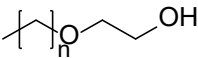
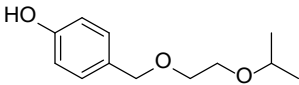
The probability of carry-over of potential impurities has been distinguished in 4 categories:

1. Unlikely to be carried over (green highlighted)
2. Likely to be depleted, but potential carry-over (yellow highlighted)
3. Likely to be carried over (blue highlighted)
4. Likely to be present in the final API (red highlighted)

Impurities of classes 2, 3 and 4 were transferred to the reaction matrix of the consecutive process step.

An extract of the reaction matrix developed at Arevipharma is shown below. For clarity reasons, this extract is not a complete listing of all potential contaminants in starting materials, reagents, solvents and potential impurities formed in the process.

Stage 1a: Formation of the intermediate IMH

Substance	Structure	Source	Carryover assessment
4-HMP		Starting material	<ul style="list-style-type: none"> Transformed by ether formation to desired product IMH or other impurities Residues of 4-HMP not fully depleted
Isopropoxyethanol		Solvent and reactant	<ul style="list-style-type: none"> Soluble in water Residues not fully depleted
1a.1 (n = 0-3)		Potential contaminant of isopropoxyethanol	<ul style="list-style-type: none"> Soluble in water Depletion during process step
IMH		Desired product	<ul style="list-style-type: none"> No depletion

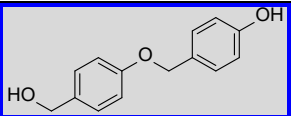
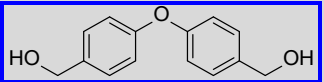
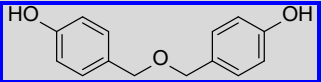
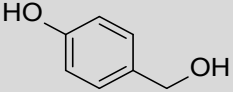
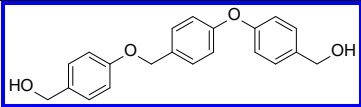
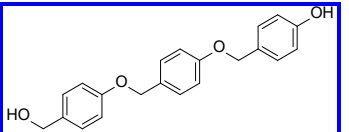
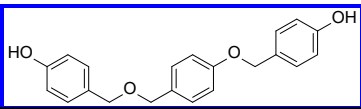
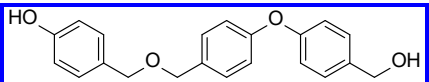
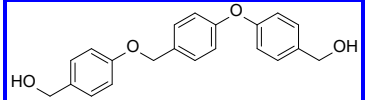
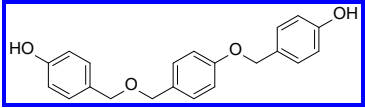
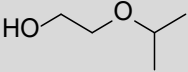
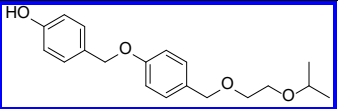
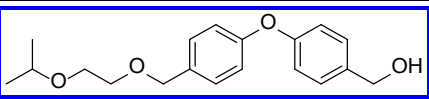
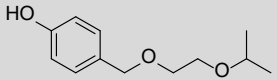
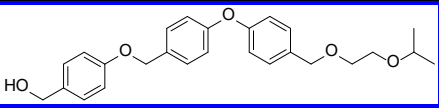
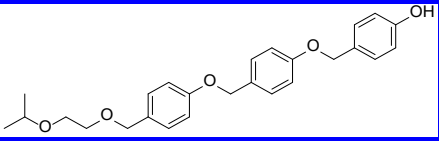
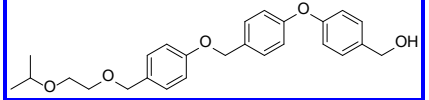
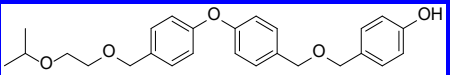
Results – Impurity Profiling of Bisoprolol Fumarate

1st generation impurities

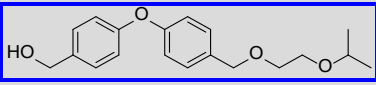
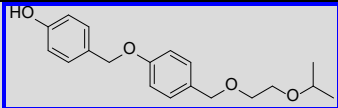
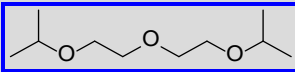
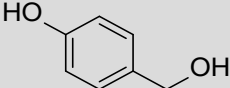
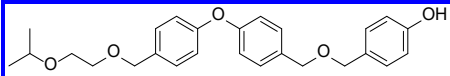
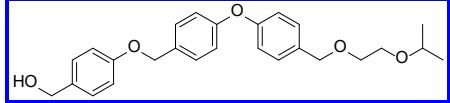
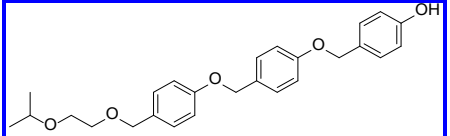
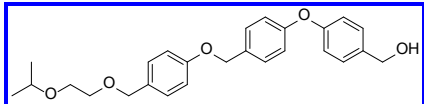
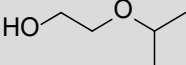
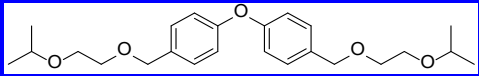
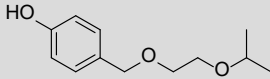
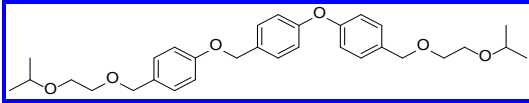
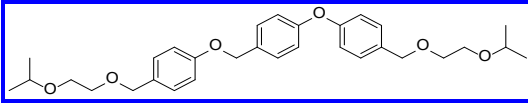
1 st gen Step 1a Formation of IMH	 4-HMP	 Isopropoxyethanol	 1a.1, n = 0-3	 IMH
 4-HMP	 1a.2	 IMH	 1a.8, n = 0-3	 1a.5
	 1a.3			 1a.6
	 1a.4			
 Isopropoxyethanol	 IMH	 1a.7	-	-
 IMH	 1a.5	-	-	 1a.9
	 1a.6	-	-	

Results – Impurity Profiling of Bisoprolol Fumarate

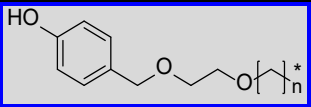
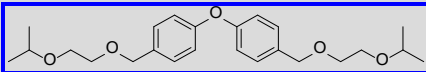
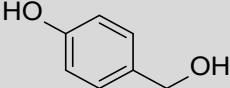
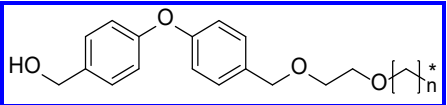
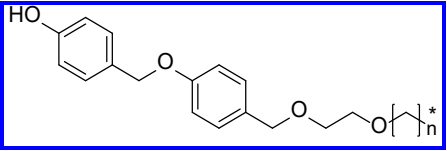
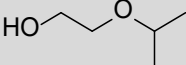
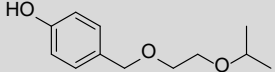
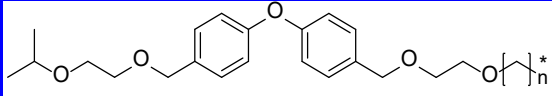
2nd generation impurities

<p>2nd gen Step 1a Formation of IMH</p>	 <p style="text-align: center;">1a.2</p>	 <p style="text-align: center;">1a.3</p>	 <p style="text-align: center;">1a.4</p>
<p>4-HMP</p> 	 <p style="text-align: right;">1a.10</p>  <p style="text-align: right;">1a.11</p>  <p style="text-align: right;">1a.12</p>	 <p style="text-align: center;">1a.15</p>  <p style="text-align: center;">1a.10</p>	 <p style="text-align: center;">1a.12</p>
<p>Isopropoxyethanol</p> 	 <p style="text-align: center;">1a.6</p>	 <p style="text-align: center;">1a.16</p>	<p style="text-align: center;">-</p>
<p>IMH</p> 	 <p style="text-align: center;">1a.13</p>  <p style="text-align: center;">1a.14</p>	 <p style="text-align: center;">1a.17</p>	 <p style="text-align: center;">1a.18</p>

Results – Impurity Profiling of Bisoprolol Fumarate

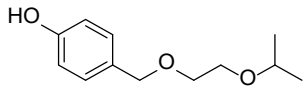
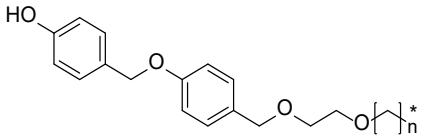
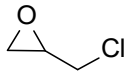
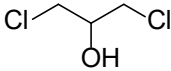
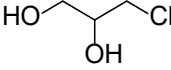
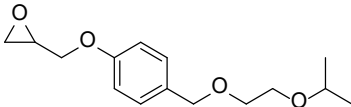
<p>2nd gen Step 1a Formation of IMH</p>	 <p style="text-align: center;">1a.5</p>	 <p style="text-align: center;">1a.6</p>	 <p style="text-align: center;">1a.7</p>
 <p style="text-align: center;">4-HMP</p>	 <p style="text-align: center;">1a.18</p>  <p style="text-align: center;">1a.13</p>	 <p style="text-align: center;">1a.14</p>  <p style="text-align: center;">1a.17</p>	-
 <p style="text-align: center;">Isopropoxyethanol</p>	 <p style="text-align: center;">1a.9</p>	-	-
 <p style="text-align: center;">IMH</p>	 <p style="text-align: center;">1a.19</p>	 <p style="text-align: center;">1a.19</p>	-

Results – Impurity Profiling of Bisoprolol Fumarate

<p>2nd gen Step 1a Formation of IMH</p>	 <p>1a.8, n = 0-3</p>	 <p>1a.9</p>
 <p>4-HMP</p>	 <p>1a.20, n = 0-3</p>  <p>1a.21, n = 0-3</p>	<p>-</p>
 <p>Isopropoxyethanol</p>	<p>-</p>	<p>-</p>
 <p>IMH</p>	 <p>1a.22, n = 0-3</p>	<p>-</p>

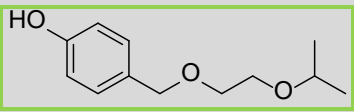
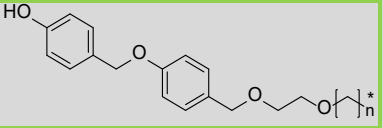
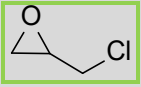
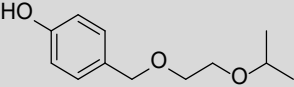
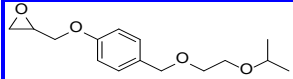
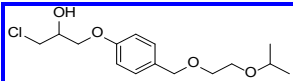
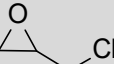
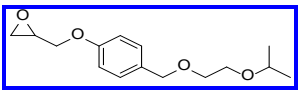
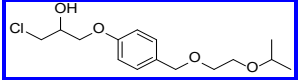
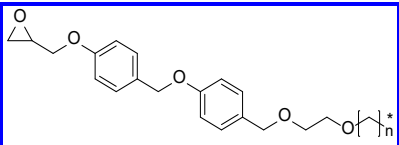
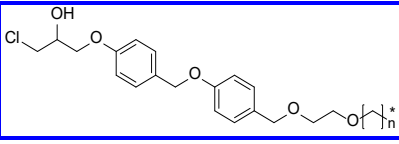
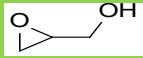
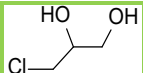
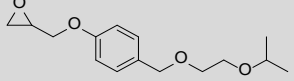
Stage 1b: Formation of the intermediate IPEP

Only selected impurities are displayed for better clarity.

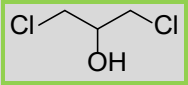
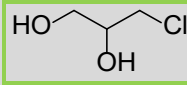
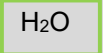
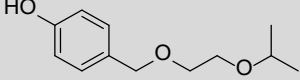
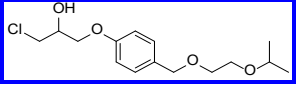
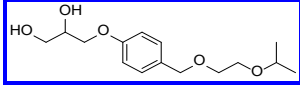
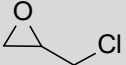
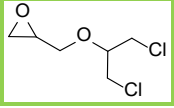
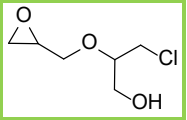
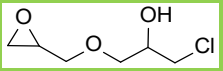
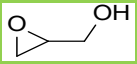
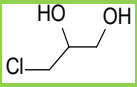
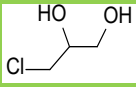
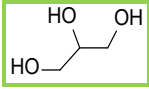
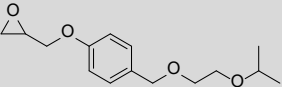
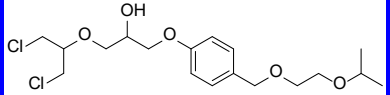
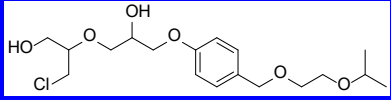
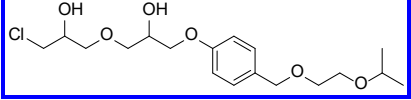
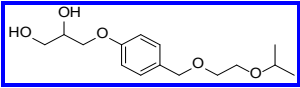
Substance	Structure	Source	Carryover assessment
IMH		Starting material	<ul style="list-style-type: none"> Transformed by reaction with epichlorohydrin and contaminants of epichlorohydrin Depletion during process step
1a.21, n = 0-3		Potential contaminant of IMH	<ul style="list-style-type: none"> Transformed by reaction with epichlorohydrin and contaminants of epichlorohydrin Depletion during process step
Epichlorohydrin		Starting material	<ul style="list-style-type: none"> Transformed by reaction with e.g. phenols and benzylic alcohols Depletion during process step
1b.1		Potential contaminant of epichlorohydrin	<ul style="list-style-type: none"> Transformed by reaction with e.g. phenols and benzylic alcohols Depletion during process step
1b.2		Potential contaminant of epichlorohydrin	<ul style="list-style-type: none"> Transformed by reaction with e.g. phenols and benzylic alcohols Depletion during process step
Water	H ₂ O	Used in the process	<ul style="list-style-type: none"> Depletion during process step
IPEP		Desired product	<ul style="list-style-type: none"> No depletion

Results – Impurity Profiling of Bisoprolol Fumarate

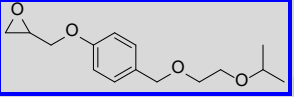
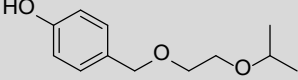
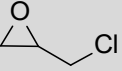
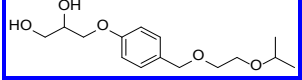
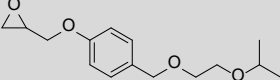
1st generation impurities

1 st gen Step 1b Formation of IPEP	 IMH	 1a.21, n = 0-3	 Epichlorohydrin
 IMH	-	-	 IPEP  1b.3
 Epichlorohydrin	 IPEP  1b.3	 1b.4, n = 0-3  1b.5, n = 0-3	-
H ₂ O	-	-	 1b.6  1b.2
 IPEP	-	-	-

Results – Impurity Profiling of Bisoprolol Fumarate

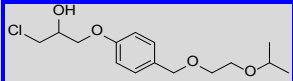
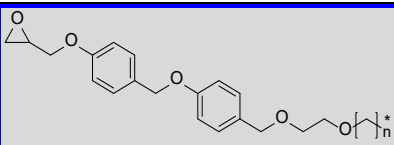
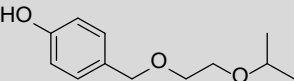
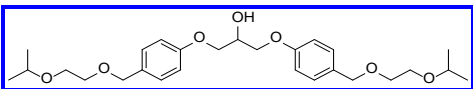
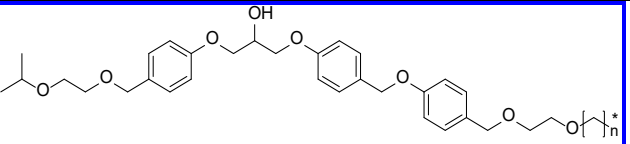
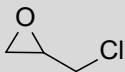
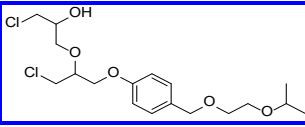
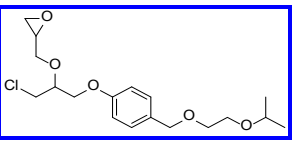
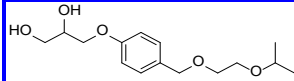
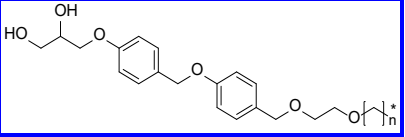
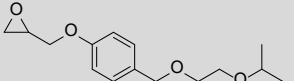
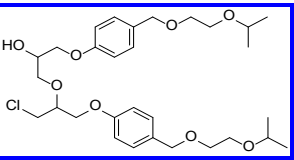
1 st gen Step 1b Formation of IPEP	 1b.1	 1b.2	 H ₂ O
 IMH	 1b.3	 1b.8	-
 Epichlorohydrin	 1b.7	 1b.9  1b.10	 1b.6  1b.2
H ₂ O	 1b.2	 1b.11	-
 IPEP	 1b.12	 1b.13  1b.14	 1b.8

Results – Impurity Profiling of Bisoprolol Fumarate

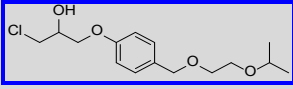
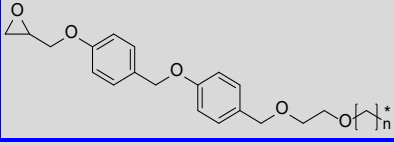
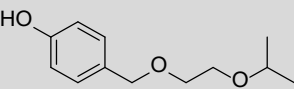
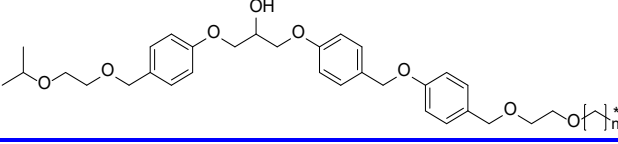
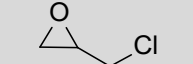
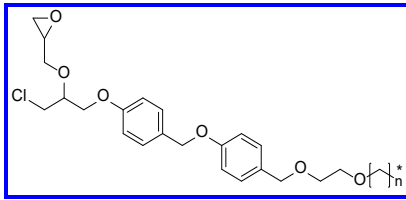
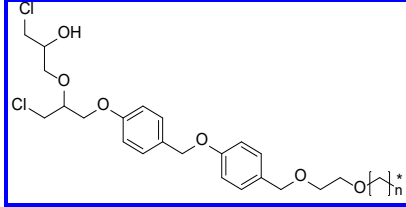
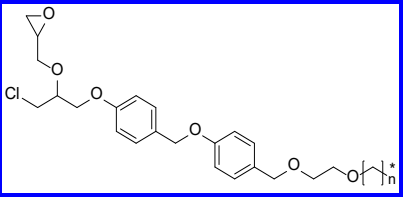
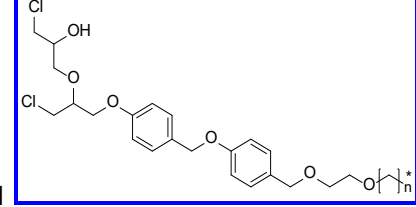
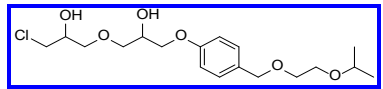
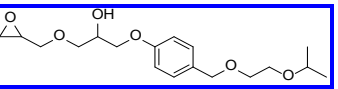
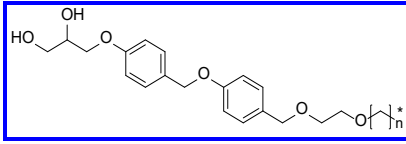
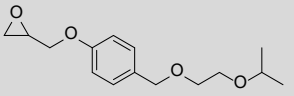
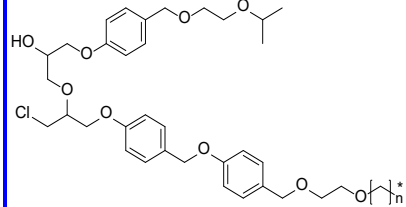
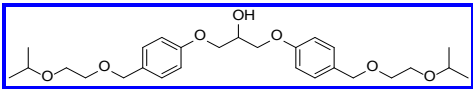
<p style="text-align: center;">1st gen Step 1b Formation of IPEP</p>	<div style="text-align: center;">  <p>IPEP</p> </div>
<div style="text-align: center;">  <p>IMH</p> </div>	-
<div style="text-align: center;">  <p>Epichlorohydrin</p> </div>	-
<p style="text-align: center;">H₂O</p>	<div style="text-align: center;">  <p>1b.8</p> </div>
<div style="text-align: center;">  <p>IPEP</p> </div>	-

Results – Impurity Profiling of Bisoprolol Fumarate

2nd generation impurities (only for selected 1st generation impurities for better clarity)

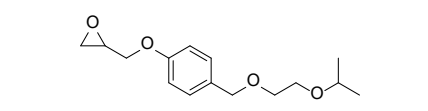
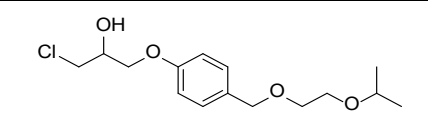
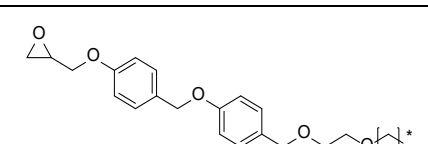
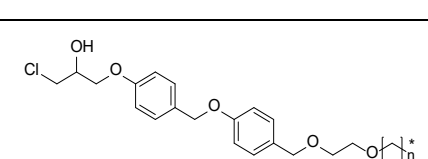
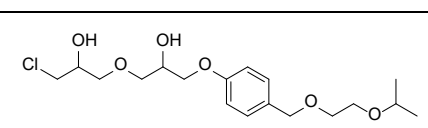
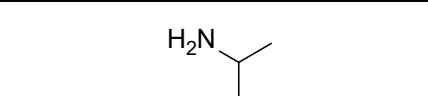
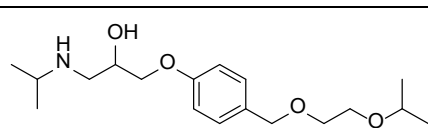
<p>2nd gen Step 1b Formation of IPEP</p>	 <p style="text-align: center;">1b.3</p>	 <p style="text-align: center;">1b.4, n = 0-3</p>
 <p style="text-align: center;">IMH</p>	 <p style="text-align: center;">1b.15</p>	 <p style="text-align: center;">1b.19, n = 0-3</p>
 <p style="text-align: center;">Epichlorohydrin</p>	 <p style="text-align: center;">1b.16</p>  <p style="text-align: center;">1b.17</p>	-
<p style="text-align: center;">H₂O</p>	 <p style="text-align: center;">1b.8</p>	 <p style="text-align: center;">1b.20, n = 0-3</p>
 <p style="text-align: center;">IPEP</p>	 <p style="text-align: center;">1b.18</p>	-

Results – Impurity Profiling of Bisoprolol Fumarate

<p>2nd gen Step 1b Formation of IPEP</p>	 <p style="text-align: center;">1b.3</p>	 <p style="text-align: center;">1b.4, n = 0-3</p>
 <p style="text-align: center;">IMH</p>	 <p style="text-align: center;">1b.19, n = 0-3</p>	-
 <p style="text-align: center;">Epichlorohydrin</p>	 <p style="text-align: center;">1b.21, n = 0-3</p>  <p style="text-align: center;">1b.22, n = 0-3</p>	 <p style="text-align: center;">1b.21</p>  <p style="text-align: center;">1b.22</p>  <p style="text-align: center;">1b.24</p>  <p style="text-align: center;">1b.25</p>
<p style="text-align: center;">H₂O</p>	 <p style="text-align: center;">1b.20, n = 0-3</p>	-
 <p style="text-align: center;">IPEP</p>	 <p style="text-align: center;">1b.23, n = 0-3</p>	 <p style="text-align: center;">1b.15</p>

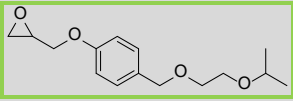
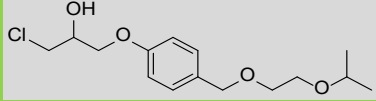
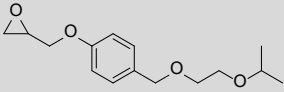
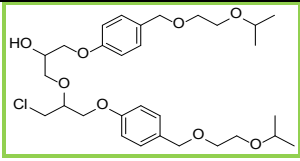
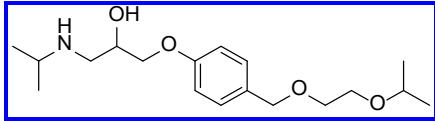
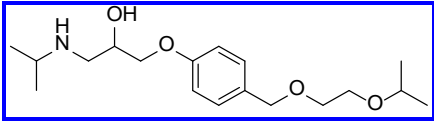
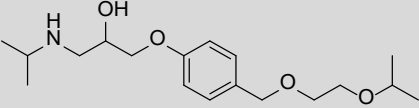
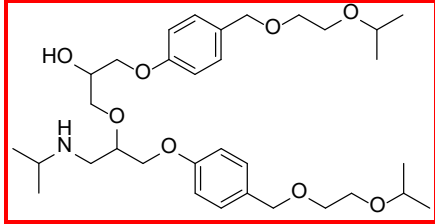
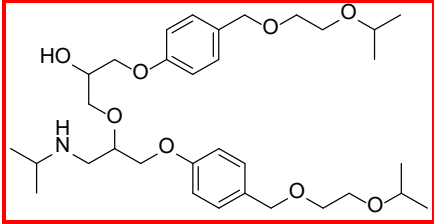
Stage 2: Formation of Bisoprolol

Only selected impurities are displayed for better clarity.

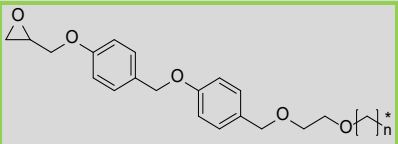
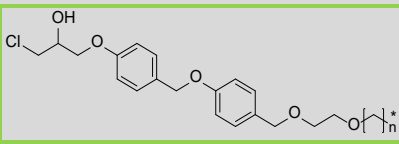
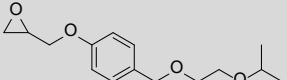
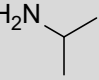
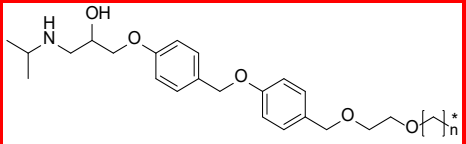
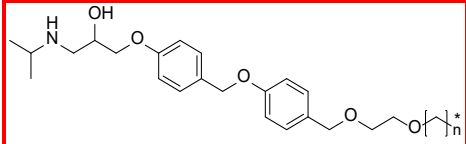
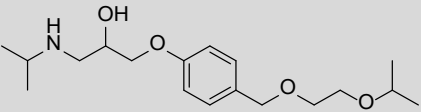
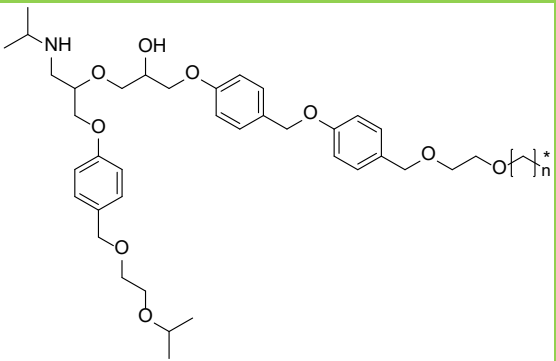
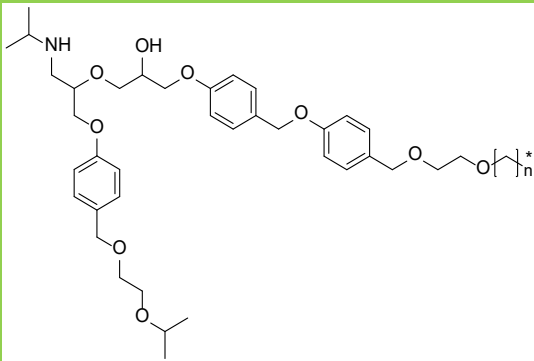
Substance	Structure	Source	Carryover assessment
IPEP		Starting material	<ul style="list-style-type: none"> Transformed by reaction with excess of isopropylamine Depletion during process step
1b.3		Potential contaminant of IPEP	<ul style="list-style-type: none"> Transformed by reaction with excess of isopropylamine Depletion during process step
1b.4 n = 0-3		Potential contaminant of IPEP	<ul style="list-style-type: none"> Transformed by reaction with excess of isopropylamine Depletion during process step
1b.5 n = 0-3		Potential contaminant of IPEP	<ul style="list-style-type: none"> Transformed by reaction with excess of isopropylamine Depletion during process step
1b.14		Potential contaminant of IPEP	<ul style="list-style-type: none"> Transformed by reaction with excess of isopropylamine Depletion during process step
Isopropylamine		Starting material	<ul style="list-style-type: none"> Transformed by reaction with excess of isopropylamine Depletion during process step
Bisoprolol		Desired product	<ul style="list-style-type: none"> No depletion

Results – Impurity Profiling of Bisoprolol Fumarate

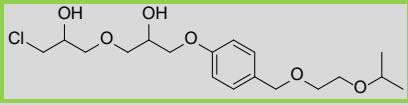
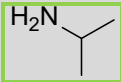
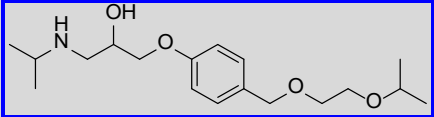
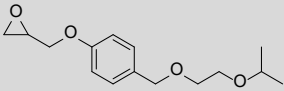
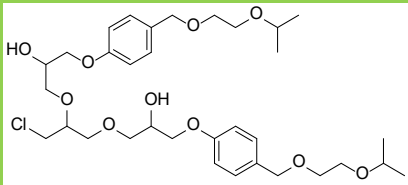
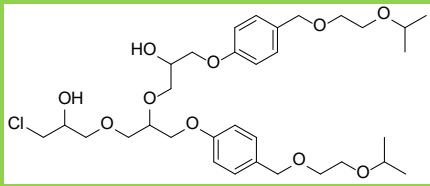
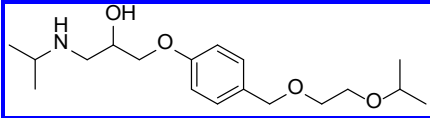
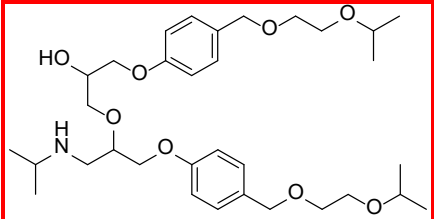
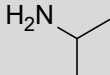
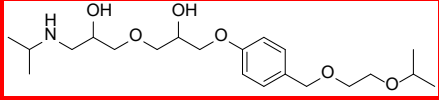
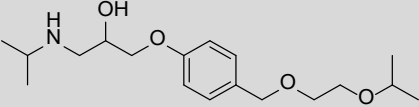
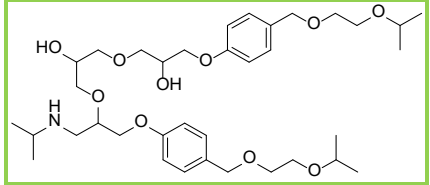
2nd generation impurities

<p>1st gen Step 1b Formation of IPEP</p>	 <p>IPEP</p>	 <p>1b.3</p>
 <p>IPEP</p>	<p>-</p>	 <p>1b.18</p>
<p>H₂N CH(CH₃)₂ Isopropylamine</p>	 <p>Bisoprolol</p>	 <p>Bisoprolol</p>
 <p>Bisoprolol</p>	 <p>2.1 = U9</p>	 <p>2.1 = U9</p>

Results – Impurity Profiling of Bisoprolol Fumarate

<p style="text-align: center;">1st gen Step 1b Formation of IPEP</p>	<div style="text-align: center;">  <p>1b.4, n = 1-4</p> </div>	<div style="text-align: center;">  <p>1b.5, n = 0-3</p> </div>
<div style="text-align: center;">  <p>IPEP</p> </div>	-	-
<div style="text-align: center;"> <p>H₂N</p>  <p>Isopropylamine</p> </div>	<div style="text-align: center;">  <p>2.2 = PI 2.16, n = 0-3</p> </div>	<div style="text-align: center;">  <p>2.2 = PI 2.16, n = 0-3</p> </div>
<div style="text-align: center;">  <p>Bisoprolol</p> </div>	<div style="text-align: center;">  <p>2.3, n = 0-3</p> </div>	<div style="text-align: center;">  <p>2.3, n = 0-3</p> </div>

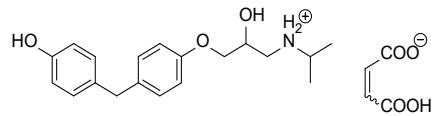
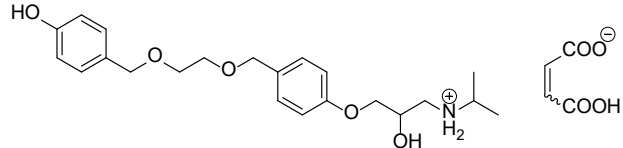
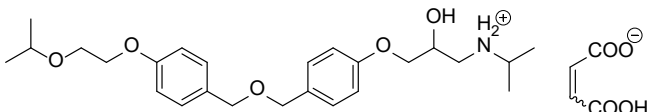
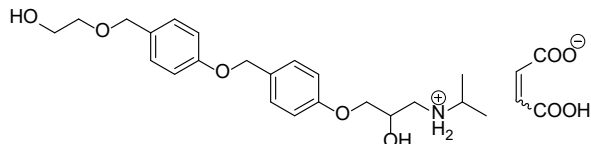
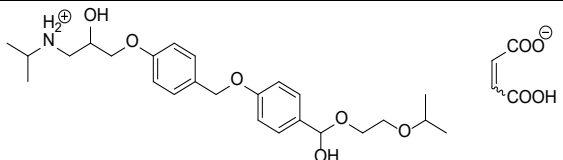
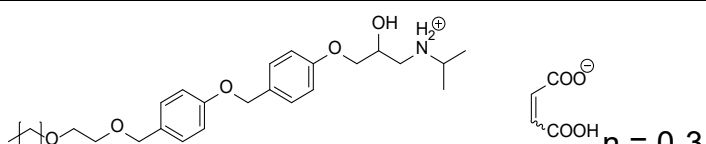
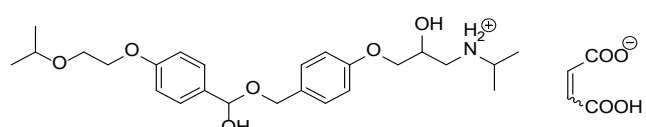
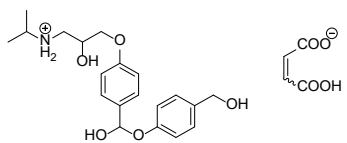
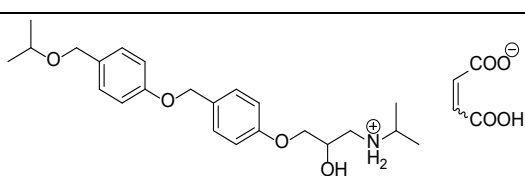
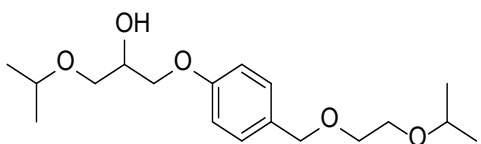
Results – Impurity Profiling of Bisoprolol Fumarate

<p style="text-align: center;">1st gen Step 2 Formation of Bisoprolol</p>	<div style="border: 1px solid green; padding: 5px; text-align: center;">  <p>1b.14</p> </div>	<div style="border: 1px solid green; padding: 5px; text-align: center;">  <p>Isopropylamine</p> </div>	<div style="border: 1px solid blue; padding: 5px; text-align: center;">  <p>Bisoprolol</p> </div>
<div style="text-align: center;">  <p>IPEP</p> </div>	<div style="border: 1px solid green; padding: 5px; text-align: center;">  <p>2.4</p> </div> <div style="border: 1px solid green; padding: 5px; text-align: center;">  <p>2.5</p> </div>	<div style="border: 1px solid blue; padding: 5px; text-align: center;">  <p>Bisoprolol</p> </div>	<div style="border: 1px solid red; padding: 5px; text-align: center;">  <p>2.1 = U9</p> </div>
<div style="text-align: center;">  <p>Isopropylamine</p> </div>	<div style="border: 1px solid red; padding: 5px; text-align: center;">  <p>2.6 = PI 2.46</p> </div>	-	-
<div style="text-align: center;">  <p>Bisoprolol</p> </div>	<div style="border: 1px solid green; padding: 5px; text-align: center;">  <p>2.7</p> </div>	-	-

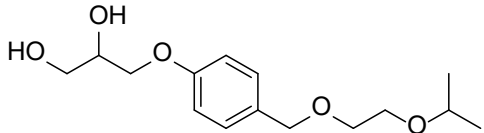
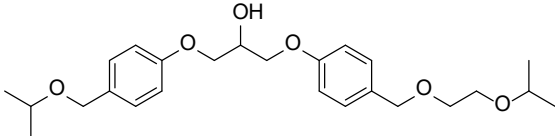
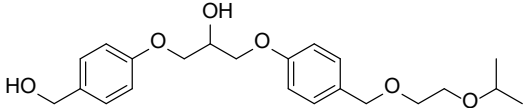
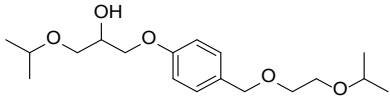
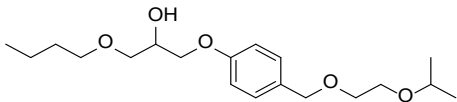
Incomplete listing of potential impurities in Bisoprolol fumarate (final API)

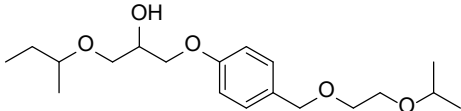
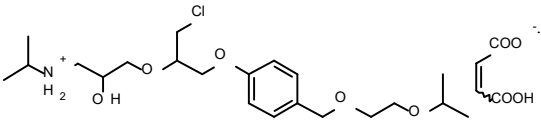
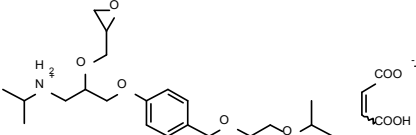
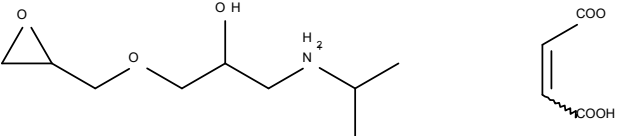
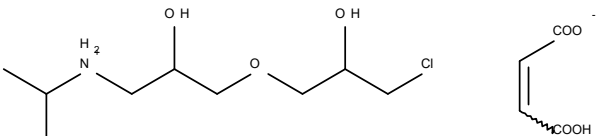
structure	name	structure	name
<p>Chemical structure of Bisoprolol fumarate (2.1) showing the bisoprolol cation and fumarate anion.</p>	2.1 (and isomers)	<p>Chemical structure of Bisoprolol fumarate (2.5) showing the bisoprolol cation and fumarate anion with a polymer chain of length n = 0-3.</p>	2.5 (and isomers)
<p>Chemical structure of Bisoprolol fumarate (2.2) showing the bisoprolol cation and fumarate anion with a different substitution pattern.</p>	2.2 (and isomers)	<p>Chemical structure of Bisoprolol fumarate (2.6) showing the bisoprolol cation and fumarate anion with a different substitution pattern.</p>	2.6 (and isomers)
<p>Chemical structure of Bisoprolol fumarate (2.3) showing the bisoprolol cation and fumarate anion with a different substitution pattern.</p>	2.3	<p>Chemical structure of Bisoprolol fumarate (2.7) showing the bisoprolol cation and fumarate anion with a different substitution pattern.</p>	2.7 (and isomers)
<p>Chemical structure of Bisoprolol fumarate (2.4) showing the bisoprolol cation and fumarate anion with a different substitution pattern.</p>	2.4 (and isomers)	<p>Chemical structure of Bisoprolol fumarate (2.8) showing the bisoprolol cation and fumarate anion with a different substitution pattern.</p>	2.8 (and isomers)

Results – Impurity Profiling of Bisoprolol Fumarate

structure	name	structure	name
	2.9		2.14 (and isomers)
	2.10 (and isomers)		2.15 (and isomers)
	2.11 (and isomers)		2.16 (and isomers)
	2.12		2.17 (and isomers)
	2.13 (and isomers)		2.18 (and isomers)

Results – Impurity Profiling of Bisoprolol Fumarate

structure	name
	1.1 (and isomers)
	1.2 (and isomers)
	1.3 (and isomers)
	1.4 (and isomers)
	1.5 (and isomers)

structure	name
	1.6 (and isomers)
	2.19 (and isomers)
	2.20 (and isomers)
	2.21 (and isomers)
	2.22 (and isomers)

Results – Impurity Profiling of Bisoprolol Fumarate

structure	name	structure	name
	2.23 (and isomers)		1.10 (and isomers)
	1.7 (and isomers)		2.25 (and isomers)
	2.24 (and isomers)		2.26 (and isomers)
	1.8 (and isomers)		1.11 (and isomers)
	1.9 (and isomers)		2.27 (and isomers)

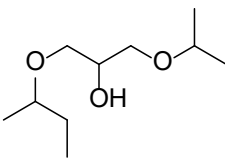
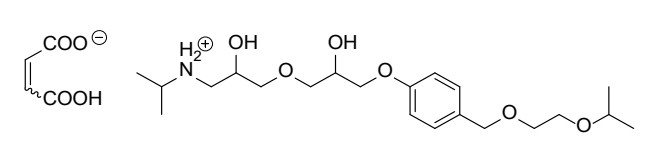
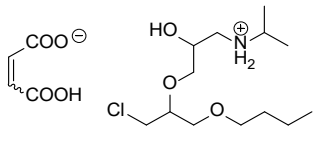
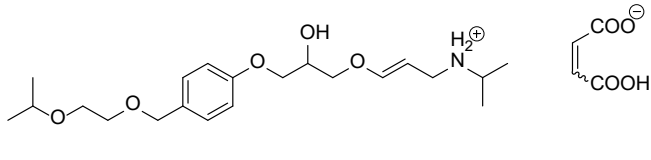
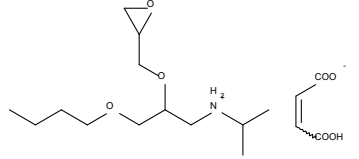
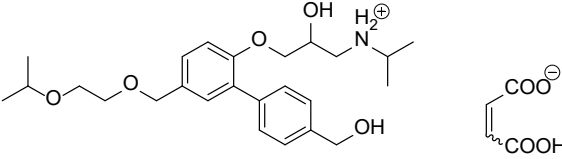
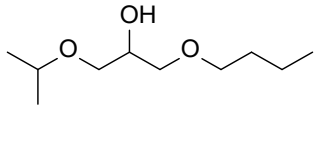
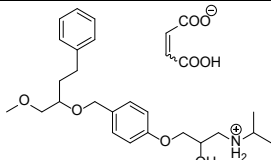
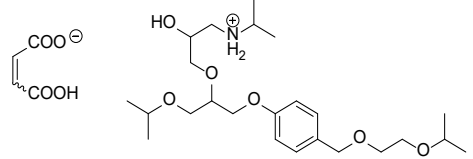
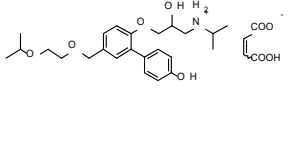
Results – Impurity Profiling of Bisoprolol Fumarate

structure	name	structure	name
	1.12 (and isomers)		1.13 (and isomers)
	2.28 (and isomers)		2.32 (and isomers)
	2.29 (and isomers)		1.14 (and isomers)
	2.30 (and isomers)		2.33 (and isomers)
	2.31 (and isomers)		2.34 (and isomers)

Results – Impurity Profiling of Bisoprolol Fumarate

structure	name	structure	name
	2.35 (and isomers)		2.39 (and isomers)
	1.15 (and isomers)		2.40 (and isomers)
	2.36 (and isomers)		1.16 (and isomers)
	2.37 (and isomers)		2.41 (and isomers)
	2.38 (and isomers)		2.42 (and isomers)

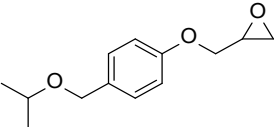
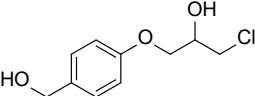
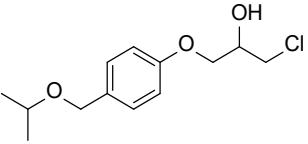
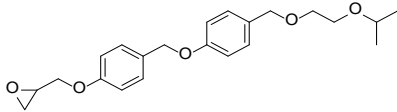
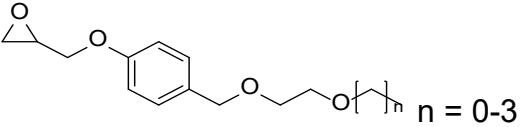
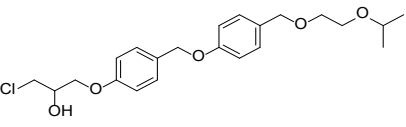
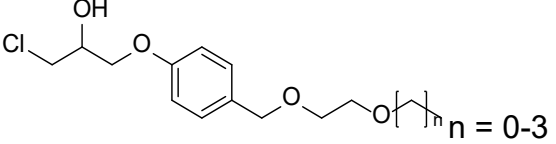
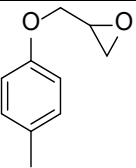
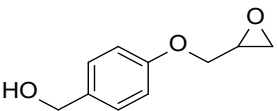
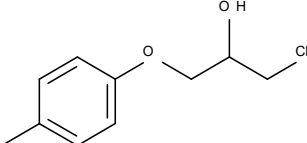
Results – Impurity Profiling of Bisoprolol Fumarate

structure	name	structure	name
	1.17 (and isomers)		2.46 (and isomers)
	2.43 (and isomers)		2.47 (and isomers)
	2.44 (and isomers)		2.48 (and isomers)
	1.18 (and isomers)		2.49 (and isomers)
	2.45 (and isomers)		2.50 (and isomers)

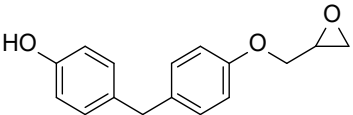
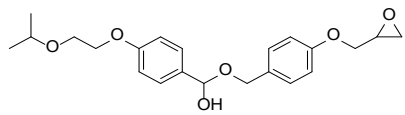
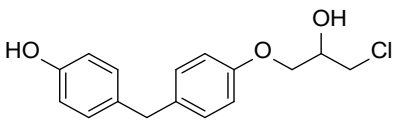
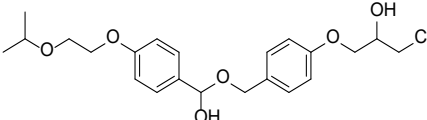
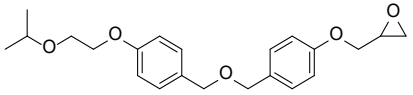
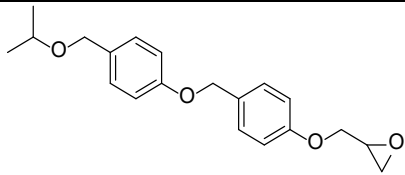
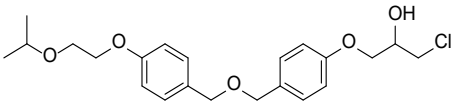
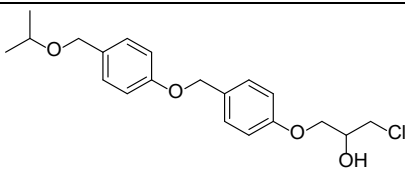
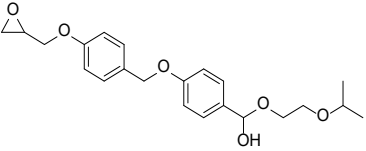
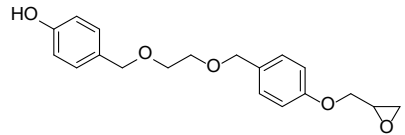
Results – Impurity Profiling of Bisoprolol Fumarate

structure	name	structure	name
	2.51 (and isomers)		1.22 (and isomers)
	2.52 (and isomers)		1.23 (and isomers)
	1.19 (and isomers)		1.24 (and isomers)
	1.20 (and isomers)		1.25
	1.21 (and isomers)		1.26

Results – Impurity Profiling of Bisoprolol Fumarate

structure	name	structure	name
	1.27 (and isomers)		1.32 (and isomers)
	1.28 (and isomers)		1.33 (and isomers)
	1.29 (and isomers)		1.34 (and isomers)
	1.30 (and isomers)		1.35 (and isomers)
	1.31 (and isomers)		1.36 (and isomers)

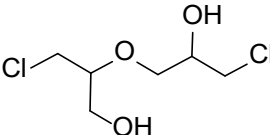
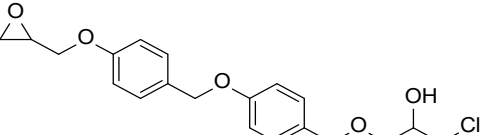
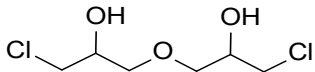
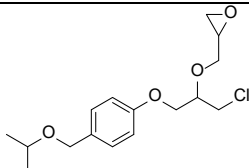
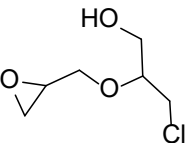
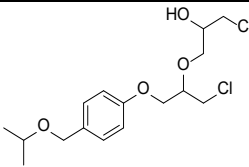
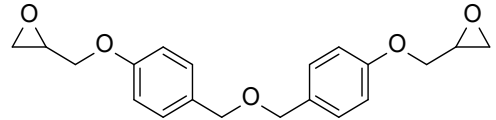
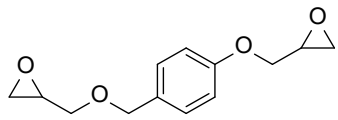
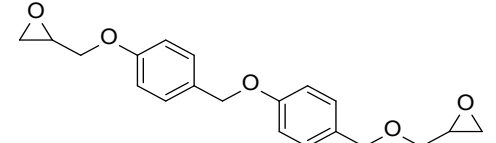
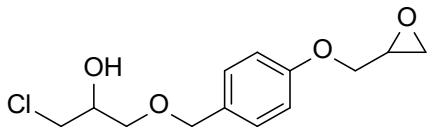
Results – Impurity Profiling of Bisoprolol Fumarate

structure	name	structure	name
	1.37		1.42 (and isomers)
	1.38		1.43 (and isomers)
	1.39 (and isomers)		1.44 (and isomers)
	1.40 (and isomers)		1.45 (and isomers)
	1.41 (and isomers)		1.46 (and isomers)

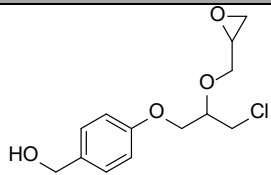
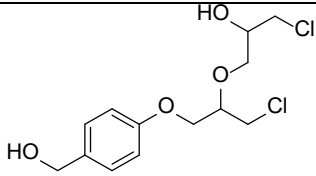
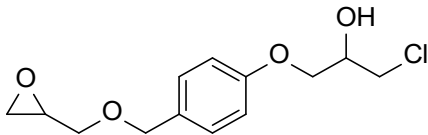
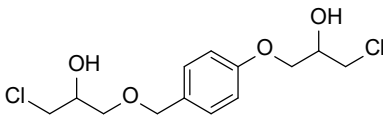
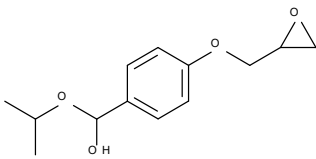
Results – Impurity Profiling of Bisoprolol Fumarate

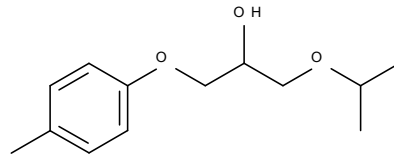
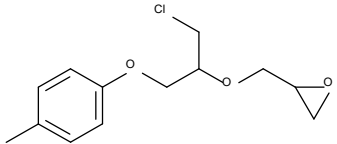
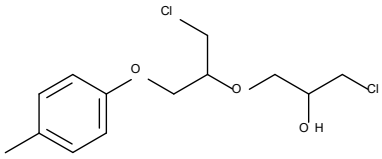
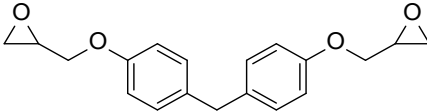
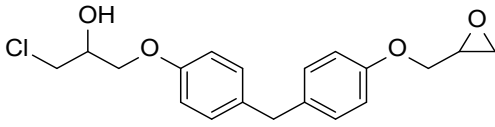
structure	name	structure	name
	1.47 (and isomers)		1.52 (and isomers)
	1.48 (and isomers)		1.53 (and isomers)
	1.49 (and isomers)		1.54 (and isomers)
	1.50 (and isomers)		1.55 (and isomers)
	1.51 (and isomers)		1.56 (and isomers)

Results – Impurity Profiling of Bisoprolol Fumarate

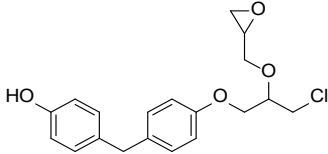
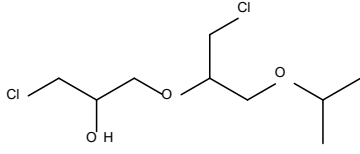
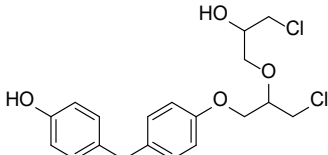
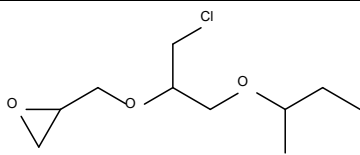
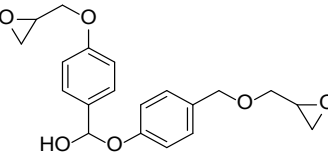
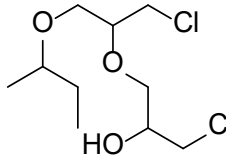
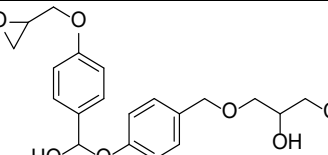
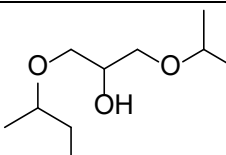
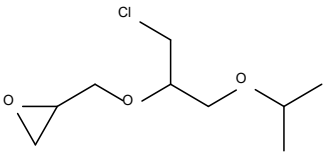
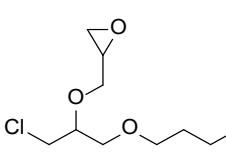
structure	name	structure	name
	1.57 (and isomers)		1.62 (and isomers)
	1.58 (and isomers)		1.63 (and isomers)
	1.59 (and isomers)		1.64 (and isomers)
	1.60 (and isomers)		1.65 (and isomers)
	1.61 (and isomers)		1.66 (and isomers)

Results – Impurity Profiling of Bisoprolol Fumarate

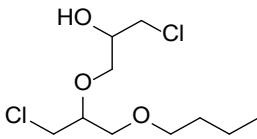
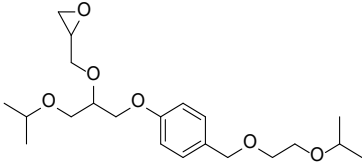
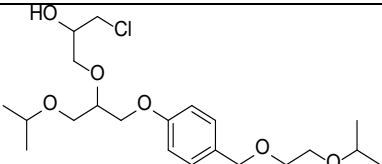
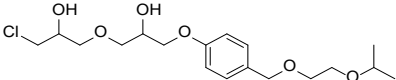
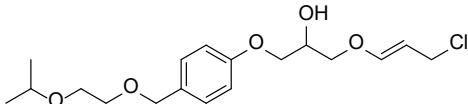
structure	name
	1.67 (and isomers)
	1.68 (and isomers)
	1.69 (and isomers)
	1.70 (and isomers)
	1.71 (and isomers)

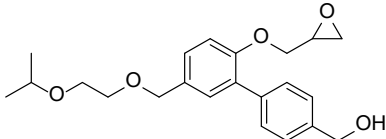
structure	name
	1.72 (and isomers)
	1.73 (and isomers)
	1.74 (and isomers)
	1.75 (and isomers)
	1.76 (and isomers)

Results – Impurity Profiling of Bisoprolol Fumarate

structure	name	structure	name
	1.77 (and isomers)		1.82 (and isomers)
	1.78 (and isomers)		1.83 (and isomers)
	1.79 (and isomers)		1.84 (and isomers)
	1.80 (and isomers)		1.85 (and isomers)
	1.81 (and isomers)		1.86 (and isomers)

Results – Impurity Profiling of Bisoprolol Fumarate

structure	name
	1.87 (and isomers)
	1.88 (and isomers)
	1.89 (and isomers)
	1.90 (and isomers)
	1.91 (and isomers)

structure	name
	1.92 (and isomers)

4 Final Discussion

4.1 Sources of impurities in active pharmaceutical ingredients and medicinal products

The sources of impurities of APIs and medicinal products are various: Impurities can arise during the API synthesis upon side-reactions of the used reactants, reagents, catalysts, residual solvents etc., but also from impurities of the used materials and their reactions [1-8]. Furthermore, purification and salification steps [9], reactions of the API with excipients (and their impurities) as well as degradation products must be considered when establishing an impurity profile of a medicinal product [10]. Even though these sources are well-known, the occurrence of unexpected impurities is a recurring problem. A prominent example is the contamination of sartans with nitrosamines [11], prompting the search for nitrosamines in other substance classes and leading to the detection of nitrosamines in e.g. ranitidine, metformin, and rifampicin [12-14]. Another example is the contamination of the aminoglycoside antibiotic gentamicin sulfate with histamine [15]. Both 4-methyl-1-nitrosopiperazine (MeNP) in rifampicin and histamine in gentamicin, which were analyzed in this work, had not been considered in their compendial monographs [16, 17], but their emergences could be explained by the respective synthesis procedure.

The high risk of MeNP formation upon the production of rifampicin is displayed in the fact that all analyzed batches were contaminated (15 batches from 4 manufacturers). The *acceptable intake limit* of 0.16 ppm was exceeded by far in all batches [14]. However, the regulatory authorities stated that the intake of a single dose of rifampicin contaminated with up to 5 ppm MeNP for the post-exposure prophylaxis (PEP) of leprosy is acceptable considering the risks of a possible leprosy infection [18]. In contrast to the single dose in PEP, the nitrosamine exposure is distinctly higher in the standard therapy of tuberculosis, where rifampicin is used for 6 months in combination with other antimycobacterial drugs (isoniazid, pyrazinamide, ethambutol) [19]. Considering the synthesis' high potential for MeNP formation and the fact that all analyzed batches were affected, the avoidance of rifampicin might be beneficial, making necessary the development of alternative therapeutic regimens.

The emergence of histamine in gentamicin shows the relevance of the quality of raw materials used in the production process of APIs and medicinal products. Histamine,

a contaminant of the fish peptone used upon fermentation, was carried through the entire production process into the medicinal product. Hence, the quality of raw materials can have a major impact on the quality of the final product. Moreover, the applied purification processes were not able to remove histamine from the crude product. In consequence, the European Pharmacopoeia general monograph *Products of Fermentation* was adapted and now requires testing of the raw materials regarding histidine, the precursor of histamine, and proof that the selected purification processes are capable of removing histamine (and other biogenic amines) [20].

4.2 Methods in the analysis of drug impurities

4.2.1 Targeted approaches

The standard techniques applied in the impurity profiling of APIs are targeted approaches. The synthesis is assessed to estimate the risk of the formation of potentially mutagenic impurities, stress tests are performed to recognize degradation products, and analytical procedures are established to control present impurities, mostly using HPLC-UV, but also HPLC-MS and NMR [21]. The limits stated in respective ICH guidelines determine which actions must be taken upon the appearance of impurities. This approach proved suitable in many cases, but poses the risk of disregarding relevant impurities, as only substances exceeding certain thresholds in the applied tests need to be elucidated or characterized regarding their toxicologic potential. In consequence, impurities, which are not detected by the applied method(s) or are genotoxic at a very low concentration might not be recognized.

In the analysis of rifampicin, gentamicin, naproxen, and their respective impurities, targeted approaches were applied. In all cases, the identity of the impurities was known, and the respective contents were to be determined. For the quantification of MeNP in rifampicin capsules, an LC-MS/HRMS method published by the FDA was used [22]. The method made use of a reversed phase phenyl-hexyl column and tandem HRMS detection of a characteristic MeNP fragment, making the method highly selective [23]. Although the method's system suitability criteria were met, the quantification was performed by linear regression instead of the proposed one-point calibration. Obviously, the linear ranges of the instruments used upon method development/validation (qOrbitrap) and the instrument used in this work (qTOF) differed significantly. Even though one-point calibration is feasible in many cases, it is prone to low precision [24, 25]. Robust techniques should be applied in methods

intended for the use in different laboratories and with different instrumentations to guarantee reliable results.

The contamination of gentamicin with the biogenic amine histamine was investigated by means of an LC-MS/MS method applying quadratic regression with an external standard. Due to the high polarities of the aminoglycoside and histamine, *hydrophilic interaction liquid chromatography* (HILIC) was applied. The triple quadrupole mass spectrometer was run in the highly selective and sensitive *multiple reaction monitoring* (MRM) mode [26], monitoring two characteristic fragments of histamine. Only small amounts of histamine were detected in the analyzed samples, below the limit for anaphylactic reactions [27]. However, the samples had been stored at room temperature at the University of Würzburg for about 15 years, which prompts the question of the stability of histamine. The free base of histamine is hygroscopic and air sensitive [28]. As the last step of the preparation of gentamicin sulfate is the salification with sulfuric acid [29], histamine is conjectured to be present as sulfate salt. No stability data are available for histamine sulfate, but no instabilities are reported for other histamine salts (dihydrochloride and biphosphate) [30, 31]. As all sample components are present as solids, degradation of histamine is expected to be neglectable. Additional LC-MS analyses were performed to check a possible correlation of the contamination with histamine and the aminoglycoside impurity sisomicin, which is a lead impurity of gentamicin. Here, zwitterionic HILIC was applied for the separation of the aminoglycosides and coupled to MS detection via a quadrupole ion trap. No correlation of the two contaminants could be found. Hence, histamine was not the causative agent of the fatalities in the 1990s.

An LC-UV method was developed and applied for the analysis of naproxen-PEG-esters (NPEG) in soft gel capsule formulations. Here, UV detection was appropriate, as the naproxen and NPEG molecule contain chromophores and an adequate sensitivity was reached. The contents of NPEG were in the range of 0.15-0.37%, calculated as relative peak area. The influences of the drug load, the water and lactic acid concentration, and the pH could be explained by the type of the reaction, an acid catalyzed condensation [32]. The results clarified the influences of the formulation on NPEG formation, but a more detailed investigation can be achieved by analysis of more formulations. For example, the water concentration influences the pH of the formulation. Thus, the observed effect of the water concentration on the NPEG

formation was due to both factors. The isolated effects can be measured by variation of the pH at constant water concentrations, and vice versa.

4.2.2 Untargeted approaches

Untargeted approaches applying modern and highly sensitive mass spectrometric techniques may close the gap left by the targeted analytics and reduce the risk of missing relevant impurities. Here, mass spectrometric information about (hypothetically) all components present in a sample can be acquired within a single run by IDA or SWATH without prior information regarding the impurities' identities [33]. Structure elucidation of unknown impurities is possible based on tandem HRMS, using the exact mass and isotope pattern for the determination of molecular formulae, and fragment spectra for the elucidation of respective structures [34].

A combined approach was applied in the impurity profiling of bisoprolol fumarate, which revealed the presence of 25 impurities. 18 of them had been predicted by a reaction matrix, illustrating that the synthesis assessment is worthwhile, but might not reveal all relevant impurities, and 17 new impurities were detected in the untargeted part. The recognition of impurities in both parts of the approach showed the suitability of the procedure. However, the versatility of the approach might be increased by application of other techniques, like UV detection for chromophore-containing impurities, gas chromatography for volatile impurities, etc. The detection of chemically unstable substances like epoxides was not possible with the presented methods, but this class of impurities is not expected to be present in the API due to the high reactivity of oxirane rings [35]. The presented works are a compromise between straightforwardness and time/cost investment.

The advantages of untargeted LC-MS/HRMS approaches are their high sensitivity, the great range of detectable analytes, especially when applying different ionization techniques, and the high selectivity enabling the structure elucidation of unknown compounds. However, also with untargeted approaches, not all substances might be detectable, e.g. because they are hardly ionizable or too labile for mass spectrometric detection. Furthermore, the required instrumentation and software is more extensive than with classical approaches. Hence, untargeted approaches are less favourable for routine analytics but should be performed upon the establishment of new impurity profiles or after relevant changes in the production methods.

4.3 References

- [1] International Council for Harmonisation of Technical Requirements for Pharmaceuticals for Human Use, ICH Topic Q3A (R2) Impurities in new Drug Substances, 2006
- [2] International Council for Harmonisation of Technical Requirements for Pharmaceuticals for Human Use, ICH Topic Q1A (R2) Stability Testing of new Drug Substances and Products, 2003
- [3] International Council for Harmonisation of Technical Requirements for Pharmaceuticals for Human Use, ICH guideline M7 (R1) on assessment and control of DNA reactive (mutagenic) impurities in pharmaceuticals to limit potential carcinogenic risk, 2015
- [4] International Council for Harmonisation of Technical Requirements for Pharmaceuticals for Human Use, ICH guideline Q3D (R1) on elemental impurities, 2019
- [5] K. Zhang, J. D. Pellett, A. S. Narang, Y. J. Wang, Y. T. Zhang, Reactive impurities in large and small molecule pharmaceutical excipients – A review, *Trends Anal Chem* 101 (2018) 34-42
- [6] International Council for Harmonisation of Technical Requirements for Pharmaceuticals for Human Use, ICH guideline Q3C (R6) on impurities: guideline for residual solvents, 2019
- [7] A. H. Gainza, Reaction of halogenated hydrocarbon solvents with tertiary amines: Spectrophotometric and conductimetric study, *Int J Chem Kinet* 36 (2004) 500-509
- [8] V. G. Dongre, P. D. Ghugare, P. Karmuse, D. Singh, A. Jadhav, A. Kumar, Identification and characterization of process related impurities in chloroquine and hydroxychloroquine by LC/IT/MS, LC/TOF/MS and NMR, *J Pharm Biomed Anal* 49 (2009) 873-879
- [9] H. Buschmann, D. Jung, U. Holzgrabe, Unerwartet verunreinigt, *Deutsche Apotheker Zeitung* 159-20 (2019) 50-59
- [10] International Council for Harmonisation of Technical Requirements for Pharmaceuticals for Human Use, Impurities in New Drug Products Q3B (R2), 2006
- [11] U.S. Food & Drug Administration, FDA Updates and Press Announcements on Angiotensin II Receptor Blocker (ARB) Recalls, <https://www.fda.gov/drugs/drug-safety-and-availability/fda-updates-and-press-announcements-angiotensin-ii-receptor-blocker-arb-recalls-valsartan-losartan>, 2018 (accessed 4 January 2021)
- [12] U.S. Food & Drug Administration, FDA Updates and Press Announcements on NDMA in Zantac (ranitidine). <https://www.fda.gov/drugs/drug-safety-and-availability/fda-updates-and-press-announcements-ndma-zantac-ranitidine#:~:text=Glenmark%20Pharmaceutical%20Inc.-,FDA%20has%20advised%20companies%20to%20recall%20their%20ranitidine>

- %20if%20testing,conduct%20their%20own%20laboratory%20testing., 2020 (accessed 4 January 2021)
- [13] U.S. Food & Drug Administration, FDA Updates and Press Announcements on NDMA in Metformin. <https://www.fda.gov/drugs/drug-safety-and-availability/fda-updates-and-press-announcements-ndma-metformin>, 2020 (accessed 4 January 2021)
- [14] U.S. Food & Drug Administration, FDA works to mitigate shortages of rifampin and rifapentine after manufacturers find nitrosamine impurities. <https://www.fda.gov/drugs/drug-safety-and-availability/fda-works-mitigate-shortages-rifampin-and-rifapentine-after-manufacturers-find-nitrosamine>, 2020 (accessed 11 December 2020)
- [15] European Medicines Agency, Assessment report, Procedure under Article 5(3) of Regulation EC (No) 726/2004, Procedure no EMEA/H/A-5(3)/1468, INN/active substance: gentamicin (solution for infusion/solution for injection), 2018
- [16] Rifampicin in: European Pharmacopoeia 10.0, Council of Europe, Strasbourg, 2020
- [17] Gentamicin sulfate in: European Pharmacopoeia 9.0, Council of Europe, Strasbourg, 2017
- [18] ILEP International Federation of Anti-Leprosy Associations, Interim advice on the use of rifampicin for post-exposure prophylaxis (PEP), in light of recent information on nitrosamine impurities in rifampicin. <https://ilepfederation.org/interim-advice-on-the-use-of-rifampicin-for-post-exposure-prophylaxis-pep-in-light-of-recent-information-on-nitrosamine-impurities-in-rifampicin/>, 2020 (accessed 7th April 2021)
- [19] T. Schaberg, T. Bauer, F. Brinkmann, R. Diel, C. Feiterna-Sperling, W. Haas, P. Hartmann, B. Hauer, J. Heyckendorf, C. Lange, A. Nienhaus, R. Otto-Knapp, M. Priwitzer, E. Richter, R. Rumetshofer, K. Schenkel, O. D. Schoch, N. Schönfeld, R. Stahlmann, S2k-Leitlinie: Tuberkulose im Erwachsenenalter, *Pneumol.* 71(06) (2017) 325-397
- [20] Products of Fermentation in: European Pharmacopoeia 9.6, Council of Europe, Strasbourg, France, 2019
- [21] R. Holm, D. Elder, Analytical advances in pharmaceutical impurity profiling, *Eur. J. Pharm. Sci.* 87 (216) 118-135
- [22] U.S. Food & Drug Administration, LC-ESI-HRMS Method for the Determination of MNP in Rifampin and CPNP in Rifapentine Drug Substance and Drug Product, <https://www.fda.gov/media/142092/download>, 2020 (accessed 4th January 2021)
- [23] A. Kaufmann, P. Butcher, K. Maden, S. Walker, M. Widmer, Comprehensive comparison of liquid chromatography selectivity as provided by two types of liquid chromatography detectors (high resolution mass spectrometry and tandem mass spectrometry): "Where is the crossover point?", *Anal. Chimica Acta* 673 (2010) 60-72

- [24] A. Tan, K. Awaiye, B. Jose, P. Joshi, F. Trabelsi, Comparison of different linear calibration approaches for LC–MS bioanalysis, *J. Chromatogr. B* 911 (2012) 192-202
- [25] F. T. Peters, H. H. Maurer, Systematic Comparison of Bias and Precision Data Obtained with Multiple-Point and One-Point Calibration in Six Validated Multianalyte Assays for Quantification of Drugs in Human Plasma, *Anal. Chem.* 79 (2007) 4967-4976
- [26] R. W. Kondrat, G. A. McClusky, R. G. Cooks, Multiple reaction monitoring in mass spectrometry/mass spectrometry for direct analysis of complex mixtures, *Anal Chem* 50 (1978) 2017-2021
- [27] Fujian Fukang Pharmaceutical Co., Ltd., Investigation Report of Adverse Effects of Gentamicin Sulfate, 2017
- [28] Sigma-Aldrich, Safety Data Sheet according to Regulation (EC) No. 1907/2006: Histamine, <https://www.sigmaaldrich.com/DE/en/sds/sigma/h7125>, 2021 (accessed 06th October 2021)
- [29] U. Holzgrabe, G. Scriba, Gentamicinsulfat in: Kommentar zum Europäischen Arzneibuch, (Eds: F. Bracher, P. Heisig, P. Langguth, E. Mutschler, G. Rücker, T. Schirmeister, G. Scriba, E. Stahl-Biskup, R. Troschütz), Wissenschaftliche Verlagsgesellschaft mbH **2016** Stuttgart, Germany
- [30] Sigma-Aldrich, Safety Data Sheet according to Regulation (EC) No. 1907/2006: Histamine dihydrochloride, <https://www.sigmaaldrich.com/DE/de/sds/sigma/h7250>, 2020 (accessed 6th October 2021)
- [31] Sigma-Aldrich, Safety Data Sheet according to Regulation (EC) No. 1907/2006: Histamine biphosphate monohydrate, <https://www.sigmaaldrich.com/DE/de/sds/sigma/h7375>, 2020 (accessed 6th October 2021)
- [32] Chapter 14: Carbonsäurederivate in: T. Schirmeister, C. Schmuck, P. R. Wich, Beyer/Walter | Organische Chemie, 25th edition, S. Hirzel Verlag, Stuttgart, Germany, 2015
- [33] X. Zhu, Y. Chen, R. Subramanian, Comparison of Information-Dependent Acquisition, SWATH and MS^{All} Techniques in Metabolite Identification Study Employing Ultrahigh-Performance Liquid Chromatography-Quadrupole Time-of-Flight Mass Spectrometry, *Anal. Chem.* 86 (2014) 1202-1209
- [34] T. Kind, O. Fiehn, Advances in structure elucidation of small molecules using mass spectrometry, *Bioanal. Rev.* 2 (2010) 23-60
- [35] Chapter 6.2.4 Ausgewählte Verbindungen – Derivate der Glycole in: T. Schirmeister, C. Schmuck, P. Wich, Beyer | Walter: Organische Chemie 25, S. Hirzel Verlag, Stuttgart, Germany, 2016, pp. 191-193

5 Summary

The presented works aimed on the analysis of new impurities in APIs and medicinal products. Different subtypes of LC were coupled to suitable detection methods, i.e. UV and various MS techniques, depending on the chemical natures of the analytes and the analytical task.

Unexpected impurities in medicinal products and APIs caused several scandals in the past, concomitant with fatalities or severe side effects in human and veterinary patients. The detection of nitrosamines in sartans led to the discovery of nitrosamines in various other drugs, of which the antibiotic rifampicin was analyzed in this work. An examination of the synthesis of rifampicin revealed a high potential for the formation of 4-methyl-1-nitrosopiperazine (MeNP). An LC-MS/HRMS method suitable for the quantification of MeNP was applied in the analysis of drugs collected from Brazil, Comoros, India, Nepal, and Tanzania, where a single dose of rifampicin is used in the post-exposure prophylaxis of leprosy. All batches were contaminated with MeNP, ranging from 0.7-5.1 ppm. However, application of rifampicin containing up to 5 ppm MeNP was recommended by the regulatory authorities for the post-exposure prophylaxis of leprosy.

In the 1990s the aminoglycoside antibiotic gentamicin attracted attention after causing fatalities in the USA, but the causative agent was never identified unequivocally. The related substance sisomicin was recognized as a lead impurity by the Holzgrabe lab at the University of Würzburg: sisomicin was accompanied by a variety of other impurities and batches containing sisomicin had caused the fatalities. In 2016, anaphylactic reactions were reported after application of gentamicin. A contamination of the medicinal products with histamine, an impurity of the raw material fish peptone used upon the production, could be identified as the cause of the adverse effects. Batches of gentamicin sulfate, which had been stored at the University of Würzburg since the earlier investigations, were analyzed regarding their contamination with histamine to determine whether the biogenic amine was responsible for the 1990s fatalities as well. Furthermore, a correlation with the lead impurity sisomicin was checked. Histamine could be detected in all analyzed batches, but at a lower level than in the batches responsible for the anaphylactic reactions. Moreover, there is no correlation of histamine with the lead impurity sisomicin. Hence, the causative agent for the 1990s fatalities was not histamine and remains unknown.

Another source of impurities is the reaction of APIs with excipients, e.g. the esterification of naproxen with PEG 600 in soft gel capsules. The influence of the formulation's composition on this reaction was investigated by means of LC-UV. Therefore, the impurity naproxen-PEG-ester (NPEG) was synthesized and used for the development of a method suitable for the analysis of soft gel capsule formulations. Different formulations were stressed for 7 d at 60 °C and the relative amount of NPEG was determined. The formation of NPEG was influenced by the concentrations of water and lactic acid, the pH, and the drug load of the formulation, which can easily be explained by the chemistry behind esterification reactions.

Keeping in mind the huge variety of sources of impurities, it might be impossible to predict all potential impurities of a drug substance/product. Targeted and untargeted approaches were combined in the impurity profiling of bisoprolol fumarate. Eight versions of an LC-HRMS method were developed to enable the detection of a maximum number of impurities: an acidic and a basic buffered LC was coupled to MS detection applying ESI and APCI, both in positive and negative mode. MS and MS/MS data were acquired simultaneously by *information dependent acquisition*. In the targeted approach, potential impurities were derived from a reaction matrix based on the synthesis route of the API, while the untargeted part was based on *general unknown comparative screening* to identify additional signals. 18 and 17 impurities were detected in the targeted and the untargeted approach, respectively. The molecular formulae were assessed based on the exact mass and the isotope pattern. Theoretical fragment spectra generated by *in silico* fragmentation were matched with experimental data to estimate the plausibility of proposed/elucidated structures. Moreover, the detected impurities were quantified with respect to an internal standard.

6 Zusammenfassung

In den vorgestellten Projekten wurden neue Verunreinigungen in Arzneistoffen und Arzneimitteln untersucht. Verschiedene flüssigchromatographische Methoden wurden mit geeigneten Detektionsverfahren gekoppelt. UV-Detektion und verschiedene massenspektrometrische Techniken wurden in Abhängigkeit der chemischen Eigenschaften der Analyten und der analytischen Herausforderung ausgewählt.

Eine Kontamination von Wirkstoffen bzw. humanen und veterinären Arzneimittel mit unerwarteten Verunreinigungen löste mehrere Skandale aus, die mit Todesfällen oder ernsthaften Nebenwirkungen einhergingen. Die Identifikation von Nitrosamin-Verunreinigungen in Sartanen führte zur Entdeckung von Nitrosaminen in verschiedenen anderen Wirkstoffen, z.B. im Antibiotikum Rifampicin, das in dieser Arbeit untersucht wurde. Eine Betrachtung der Rifampicin-Synthese offenbarte ein hohes Potenzial der Bildung von 4-Methyl-1-nitrosopiperazin (MeNP). Arzneimittel aus Brasilien, Indien, Nepal, Tansania und von den Komoren wurden mittels LC-MS/HRMS bezüglich ihres MeNP-Gehaltes analysiert. Alle untersuchten Chargen waren mit MeNP im Bereich von 0.7-5.1 ppm belastet. Rifampicin wird in den genannten Ländern unter anderem als Einzeldosis zur Postexpositionsprophylaxe von Lepra eingesetzt. Für diese Indikation empfehlen die Zulassungsbehörden die Verwendung von Rifampicin mit bis zu 5 ppm MeNP.

Das Aminoglycosid-Antibiotikum Gentamicin löste in den 1990er Jahren Todesfälle in den USA aus. Die verantwortliche Verunreinigung wurde nie eindeutig aufgeklärt, doch die verwandte Substanz Sisomicin wurde durch den Arbeitskreis Holzgrabe an der Universität Würzburg als Leitverunreinigung identifiziert: Sisomicin ging mit einer Vielzahl von weiteren Verunreinigungen einher und Sisomicin-reiche Chargen hatten die Todesfälle ausgelöst. 2016 traten anaphylaktische Reaktionen nach Gentamicin-Anwendung auf. Histamin war als Verunreinigung von Fischpepton, einem Ausgangsmaterial der Produktion, in den Wirkstoff gelangt. Um zu überprüfen, ob Histamin auch für die Todesfälle in den 1990er Jahren verantwortlich war, wurden seit den früheren Untersuchungen gelagerte Gentamicin-Chargen bezüglich ihrer Verunreinigung mit Histamin untersucht. Außerdem wurde überprüft, ob es einen Zusammenhang mit dem Sisomicin-Gehalt gibt. In allen untersuchten Proben wurde Histamin gefunden, allerdings in einer geringeren Konzentration als in Chargen, die anaphylaktische Reaktionen ausgelöst hatten. Des Weiteren konnte kein

Zusammenhang mit der Leitverunreinigung Sisomicin erkannt werden. Der Auslöser der Todesfälle in den 1990er Jahren war somit nicht Histamin, sondern bleibt weiterhin unbekannt.

Ein weiterer Ursprung von Verunreinigungen ist die Reaktion des Wirkstoffs mit Hilfsstoff(en), z.B. die Veresterung von Naproxen mit PEG in Weichkapseln. Der Einfluss von Veränderungen der Formulierung auf diese Reaktion wurde mittels LC-UV untersucht. Die Verunreinigung Naproxen-PEG-Ester (NPEG) wurde synthetisiert und zur Entwicklung einer Methode zur Analyse von Weichkapsel-Formulierungen verwendet. Verschiedene Formulierungen wurden für 7 Tage bei 60 °C gestresst und deren relative Gehalte an NPEG bestimmt. Dabei war die Bildung von NPEG von der Wasser- und der Milchsäure-Konzentration, dem pH und dem Wirkstoffgehalt der Formulierung abhängig. Sämtliche Einflüsse konnten durch die Art der Reaktion (Veresterung) erklärt werden.

Vor dem Hintergrund der vielfältigen Quellen für Verunreinigungen erscheint es unmöglich, alle potenziellen Verunreinigungen eines Wirkstoffs/Arzneimittels vorherzusagen. Gerichtete und ungerichtete Ansätze wurden daher für die Erstellung eines Verunreinigungsprofils von Bisoprololfumarat kombiniert. Um eine möglichst große Anzahl von möglichen Substanzen zu detektieren, wurden 8 LC-MS/HRMS-Methoden entwickelt: je eine saure und eine basische mobile Phase der LC wurde mit massenspektrometrischer Detektion mittels ESI und APCI, jeweils im positiv- und negativ-Modus kombiniert. MS- und MS/MS-Daten wurden simultan durch *information dependent acquisition* aufgenommen. Für den gerichteten Ansatz wurde eine Reaktionsmatrix auf Basis der Synthese des Wirkstoffs angefertigt und ausgehend davon potenzielle Verunreinigungen abgeleitet. Im ungerichteten Ansatz wurden mittels *general unknown comparative screening* zusätzliche Signale identifiziert. Der gerichtete Ansatz zeigte die Anwesenheit von 18, der ungerichtete von 17 Verunreinigungen. Summenformeln wurden anhand der exakten Masse und des Isotopenmusters der Signale bewertet. Die Plausibilität von Strukturformeln wurde mittels *In-silico*-Fragmentierung abgeschätzt, wobei experimentelle und theoretische Fragmentspektren in Einklang gebracht wurden. Außerdem wurden alle detektierten Verunreinigungen mittels eines externen Standards quantifiziert.

7 Appendix

7.1 List of publications

- J. Wohlfart, U. Holzgrabe, Analysis of histamine and sisomicin in gentamicin: Search for the causative agents of adverse effects, Arch. Pharm. (2021) e2100260
- J. Wohlfart, O. Scherf-Clavel, M. Kinzig, F. Sörgel, U. Holzgrabe, The nitrosamine contamination of drugs, part 3: Quantification of 4-Methyl-1-nitrosopiperazine in rifampicin capsules by LC-MS/HRMS, J. Pharm. Biomed. Anal. 203 (2021) 114205
- J. Wohlfart, E. Jäckel, O. Scherf-Clavel, D. Jung, M. Kinzig, F. Sörgel, U. Holzgrabe, Impurity profiling of bisoprolol fumarate by liquid chromatography-high-resolution mass spectrometry: A combination of targeted and untargeted approaches using a synthesis reaction matrix and general unknown comparative screening, J. Chrom. Open 1 (2021) 100012
- F. Sörgel, M. Kinzig, M. Abdel-Tawab, C. Bidmon, A. Schreiber, S. Ermel, J. Wohlfart, A. Besa, O. Scherf-Clavel, U. Holzgrabe, The contamination of valsartan and other sartans, part 1: New findings, N. Pharm. Biomed. Anal. 172 (2019) 395-405
- O. Scherf-Clavel, M. Kinzig, A. Besa, A. Schreiber, C. Bidmon, M. Abdel-Tawab, J. Wohlfart, F. Sörgel, U. Holzgrabe, The contamination of valsartan and other sartans, Part 2: Untargeted screening reveals contamination with amides additionally to known nitrosamine impurities, J. Pharm. Biomed. Anal. 172 (2019) 278-284

7.2 Documentation of authorship

The individual contributions of each author to the published and unpublished works presented in this thesis are specified in this section.

Die Mitautoren der in dieser teilkumulativen Dissertation verwendeten Manuskripte sind sowohl über die Nutzung als auch über die angegebenen Eigenanteile informiert und stimmen dem zu.

Jonas Wohlfart

Hauptautor/in

Verweis: E-Mail hinterlegt

Ulrike Holzgrabe

Korrespondenzautor/in

Verweis: E-Mail hinterlegt

Würzburg, 03.01.2022

Prof. Dr. Ulrike Holzgrabe

Erklärung zur Autorenschaft

The nitrosamine contamination of drugs, part 3: Quantification of 4-Methyl-1-nitrosopiperazine in rifampicin capsules by LC-MS/HRMS

Jonas Wohlfart, Oliver Scherf-Clavel, Martina Kinzig, Fritz Sörgel, Ulrike Holzgrabe

Journal of Pharmaceutical and Biomedical Analysis 203 (2021) 114205

Jonas Wohlfart (JW), Oliver Scherf-Clavel (OSC), Martina Kinzig (MK), Fritz Sörgel (FS), Ulrike Holzgrabe (UH)												
Autor	JW	OSC	MK	FS	UH							Σ in Prozent
Studiendesign	5	5			5							15
Experimentelle Arbeit	30											30
Datenanalyse und Interpretation	5	2.5			2.5							10
Verfassen der Veröffentlichung	20											20
Korrektur der Veröffentlichung		5	5	5	5							20
Koordination der Veröffentlichung					5							5
Summe	60	12.5	5	5	17.5							100

Die Mitautoren der in dieser teilkumulativen Dissertation verwendeten Manuskripte sind sowohl über die Nutzung als auch über die angegebenen Eigenanteile informiert und stimmen dem zu.

Jonas Wohlfart

Hauptautor/in

Verweis: E-Mail hinterlegt

Oliver Scherf-Clavel

Koautor/in

Verweis: E-Mail hinterlegt

Martina Kinzig

Koautor/in

Verweis: E-Mail hinterlegt

Fritz Sörgel

Koautor/in

Verweis: E-Mail hinterlegt

Ulrike Holzgrabe

Korrespondenzautor/in

Verweis: E-Mail hinterlegt

Würzburg, 03.01.2022

Prof. Dr. Ulrike Holzgrabe

Erklärung zur Autorenschaft

Analysis of Naproxen-PEG-Esters in Soft Gel Capsule Formulations

Jonas Wohlfart, Ulrike Holzgrabe

Unpublished Manuscript

Jonas Wohlfart (JW), Ulrike Holzgrabe (UH)												
Autor	JW	UH										Σ in Prozent
Studiendesign	5	5										10
Experimentelle Arbeit	35											35
Datenanalyse und Interpretation	7.5	7.5										15
Verfassen des Manuskripts	30											30
Korrektur des Manuskripts		10										10
Summe	77.5	22.5										100

Die Mitautoren der in dieser teilkumulativen Dissertation verwendeten Manuskripte sind sowohl über die Nutzung als auch über die angegebenen Eigenanteile informiert und stimmen dem zu.

Jonas Wohlfart

Ulrike Holzgrabe

Hauptautor/in

Korrespondenzautor/in

Verweis: E-Mail hinterlegt

Verweis: E-Mail hinterlegt

Würzburg, 03.01.2022

Prof. Dr. Ulrike Holzgrabe

Erklärung zur Autorenschaft

Impurity profiling of bisoprolol fumarate by liquid chromatography-high resolution mass spectrometry: A combination of targeted and untargeted approaches using a synthesis reaction matrix and general unknown comparative screening

Jonas Wohlfart, Elisabeth Jäckel, Oliver Scherf-Clavel, Dirk Jung, Martina Kinzig, Fritz Sörgel, Ulrike Holzgrabe

Journal of Chromatography Open 1 (2021) 100012

Jonas Wohlfart (JW), Elisabeth Jäckel (EJ), Oliver Scherf-Clavel (OSC), Dirk Jung (DJ), Martina Kinzig (MK), Fritz Sörgel (FS), Ulrike Holzgrabe (UH)

Autor	JW	EJ	OSC	DJ	MK	FS	UH					Σ in Prozent
Studiendesign	3	3	3	3			3					15
Experimentelle Arbeit	25											25
Datenanalyse und Interpretation	25	5										30
Verfassen der Veröffentlichung	10	5										15
Korrektur der Veröffentlichung		2	2	1	1	1	5					12
Koordination der Veröffentlichung				1			2					3
Summe	58	15	5	5	1	1	15					100

Die Mitautoren der in dieser teilkumulativen Dissertation verwendeten Manuskripte sind sowohl über die Nutzung als auch über die angegebenen Eigenanteile informiert und stimmen dem zu.

Jonas Wohlfart

Hauptautor/in

Verweis: E-Mail hinterlegt

Edith Jäckel

Koautor/in

Verweis: E-Mail hinterlegt

Oliver Scherf-Clavel

Koautor/in

Verweis: E-Mail hinterlegt

Dirk Jung

Koautor/in

Verweis: E-Mail hinterlegt

Martina Kinzig

Koautor/in

Verweis: E-Mail hinterlegt

Fritz Sörgel

Koautor/in

Verweis: E-Mail hinterlegt

Ulrike Holzgrabe

Korrespondenzautor/in

Verweis: E-Mail hinterlegt

Würzburg, 03.01.2022

Prof. Dr. Ulrike Holzgrabe